

Geophysical exploration of Antarctic blue ice areas (BIAs) for paleoclimate applications

A doctoral thesis by Anna Sinisalo

Academic Dissertation to be presented with the assent of the Faculty of Science,
University of Oulu, for public discussion in Arktikum (Aurora hall), Rovaniemi,
on November 16th, 2007, at 12 noon.

Copyright 2007
Arctic Centre

Supervised by
Research professor John Moore
Professor Sven-Erik Hjelt

Opponent
Professor Jon Ove Hagen

Examiners
Doctor Elisabeth Isaksson
Doctor Francisco J. Navarro

Publisher
Arctic Centre, University of Lapland

Cover photos
FINNARP/Aslak Grinsted

Layout
Liisa Karintaus

ISSN 1235-0583
ISBN 978-952-484-159-7

Edita Prima Oy
Helsinki 2007

Anna Sinisalo

Geophysical exploration of Antarctic blue ice areas (BIAs) for paleoclimate applications

Faculty of Science
Department of Physical Science
Division of Geophysics
University of Oulu
PO Box 3000
FI-90014
University of Oulu
Finland

Arctic Centre
University of Lapland
PO Box 122
FI-96101 Rovaniemi
Finland

Abstract

Antarctic blue ice areas (BIAs) cover about 1 % of Antarctic surface area. The BIAs are known to have very old ice at the surface. This ice could be of great value for paleoclimatic purposes but the dating of the surface blue ice is demanding. Only few BIAs have been studied for paleoclimatic purposes although the temporal resolution in paleoclimatic data collected from the surface of a BIA can be higher than those of any of the vertical Antarctic ice cores.

In this study, we focus on Scharffenbergbotnen, a blue ice area in Dronning Maud Land, Antarctica. Surface mass balance, ice flow velocities, and age gradient of the surface blue ice are determined by stake, ground penetrating radar, and differential GPS measurements. We estimate the surface age gradient and the age of our blue ice samples by adjusting a flowmodel to match with radiocarbon ages of the ice samples from the same area. The age gradients estimated by the flowmodel, by following isochrones with a ground penetrating radar, and by high resolution isotopic analysis are rather consistent.

An isotopic analysis of a limited set of snow and blue ice samples can provide a fast and easy way to make a first estimation of the age of a BIA. A 101-m long continuous surface profile was also analysed for stable water isotopes from Scharffenbergbotnen BIA. According to the dating model the time period sampled is about a 500-year span of the mid-Holocene. The isotopic analysis imply that the mid-Holocene samples in Scharffenbergbotnen originate from a cooler climate period than the present. Furthermore, comparison with 10500 year old ice shows that the modern climate is about $1.0 \pm 0.3^\circ\text{C}$ warmer than the early Holocene climatic optimum in Scharffenbergbotnen.

Many of the BIAs in mountainous areas of Dronning Maud Land are of Holocene origin. Changes in ice sheet thickness control the existence of the BIAs in the mountainous areas. Scharffenbergbotnen BIA was much smaller in the last glacial maximum than it is today. However, there are significant differences between the ice sheet elevation history in the mountainous areas of Dronning Maud Land and in central East Antarctica and Transantarctic mountains.

This work emphasises that geophysical data must be combined with ice core analysis to get a reliable paleoclimate record. Although dating can be demanding, BIAs can provide high resolution paleoclimatic data that cannot be extracted from anywhere else.

Keywords: Antarctic blue ice area, geophysics, paleoclimate, surface mass balance, GPR, GPS

Acknowledgements

I would like to thank my supervisor research professor John Moore for introducing me the world of glaciology, and for sharing his innovative scientific ideas. I am grateful for my professors Sven-Erik Hjelt, and Pertti Kaikkonen for allowing me to specialise in glaciology, and for the co-operation between the universities of Oulu and Lapland. I also thank all my co-authors, colleagues, and contributors. Especially, I would like to express my deepest gratitude to my colleagues and friends Aslak Grinsted, and Kristiina Virkkunen, and my field team mate Jari Vehviläinen. Two reviewers, Dr. Elisabeth Isaksson and Dr. Francisco Navarro gave me plenty of valuable comments and suggestions that helped me to improve the manuscript.

Numerous people have supported me in various ways during these years of research. I am sorry for not being able to list all the names here but I would like to express my gratitude to all of those who have been involved in this work. These people include colleagues and friends at the Arctic Centre; at the Divisions of Geophysics of the universities of Oulu and Helsinki; at the Institute of Marine and Atmospheric Utrecht, the Netherlands; and the expedition members of FINNARP 1999-2000, 2000-2001, 2003-2004, and SANAE 39 and 40.

Finnish Antarctic Research Program (FINNARP 1999-2000, 2000-2001, and 2003-2004) provided the field logistics. This work was primarily funded by the Academy of Finland (project no.43921). Parts of this work were funded by the Arctic graduate school ARKTIS, the Thule Institute, and by grants from the Faculty of Science, Oulu University and the University Pharmacy Foundation (Oulu).

Finally, I would like to thank Kalle and my whole family, and the dear friends for all the support and encouragement, and more important, for all the fun moments outside of the office.

List of original papers

I **Sinisalo, A.**, J. Moore, R. van de Wal, R. Bintanja and S. Jonsson, 2003a. A 14-year mass balance record of a blue ice area in Antarctica. *Ann. Glac.* 37, p. 213-218.

II **Sinisalo, A.**, A. Grinsted, J. Moore, E. Kärkäs and R. Petterson, 2003b. Snow accumulation studies in Antarctica with ground penetrating radar using 50, 100 and 800 MHz antenna frequencies. *Ann. Glac.* 37, p. 194-198.

III **Sinisalo, A.**, A. Grinsted, and J. C. Moore, 2004. Dynamics of the Scharffenbergbotnen blue-ice area, Dronning Maud Land, Antarctica, *Ann. Glac.* 39, p. 417-423.

IV **Sinisalo, A.**, A. Grinsted, J. C. Moore, H. A. J. Meijer, T. Martma, and R. S. W. van de Wal, 2007. Inferences from stable water isotopes on the Holocene evolution of Scharffenbergbotnen blue ice area, East Antarctica. *J. Glaciol.* 53(182), 427-434.

A. Sinisalo was mainly responsible for interpretation of the data, and writing the papers. She made the ground penetrating radar (GPR), and differential GPS measurements in 1999/2000, 2000/2001, and 2003/2004, and carried out the data processing and data analyses discussed in the papers. She led the field team that extracted the 101-m ice core discussed in paper IV, and participated in some of the sampling work.

The papers I-IV are reprinted from the Journal of Glaciology/Annals of Glaciology with permission of the International Glaciological Society.

Contents

1	Introduction	8
2	Antarctic blue ice areas (BIAs)	10
2.1	Definition	10
2.2	Geographical distribution	10
2.3	Ice flow	12
2.4	Meteorology	12
2.5	Surface characteristics	13
2.6	Classification of blue ice areas	15
2.7	Dating	16
2.7.1	Meteorites	16
2.7.2	Radiodating	17
2.7.3	Isotopic dating	17
2.7.4	Dating of tephra layers	18
2.7.5	Geomorphology	18
2.7.6	Ice flow modelling	18
2.7.7	Combination of methods	19
2.8	Blue ice areas and climate	19
3	Methods	21
3.1	Precise GPS	21
3.2	Ground penetrating radar (GPR)	22
3.3	Mass balance studies	23
3.4	Dip angles of isochrones and surface age gradient in BIAs	23
3.5	Blue ice, firn, and snow samples	23
3.6	Isotopic analysis	24
4	Study area	25
5	Results and discussion	26
5.1	Mass balance and dynamics of the BIAs (Papers I-IV)	26
5.2	Paleoclimate data (Paper IV)	27
5.3	Dating of surface blue ice (Paper III and IV)	28
5.4	On the age and stability of the BIAs (Paper IV)	31
5.5	Suggestions for future studies	33
6	References	34

I INTRODUCTION

Antarctica plays a significant role in the global climate system. To understand the significance of current climate change, and to potentially predict future changes in atmospheric circulation and temperature, we need to examine climate series that are longer than available instrumented records. As global climate is complex it is important to have site-specific paleoclimatic data. Traditionally, paleoclimate has been studied from the analysis of deep ice cores. There are only few deep drilling projects, however, covering tens or hundreds of thousands of years of climate history in Antarctica (Epica community members, 2004; Petit and others, 1999; Watanabe and others, 2003), and these projects are very expensive and time-consuming.

Antarctic paleoclimate data are available not only from the deep ice cores but also from the surface of Antarctic blue ice areas (BIAs). Many of these BIAs are known to have very old ice at the surface (Whillans and Cassidy, 1983; Bintanja, 1999). The surface blue ice provides also higher temporal resolution than deep ice cores (Moore and others, 2006; Sinisalo and others, 2007). Thus, shallow or horizontal surface cores from BIAs may complement the deep ice cores to get an insight to the climate history (Sinisalo and others, 2007; Moore and others, 2006; Custer, 2006; Popp and others, 2004).

The first scientific description of an Antarctic BIA was given by Schytt (1961) though there is a good general introduction by Giaever (1954) concerning the first expedition to visit a BIA. The expedition members discovered the amazing stability of the snow-blue ice boundary by placing match sticks at the boundary –many of which were still in place and not buried several months later. Schytt (1961) noted that crystal size of the blue ice indicated a deep source for the ice. Crary and others (1961) first described the surface characteristics of BIA and discussed formation of BIAs by horizontal compressive forces with katabatic winds removing snow accumulation.

Much of the early scientific interest in Antarctic BIAs was due to their nature as meteorite collectors (Cassidy and others, 1977; Whillans and Cassidy, 1983; Nishiizumi and others, 1989). The initial discovery of meteorites was made in the Yamato Mountains (Fig. 1) by Yoshida and others (1971) in 1969. Since then, more than 25 000 meteorites have been found on Antarctic BIAs (Harvey, 2003). Consequently, the ice flow regime was studied and ice flow models were published for several BIAs to explain the meteorite findings (Naruse and Hashimoto, 1982; Whillans and Cassidy, 1983; Azuma and others, 1985). When researchers started to understand the flow regime of the BIAs, they got also interested in the paleoclimate record stored on the surface of BIAs (Bintanja, 1999; Moore and others, 2006; Sinisalo and others, 2007; Custer and others, 2006; Popp, 2004).



Fig. 1. *Some Antarctic BIAs of scientific interest. SBB=Scharffenbergbotnen, YM=Yamato Mountains, Mt.M=Mt. Moulton, AH=Allan Hills, FM=Frontier Mountain. SBB also indicates the location of Heimefrontfjella mountain range.*

Several studies have been made on the mass balance of various BIAs (e.g. Jonsson and Holmlund, 1990; Jonsson, 1992; Sinisalo and others, 2003a, Faure and Buchanan, 1991; Schultz and others, 1990), on the meteorological conditions of BIAs (e.g. Bintanja and van den Broeke, 1995a; Bintanja and van den Broeke, 1995b; Bintanja, 2000; Bintanja and Reijmer, 2001), on the blue ice surface properties (Bintanja and others, 2001), and on the moraines in the BIAs and their surroundings (Lintinen and Nenonen, 1997; Hättestrand and Johansen, 2005).

The dating of the surface blue ice is demanding since the traditional ice core dating methods cannot be easily applied for the BIAs where the layering is far from horizontal. Previously, blue ice samples from various BIAs have been dated by meteorite terrestrial ages found on their surface (e.g. Nishiizumi and others, 1989; Whillans and Cassidy, 1989), by ^{14}C dating of ice (van Roijen, 1995; van der Kemp and others, 2002), by radiometric dating of tephra layers found at the surface of BIAs (Wilch and others, 1999), and by stratigraphic comparison with well-dated ice cores (Moore and others, 2006). There are several BIAs in e.g. Yamato mountains, and Allan Hills (Fig. 1) where the surface blue ice is estimated to be tens or hundreds of thousands of years old (Nishiizumi and others, 1989; Whillans and Cassidy, 1989; Welten and others, 2000). However, there are still only a few paleoclimate records from BIAs although the temporal resolution in such data can be higher than those from any of the other Antarctic ice cores (Moore and others, 2006; Sinisalo and others, 2007).

The main objectives of this work are

- To understand better the dynamics of the Antarctic BIAs;
- To investigate possibilities to extract climate proxies from the surface of the BIAs;
- To understand better the temporal stability of Antarctic BIAs.

The easily recoverable ancient surface ice of the BIAs could be of great value for paleoclimatic purposes if the dynamics and the internal structure of the BIAs were better known (Bintanja, 1999). Despite the studies introduced earlier in this chapter there are still many open questions related to the Antarctic BIAs remaining, for example their general stability under different climate regimes, and the surface age gradient of individual BIAs of interest.

2 ANTARCTIC BLUE ICE AREAS (BIAs)

In this section, we shortly introduce the Antarctic BIAs that have been of primary interest of the scientific community, and summarize the current scientific knowledge, and the latest results that have been published concerning these areas. We also summarize the review of BIAs by Bintanja (1999), and update the scientific research of Antarctic BIAs since then.

2.1 Definition

BIAs are bare ice fields that the wind keeps clean of snow, and their area can vary from a few hectares to thousands of square kilometres. Blue ice extent may vary because of weather changes, seasonal effects, and climate change although these changes are usually not well defined. Bintanja (1999) defines BIAs as areas where

- surface mass balance is negative,
- sublimation forms the main ablation process, and
- surface albedo is relatively low.

BIAs appear blue (Fig.2) as does all ice of sufficient thickness due to the strong absorption of the red band of the solar radiation spectrum by the ice. However, blue ice is normally less dense than solid ice, and the presence of air bubbles makes the colour lighter than that of the bubble-free solid ice due to their relatively uniform scattering of light (Bintanja, 1999).

2.2 Geographical distribution

BIAs cover about 0.8-1.6 % of Antarctic surface area (Winther and others, 2001). They are scattered widely over the continent appearing mainly in the vicinity of mountain



Fig. 2. *A BIA in the Scharffenbergbotnen valley surrounded by mountains.
Photo: FINNARP/Anna Sinisalo*

ranges and nunataks as they are likely to form at locations where ice flow is dammed by outcropping nunataks or slowed down by subglacial bedrock ridges (e.g. Faure and Buchanan, 1991), precipitation is low and the annual mean wind speed relatively high (Van den Broeke and Bintanja, 1995). These phenomena explain why Antarctica is the only place on Earth where BIAs exist.

There are only few BIAs that have been studied in detail. They are located (see Fig. 1) in the vicinity of Yamato mountains (e.g. Moore and others, 2006), the Allan Hills (e.g. Faure and Buchanan, 1991; Schultz and others, 1990; Spikes, 2000), Mt. Moulton (e.g. Wilch, 1999), and Heimefrontfjella mountain range in Dronning Maud Land (e.g. Bintanja 1999; this publication). In addition, there are other BIAs, such as Frontier Mountain BIA (Perchiazzi and others, 1999) that have been studied less intensively (Fig. 1). Meteorites have been collected mainly from Yamato mountains (Yoshida and others, 1971; Nishiizumi and others, 1989), Allan Hills (Cassidy and others, 1977; Nishiizumi and others, 1989) and Transantarctic mountains in general (Welten and others, 2000); and paleoclimate data from Yamato Mountains (Moore and others, 2006), Mt. Moulton (Custer, 2006; Popp and others, 2004), and Scharffenbergbotnen in the Heimefrontfjella mountain range (Sinisalo and others, 2007).

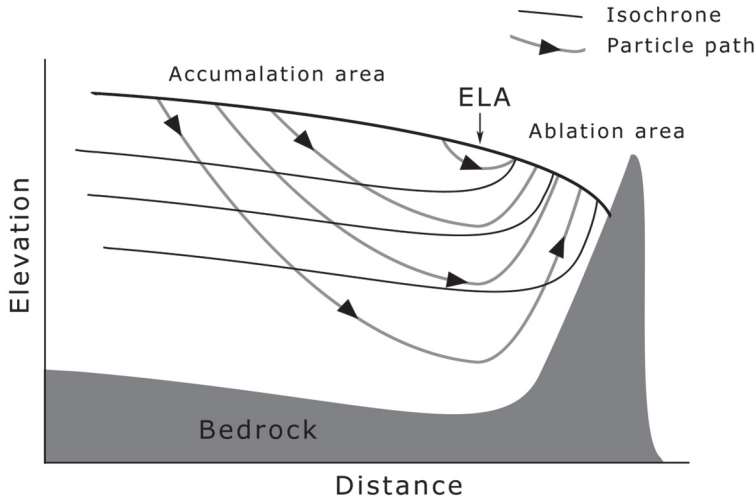


Fig. 3. *A sketch of ice flow in a BIA. The flow direction is from left to right. Equilibrium line (ELA) separates the snow covered accumulation area from the ablation area i.e. the BIA. The isochrones that represent an individual annual layer come up to the surface of the BIA eventually resulting in near-vertical layering. The oldest ice layers are found at the surface at the end of the BIA on right.*

2.3 Ice flow

The definition of the BIAs leads to a net upward component in the ice flow pattern in those areas. Thus, old ice layers originally buried deep in firn flow up to the surface and consequently there is very old ice at the surface of the BIA (Fig. 3).

Ice flow regime is very complex at many large BIAs located at mountain ranges where bedrock topography and outcropping nunataks mix the flow. This is the case e.g. at many locations of Yamato Mountains and Allan Hills (e.g. Moore and others, 2006; Grinsted and others, 2003). On the other hand, current flow regime may also be simple as e.g. in Scharffenbergbotnen (Grinsted and others, 2003; Sinisalo and others, 2004; and 2007). The flow history may also have varied significantly over a climatic cycle at each location which makes dating of surface ice more complicated. The oldest surface ice used for paleoclimate purposes vary from Holocene ice (Sinisalo and others, 2007; this publication) up to about 150 000 years (Popp and others, 2004).

2.4 Meteorology

The formation and maintenance of the BIAs is facilitated by specific meteorological conditions induced by nearby mountains (Bintanja and Van den Broeke, 1995a and

1995b). According to Bintanja and Reijmer (2001), the meteorological conditions over the BIA differ from those over the snow covered surroundings due to

- 1) differences in surface characteristics, such as albedo, extinction characteristics for solar radiation, and surface aerodynamic roughness, between blue ice and snow, and
- 2) differences in topographic setting or nearby orography.

The air over the BIA is warmer and the relative humidity is lower than over a snow site, and these conditions contribute to the significantly higher sublimation rates over BIAs than over snow (Bintanja and Reijmer, 2001). They can be attributed to adiabatic warming of the descending katabatic flow, aided by diabatic warming due to radiation and by entrainment of warm air from aloft into the boundary layer (Bintanja and Reijmer, 2001). The surface winds over BIAs are generally more gusty than those over adjacent snow fields but the average wind speeds are comparable with each other (Bintanja, 1999).

2.5 Surface characteristics

Antarctic BIAs have special surface characteristics such as low albedo, and aerodynamic smoothness in comparison to the surrounding snow and ice covered areas. These characteristics aid formation and maintenance of the BIAs (Bintanja and Van den Broeke, 1995a, 1995b; Bintanja and Reijmer, 2001).

The surface of BIAs is generally rippled (Fig. 4; Bintanja and others, 2001). Bintanja and others (2001) suggest that the only possible mechanism for blue-ice ripple formation is sublimation, occurring whenever there is wind forcing. The orientation of the crests of the ripples is perpendicular to that of the direction of the strongest winds. The measured wave-heights in different BIAs vary between 2 and 10 cm, and the wave-length between 5 and 24 cm (Bintanja and others, 2001; Mellor and Swithinbank, 1989; Weller, 1968). The annual average-wave height does not vary over time. The wave-height increases in the summer as the troughs of the ripples experience more sublimation than the crests, but the increase is compensated in winter (Bintanja and others, 2001).

Dust or tephra bands (Fig. 4) are found in the surface of many BIAs where they usually appear perpendicular to the ice flow (Bintanja, 1999). However, dust bands in the Allan Hills and the Yamato Mountains have been observed to curl back as much as 180° in some cases (Koeberl, 1990). Koeberl (1990) found that the dust bands at the Antarctic BIAs are mostly of volcanic origin and may be correlated with individual Cenozoic volcanoes in Antarctica and sub-antarctic regions. When volcanic eruptions disperse large quantities of volcanic dust over Antarctica, where it falls on snow accumulation areas. It will be buried under new snow layers and incorporated in the ice, and transported to the ablation zones with the ice flow. Such dust bands on the surface of



Fig. 4. *Surface characteristics of a BLA. Dust bands can appear as distinct narrow stripes (left) or as more than metre wide bands at the surface of a BLA. Supraglacial moraines and cryoconite holes are visible on the dust band on the right. Photo: Left: FINNARP/Anna Sinisalo, right: FINNARP/Aslak Grinsted*

the BIAs constitute isochronous layers. Grain size is usually smaller for volcanic debris than bedrock debris.

There are also other possible sources for soluble and insoluble impurities than volcanoes. The most important other sources according to Koeberl (1990) include

- 1) material from subglacial bedrock debris scraped up from the ground by the movement of the glacier,
- 2) cosmic particles falling as micrometeorites or meteorite ablation spherules, and
- 3) continental and marine dust and aerosols transported by wind.

Cryoconite holes indicate melting and they can be found on low altitude BIAs (Bintanja, 1999). They are round-shaped, transparent patches of ice (Fig. 4) that form due to absorption of solar radiation by dark particles or stones, causing their temperature to rise above the melting point (Bintanja, 1999). The stone will slowly sink into the ice until a depth where shortwave heating is diminished and equals conductive cooling. Bintanja (1999) suggests that depth to be a few decimetres.

2.6 Classification of blue ice areas

BIAs can be divided according to their flow regime (Grinsted and others, 2003) into

- 1) open type of BIAs, and
- 2) closed type of BIAs.

This division is relevant to the possible surface-age distribution of the BIA. The ice flow in an open type of BIA is not dammed by mountains, nunataks or bedrock topography but ice flows through the BIA and the oldest layers of ice do not come to the ice surface at all. The dipping angles of the outcropping isochrones are smaller than at the surface of the closed type BIA. Closed type of BIAs are located at mountain ranges where their flow is dammed and the oldest layers of ice will be found in the surface closest to the mountains as if the layers had climbed up the mountain slope (Fig. 3). For example, the Yamato mountains that form the largest known BIA is an open-type of BIA, and Scharffenbergbotnen is a closed-type of BIA.

Bintanja (1999) divided BIAs into four types that were based on the geographical setting and ice flow characteristics of the BIA. This classification of BIAs into Type I-IV was originally presented by Takahashi and others (1992).

- 1) Type I BIAs are associated with mountains protruding through the ice. They are situated in the lee of an obstacle, which acts as a barrier for snowdrift. The length of these BIAs can be estimated to be roughly 50 to 100 times the height of the obstacle relative to the ice surface (Takahashi and others, 1992). This is the most common type of BIA (Bintanja, 1999). Scharffenbergbotnen is an example of the type I BIAs
- 2) Type II BIAs are located on a valley glacier. The descending katabatic winds cause net erosion of the surface and a local divergence of snowdrift, eventually leaving bare blue ice.
- 3) Type III BIAs are located on relatively steep slopes without mountains protruding through the ice. The increasing surface slope accelerates the downslope katabatic winds, causing a divergence of snowdrift transport similar to type II (Takahashi, and others, 1992). The Yamato mountains is of this type.
- 4) Type IV BIAs are situated at the lowest part of a glacier basin. Accelerating katabatic winds in the basin remove the snow from the surface.

Winther and others (2001) divided the BIAs according to their spectral reflectance in satellite imagery into

- 1) melt-induced blue ice areas, and
- 2) wind-induced blue ice areas.

Melt-induced BIAs have generally higher concentration of ice-bound snow crystals at lower elevations than in the wind-induced BIAs due to repeated melt-freeze cycles

(Winther, 1994). They are located on slopes in coastal areas where climate conditions together with favourable surface orientation sustain conditions for surface and near-surface melt whereas wind-induced BIAs occur near mountains or on outlet glaciers, often at higher elevations (Winther and others, 2001). Bintanja's (1999) definition of BIAs (see chapter 2.1.), however, excludes type 1 BIAs as sublimation is the dominant ablation mechanism of a BIA, and it is clear that only the wind-induced BIAs can be useful for paleoclimate studies.

2.7 Dating

The principal problem in interpreting blue ice samples has been dating the ice. Dating of blue ice samples is much more problematic than that of deep cores. The surface age has been estimated by various methods for many Antarctic BIAs. The individual methods, however, do not provide a reliable continuous dating over the surface of a BIA but represent either dating of a specific layer as e.g. dating of tephra layers, or an estimate of the age distribution of the overall surface as in most of the modelling efforts.

Age estimates of the BIAs have been made based on the terrestrial age of meteorites collected from the surface of BIAs (Cassidy and others, 1992; Corti and others, 2003; Delisle, 1993), analysis of radioactive compounds in ice samples (Fireman, 1986; Van der Kemp and others, 2002; van Roijen, 1996), and on dating englacial tephra layers (McIntosh and Dunbar, 2004). Other methods include ice flow modelling using different sets of parameters (e.g. Grinsted and others, 2003), stable isotopic values (Sinisalo and others, 2007), and electrical measurements of blue ice in comparison to the records analysed from well-dated deep cores (Moore and others, 2006). It is clear, that the best results can be obtained by combination of methods as one method alone cannot usually provide an unambiguous estimate.

2.7.1 Meteorites

The terrestrial ages of meteorites found on a BIA can be used as a measure of the age of the surface blue ice. The terrestrial ages of Antarctic meteorites determined using radioactive cosmogenic nuclides have been up to more than two million years (Welten and others, 1995; Scherer and others, 1997) but are usually less than 500 thousand years (Welten and others, 2000).

Meteorites have been found from the surface of many Antarctic BIAs, most of which are located in the Transantarctic mountains (Whillans and Cassidy, 1983; Cassidy and others, 1992; Corti and others, 2003; Delisle, 1993; Welten and others, 2000). Usually the meteorites have fallen on the snow accumulation areas that are much larger than the actual BIAs. Then they are transported englacially to the BIA where they come to the surface along the flow. The meteorites remain at the surface as ice around them ablates away. Thus, the blue ice around the meteorites is of same age or younger than the

meteorites, and the meteorite age provides the upper limit for the age of the blue ice around it assuming no direct infall of meteorites to the BIA's surface.

The accuracy of dating meteorites is still about 30 ky at its best (Welten and others, 2000). The main uncertainty in dating surface blue ice using meteorite terrestrial ages, however, is due to possible past changes of ice flow. Goldstein and others (2004) suggested that the old meteorites found on the surface of a BIA have experienced a multi-stage history of ice accumulation and/or ice flow and the ice found at the surface of the BIA is significantly younger than the youngest meteorites dated in the area (Nishizumi and others, 1989). In some cases, the meteorite concentrations have also been reported to form by direct infall to the BIA surface (Huss, 1990). Then the terrestrial age of meteorites is a measure of the minimum age of the BIA since it gives an indication of how long the BIA has acted as a meteorite accumulation area as the meteorites have not ever been buried in snow. Small meteorites may also have been blown downstream from their original place by wind, and as a result, meteorites accumulated on blue ice are younger than the ice around them.

No meteorites have been found in the mountainous BIAs in Dronning Maud Land. The possible explanations for the lack of meteorites are:

- 1) young age of the BIAs (Sinisalo and others, 2007; this publication);
- 2) meteorites may have melted back into the blue ice forming cryoconite holes (Fig. 4) during the high insolation days during summer; or
- 3) meteorites may be “hidden” by supraglacial debris on the surface of a BIA (Fig. 2; Hätterstrand and Johansen, 2005).

2.7.2 Radiodating

Van Roijen (1996) developed a method for dating blue ice by measuring ^{14}C concentrations from air trapped in the ice. This was originally made by Fireman and Norris (1982). In Van Roijen's method, measured ^{14}C depth profiles in blue ice are translated into carbon ages with a correction made for in situ produced ^{14}C . The radiocarbon ages can be further converted to calendar ages using a radiocarbon calibration curve by Reimer and others (2004). The first ^{14}C ages had large uncertainties of up to several thousands of years (Van Roijen, 1996). Van der Kemp and others (2002) improved the method and managed to decrease the uncertainty of a carbon age to ± 400 years. This method, however, requires large ice samples and does not provide an age span but an average age for the ice analysed.

2.7.3 Isotopic dating

The ratios of heavy to light atoms of both oxygen and hydrogen in ice and snow, expressed as $\delta^{18}\text{O}$ and δD values, respectively, provide a simple method to determine whether the samples at a given site were deposited during a glacial or an interglacial sim-

ply from the isotopic composition. Different climatic periods have different signatures in stable water isotopes (e.g. Petit and others, 1999), and a rapid, relatively large change of in δD or $\delta^{18}O$ in Antarctic ice is an indicator of a change between interglacial and glacial climates (e.g. Masson and others, 2000).

The isotopic analysis methods and corrections needed to compare the isotopic values of ice and snow samples of different ages are discussed in section 3.6, and the paper by Sinisalo and others (2007). The limitation of this method is that it can only be used to make the division between samples of glacial and interglacial origin as described above.

2.7.4 Dating of tephra layers

Volcanic ash or tephra layers have been radioisotopically dated by using uranium-series and cosmogenic nuclide age data collected from the surface of BIAs in the Allan Hills (Goldstein and others, 2003; Fireman, 1986), Yamato Mountains (Nishiizumi and others, 1979), and at Mt. Moulton (Wilch, 1999; McIntosh and Dunbar, 2004) (see Fig. 1 for the locations). In addition, the grain size analysis of volcanic ash fragments can provide information about the distance to the source area (Nishio and others, 1984)

There are problems, however, in this method as the tephra bands tend to disappear over hundred metre scales, and it may be difficult to follow the tephra layers from a large enough deposit to date to the place where a core is taken. Large differences in results of uranium-series dating were also found for similar blue ice samples from Allan Hills (Goldstein and others, 2004; Fireman, 1986). The reasons are not entirely clear but the main difference appears to be in sample processing (Goldstein and others, 2004).

2.7.5 Geomorphology

The supraglacial moraine structures can provide useful information about the age of a BIA. Hättestrand and Johansen (2005) studied moraines in Scharffenbergbotnen BIA, and found that supraglacial moraines were deposited during last glacial maximum (LGM). They concluded that the survival of these moraines in the area until present day indicates that there was a local ablation centre, and probably a BIA in Scharffenbergbotnen at LGM. The moraines on the slopes of surrounding nunataks suggest that the surface elevation of the BIA has been higher during last glacial maximum, and striae and gouges in the outcropping bedrock indicate past ice flow directions (Hättestrand and Johansen, 2005). Similarly, old supraglacial moraines and ice flow indicators in the bedrock in other BIAs can be used for reconstructing the former ice flow, and existence, surface elevation, and extent of the BIA.

2.7.6 Ice flow modelling

First modelling efforts on BIAs were made to explain the meteorite findings on the

surface of BIAs. Nasure and Hashimoto (1982) made a simple flow model to date a BIA upstream of a nunatak in Yamato Mountains based on the continuity equation (Nye, 1953). Azuma and others (1985) produced a much more sophisticated model for a South Yamato BIA near another nunatak, and Whillams and Cassidy (1983) modeled the flow in Allan Hills BIA with similar assumptions. Since then various flow models have been applied for Antarctic BIAs (e.g. Van Roijen, 1996; Spikes, 2000).

In this work, we use the model by Grinsted and others (2003). It is a volume conserving model which assumes constant ice sheet geometry over time, i.e. steady state flow. In addition to Scharffenbergbotnen, this model has been applied to Allan Hills (Grinsted and others, 2003) and to Yamato Mountains (Moore and others, 2006). The modelling efforts of Scharffenbergbotnen show that it is important to combine other geophysical data with the modelling (Grinsted and others, 2003; Sinisalo and others, 2007).

2.7.7 Combination of methods

It is clear that the best confidence in dating blue ice can be reached by combining many dating methods together. Generally, this means tuning flow models with other methods. First, a flow model can be used to gain an initial expectation of plausible surface age distribution, vertical age span, and the source region of the ice. Other dating methods, such as radiocarbon dating, meteorite terrestrial ages, or tephra layer dating should be used to check on the model plausibility in the areas where these kinds of data are available.

After adjusting the ice flow model to match with the other dating methods, high-resolution records of ice chemistry, gas composition, and isotopic values in ice, or electrical stratigraphy, can be used for matching the data with records from other ice cores. However, the forest of peaks in such records, and the flexibility in surface age and age span means that the method must be used with caution and strong constraints (Moore and others, 2006). Ice crystal size data have also been found useful for confirming an age span for a blue ice core (Moore and others, 2006).

Various data available can be used with the model in an iterative way to estimate the age distribution in a BIA. The flow modelling can also provide other useful information about the study area, such as the surface age distribution along the flowline over the whole BIA, temporal changes in the size of the BIA, and ice flow velocities, and constrain modeled elevation changes and accumulation patterns over the region (Moore and others, 2006; Sinisalo and others, 2007).

2.8 Blue ice areas and climate

The relations between blue ice extent and climate are not straightforward. Blue ice extent has varying sensitivity to climatic parameters, and climate change will affect the

processes creating blue ice in several ways (Orheim and Lucchitta, 1990). Changes in air temperature will affect energy available for surface ablation, and changes in precipitation, and wind direction and strength will affect accumulation (Orheim and Lucchitta, 1990).

It is clear that large reductions in exposed BIA are more likely than large increases, and that increasing a BIA can be expected to take a longer time than decreasing it (e.g. Bintanja, 1999; Brown and Scambos, 2004). As a BIA cannot expand onto a nunatak area, aerial increase must take place into adjacent snow fields by the relatively slow processes of either dry snow metamorphosis, or exposure of sub-surface ice (Orheim and Lucchitta, 1990). Additionally, present day BIAs above 2000 m have remarkably similar ablation rates (Bintanja, 1999), which implies that changing climate does not affect ablation rates of high elevation BIAs greatly. A decrease of the BIA, on the other hand, can happen quickly as a result of increased accumulation or possibly of changed wind patterns (Bintanja and Van den Broeke, 1995a). Seasonal, and even annual variations in BIA extent due to snow accumulation events may be large and significant area reductions may occur (Brown and Scambos, 2004). Minimum in the BIA extent is reached in winter (Brown and Scambos, 2004). Snow may accumulate over a long time period but then rapidly removed by a large storm in a few days.

When a BIA has formed, it tends to persist due to two conservative feedback processes. These processes may enable BIAs to persist and possibly expand in the downwind direction. Firstly, the relatively low albedo of the blue ice increases the absorption of solar radiation, which increases the energy available for sublimation. Secondly, the smooth blue ice surface prevents drifting snow from becoming attached, resulting in zero accumulation in the longer term. (Bintanja, 1999)

Although BIAs seem to be rather stable under different climate regimes due to the feedback mechanisms described above, climate change also affects ice flow patterns and may even change the ice flow direction in some areas. This can have a significant influence on the BIA extent in a long term (Bintanja, 1999; Sinisalo and others, 2007).

There have been attempts to estimate areal changes in individual BIAs (Brown and Scambos, 2004; Spikes, 2000; Orheim and Lucchitta, 1990), and the total extent of Antarctic BIAs using satellite images (Winther and others, 2001). Increasing accumulation leading to a general decrease in blue ice can be easily detected, whereas increased ablation is more difficult to observe and requires more permanent change before it will be noticed. Since the possible permanent changes in blue ice extent are very slow and satellite images exist only over some decades, there has not been any change observed that could be interpreted as a climate signal. However, satellite imagery shows potential to be a useful tool in the future.

3 METHODS

During this work we have performed various geophysical measurements on BIAs in DML, Antarctica. We used differential GPS, and ground penetrating radar (GPR) for ice flow, and mass balance studies. The relevant details of the methods, such as measuring parameters, and equations applied, are provided in the papers I-IV. The data were used in an ice flow model by Grinsted and others (2003). Firstly, the model was used with higher resolution for blue ice/firn transition zone in Scharffenbergbotnen BIA (Sinisalo and others, 2004), and secondly, it was adjusted with other dating methods and applied in the whole Scharffenbergbotnen BIA (Sinisalo and others, 2007). Mass balance and flow modelling studies were made to estimate the stability of the BIA. The GPR studies of internal structure of accumulation areas, and differential GPS measurements of the ice flow were made to learn about the dynamics of the BIAs, and to estimate the surface age distribution of the blue ice with flow modelling and isotopic data of surface blue ice.

3.1 Precise GPS

We used two antenna-receiver systems in all GPS measurements (Javad Positioning System with a Hiper antenna-receiver or Legacy E antennas and receivers). A base station was established on a fixed point on bare rock in the vicinity of the study areas (Fig. 5),

Fig. 5. *JPS Legacy E antenna on a stake (left) and the base station with a Hiper antenna-receiver placed on a fixed point on the bedrock (right). The base station was connected to a solar panel. Photos: FINNARP/Anna Sinisalo.*



and all the other positions were then measured relative to the fixed point.

The GPR technique involved driving the profile lines on a snowmobile carrying a differential GPS. In addition to the positioning of the GPR profiles, the differential GPS was also used for static stake measurements of the horizontal ice surface velocity (Sini-salo and others, 2003b; Sinisalo and others, 2004), kinematic surface profiling of the BIAs, and to determine exact positions of various ice and snow sampling points.

The recording time for static point measurements varied from 2 minutes up to 15 minutes. The accuracy of the relative measurements is in order of millimetres. The main error source in the stake measurements was the accuracy of measuring the stake height, that we estimated to be ± 0.5 cm.

3.2 Ground penetrating radar (GPR)

We used a commercial RAMAC GPR (Malå Geoscience) with 800 MHz, 100 MHz, and 50 MHz antennas (Sinisalo, 2003b; 2004). The radar technique involved driving the profile lines on a snowmobile carrying a differential GPS. The radar transmitter and receiver antennas for the 50 MHz measurements were mounted on a non-metallic sledge, which was pulled 7 m behind the snowmobile (Fig. 6). The radar control unit and computer were mounted on the snowmobile together with the roving GPS receiver. The 800- and 100-MHz antennas were shielded units and could be pulled closer behind the snowmobile – the 100-MHz system was pulled about 5 m behind in its own sealed housing, the 800-MHz system was pulled about 2 m behind the snowmobile using rigid struts to keep it at a fixed distance.

GPR data were collected on a laptop computer. Post-processing of the data was done using the Haescan program (Roadscanners Oy). Amplitude zero-level correction was applied, background noise was removed and vertical high pass and low pass filtering in time domain was performed.

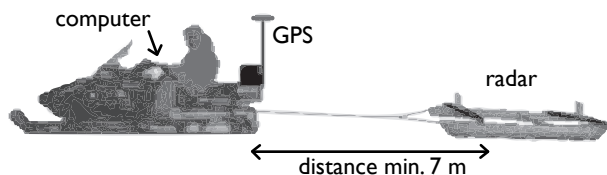


Fig. 6. *Setting of GPR measurements performed with the 50 MHz antennas.*

3.3 Mass balance studies

Stake measurements are the simplest way to determine the mass balance at a location (Sinisalo and others, 2003a). The disadvantage is that a stake represents a point measurement and mass balance can strongly vary over short distances.

The stake measurements were supplemented by ground penetrating radar (GPR) studies (Sinisalo and others, 2003b; Sinisalo and others, 2004). They can be used to integrate the separate short time series from stake data into more reliable mass balance profiles. First, the radar isochrones tracked with the GPR must be dated to study the mass balance variability. We modeled the densification rate and age-depth and radar travel-time depth relations by using the densification model of Herron and Langway (1980) and an empirical equation by Robin (1975) (Sinisalo and others, 2003b; 2004). A correction for strain thinning of layers with depth was made in order to calculate the age of the isochrones at each depth by using the simple model by Nye (1963). The measured GPR mass balance profiles were then extrapolated to produce a mass balance map over the study area (Sinisalo and others, 2004).

3.4 Dip angles of isochrones and surface age gradient in BIAs

The GPR was used to determine the surface age gradient of the blue ice and to study the dip angles of the isochrones at the firn/blue ice transition zone (Sinisalo and others, 2004). The dating method is described in the previous section and in more detail in Sinisalo and others (2004). The GPR isochrones were followed from the accumulation area to the firn/blue ice transition zone where these layers come up the surface. The GPR data were migrated to obtain true angles for the dipping horizons assuming a constant permittivity for the firn pack above the layers. The surface-age distribution in the firn/blue ice transition zone was determined by following three dated GPR isochrones to the surface.

3.5 Blue ice, firn, and snow samples

Blue ice cores can give a better temporal resolution of paleoclimatic data than deep ice cores from the low accumulation continental interior due to their different kind of geographic location and flow history than in-situ accumulated and horizontally layered deep cores (Moore and others, 2006; Sinisalo and others, 2007). We collected a 101-m long horizontal ice core from the surface of a BIA (Sinisalo and others, 2007). This ice core was collected by electric chain saws along the flowline in austral summer 2003/2004. In this work, we also use results of isotopic analysis of previously collected shallow blue ice cores, firn samples and a 52-m vertical blue ice core drilled by a Dutch field party in 1997/1998 (Bintanja and others, 1998).

3.6 Isotopic analysis

We made use of the ratios of heavy to light atoms of both oxygen and hydrogen expressed as $\delta^{18}\text{O}$ and δD values, respectively. $\delta^{18}\text{O}$ is defined as the deviation of a sample from the composition of the Vienna Standard Mean Ocean Water (V-SMOW) standard:

$$\delta^{18}\text{O} = f \left[\left[\left(\frac{{}^{18}\text{O}}{{}^{16}\text{O}} \right)_{\text{sample}} / \left(\frac{{}^{18}\text{O}}{{}^{16}\text{O}} \right)_{\text{v-smow}} \right] - 1 \right] \quad (1)$$

The $\delta^{18}\text{O}$ and δD are both presented with respect to the international consensus VSMOW-SLAP scale (Gonfiantini, 1984). On this scale, $\delta^{18}\text{O}$ is defined as the deviation of a sample from the composition of the Vienna Standard Mean Ocean Water (VSMOW) calibration material in which the laboratory-specific normalisation factor f is chosen such that an analysis of Standard Light Antarctic Precipitation (SLAP) would yield the assigned value of -55.5‰. Similarly, the assigned value for δD is -428 ‰. The normalisation factor f is close to unity, but still its value, and therefore the procedure matters especially for isotopically light samples, such as the Antarctic ice in this study.

The $\delta^{18}\text{O}$ analyses and δD analyses of the blue ice and firn samples were made in the Centre for Isotope Research, University of Groningen, the Netherlands, and at the University of Technology, Tallinn, Estonia. Details of the analyses are given in Sinisalo and others (2007).

When comparing isotopic values of samples of different ages, we corrected the measured values for elevation changes in the past, and the change in the isotopic composition of ocean surface waters in the source area due to the deglaciation (Sinisalo and others, 2007). For example, the change of isotopic composition of surface sea water due to deglaciation $\Delta\delta^{18}\text{O}_{\text{SW}}$ was about +1.1‰ at LGM compared with the present value (Labeyrie and others, 1987), and the decrease in surface elevation of 200-250 m in Scharffenbergbotnen after the last glacial maximum (Hättestrand and Johansen, 2005) corresponds to a change of 1.2-1.5‰ in $\delta^{18}\text{O}$ using the present day altitudinal lapse rate for $\delta^{18}\text{O}$ values (Isaksson and Karlén, 1994). These corrections are especially important when the differences in isotopic values are not large, and they are used to estimate past temperatures.

We used the present-day spatial dependence of isotopic fractionation on temperature from Isaksson and Karlén (1994) as a surrogate of the temporal dependence to interpret isotopic profiles (e.g. Delaygue and others, 2000). This allowed us to estimate the relative temporal temperature changes in the study area. Details of the calculations are presented in Sinisalo and others (2007).

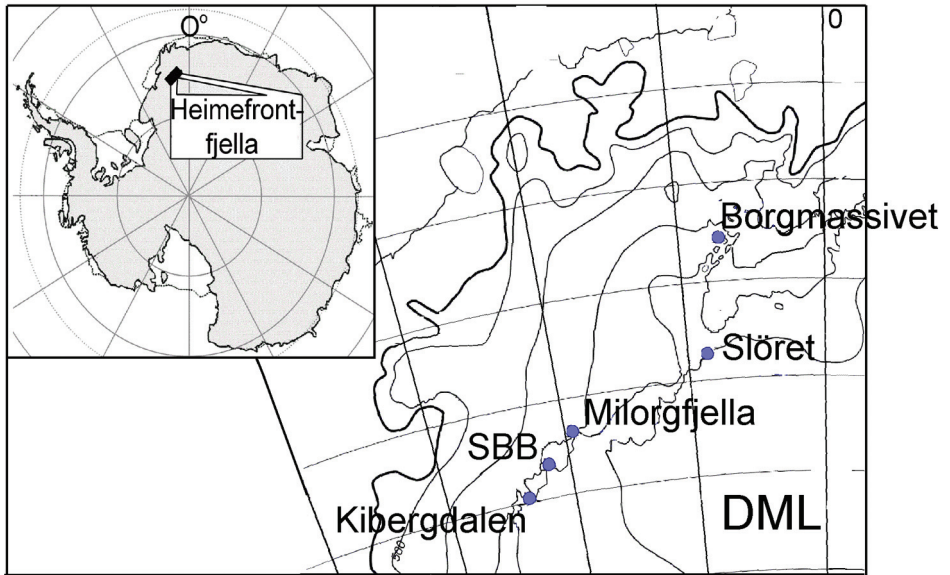


Fig. 7. Locations of five BIAs in Dronning Maud Land (DML) that were preliminarily studied during this work. Kibergdalen, Scharffenbergbotnen (SBB), and Milorgfjella are located in the Heimefrontfjella mountain range. Slöret is in Kirwanveggen mountain range and Borgmassivet is a BIA on a lee side of a mountain area having the same name.

4 STUDY AREA

For this work, we visited five BIAs located in the mountainous areas of eastern DML (Fig. 7). Preliminary study of the internal dynamics of these areas was made with GPR, and several snow/firn and blue ice samples were collected from these areas. Based on the preliminary studies, we chose Scharffenbergbotnen (Fig. 7) for the main focus as it is the best-studied BIA from the glaciological point of view, and it has a relatively simple flow regime (Sinisalo and others, 2004). In addition, we discuss GPR and $\delta^{18}\text{O}$ data collected from a high-elevation BIA in Slöret (Fig. 7) as reference data in the Chapter 5.

Scharffenbergbotnen is a closed-type BIA (Fig. 8; Grinsted and others, 2003), and it represents type I BIA in the classification of BIAs by Takahashi and others (1992) as mentioned earlier. Slöret is an open-type BIA located at the edge of the Antarctic plateau (Fig. 8) at about 2300 m a.s.l. where the ice sheet flows over the Kirwanveggen mountain range. Slöret is of type III, and the other BIAs visited during the work are of type I (Fig. 7) according to the classification by Takahashi and others (1992).

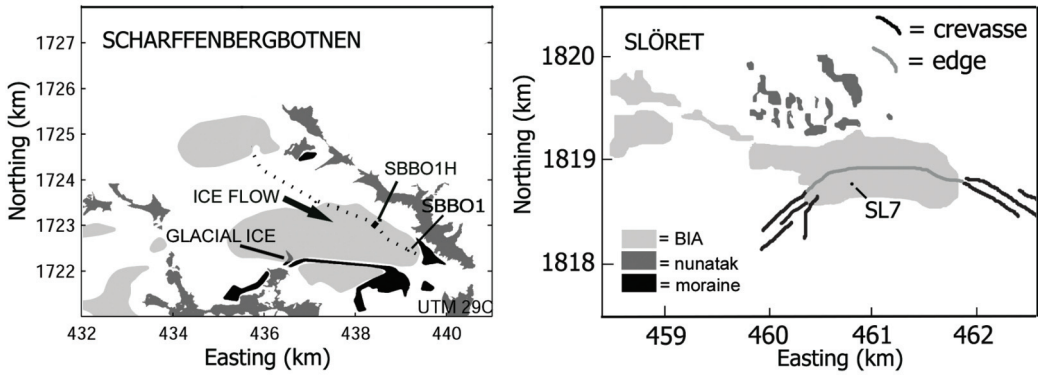


Fig. 8. *Left: Scharffenbergbotnen BLA. The 101-m horizontal ice core collected (SBB01H), 52-m vertical blue ice core (SBB01), the ice flowline used in the modelling (dotted line), and the place where ice from glacial period was found are marked. Right: Slöret BLA. The edge of the Antarctic plateau and the biggest crevasses are marked. A 7-m blue ice core (SL7) is marked with a dot. The ice flow velocities in Slöret BLA could not be measured as they were too low to be significant during the two-week measuring period. Based on surface slopes we can estimate that the main flow direction is from inland towards the edge (from bottom to top in the figure).*

5 RESULTS AND DISCUSSION

5.1 Mass balance and dynamics of the BIAs (Papers I-IV)

Surface mass balance observations in Scharffenbergbotnen valley over a 14-year time period by direct stake measurements showed large spatial and temporal variations in the net balance without any clear trend (Sinisalo and others, 2003a). We found marginally significant increases in snow accumulation, and in ablation in the blue ice area farthest from the equilibrium zone (both at the 95% confidence level). However, the observed changes in mass balance gradient are small, especially when compared with large changes observed elsewhere in Antarctica even relatively close to the BIA.

To study mass balance over longer time periods, we compared three different GPR antenna frequencies (50, 100, and 800 MHz) for accumulation studies within the uppermost 50 m of the snow pack in Antarctica. We found that the lower frequencies are particularly useful when determining the accumulation rates further in the past or over longer time periods (Sinisalo and others, 2003b). The advantage of using the higher frequency antennas is the better resolution and capability to follow the near-surface layers. However, the low frequency signals have much greater depths of penetration and they

tend to show only the strongest and most continuous reflectors that are useful when following the individual layers (Sinisalo and others, 2003b; 2004).

With the GPR, large areas can be covered quickly, and the temporal and spatial variability in snow accumulation obtained. Moreover, the accumulation survey can be made even in the absence of deep ice cores to directly date the radar layering (Sinisalo and others, 2003b). In that case, however, it is important to bear in mind the sensitivity of the age model to the rather large interannual variability of precipitation and the snow density. Using the radar layering proved to be a much better method of estimating accumulation rate over a large area than a usually short series of stake measurements.

Sinisalo and others (2004) found that the surface mass balance in Scharffenbergbotnen valley is negative, and the inflow through the northwestern gate should balance it if the valley was in steady state. However, the recent observations do not support such a high inflow (unpublished data), and the net mass balance may remain negative in the valley. Our data indicate that the Scharffenbergbotnen BIA used to be much smaller than it is today (Sinisalo and others, 2007). Previous studies show that the surface of the BIA used to be 200-250 m higher at LGM (Hätterstrand and Johansen, 2005), and it is likely that lowering of the ice surface in the valley started when the surface of the surrounding ice sheet reached a point where the outcropping mountains made a barrier to ice inflow over the side walls of the valley. There is no evidence, however, on when the lowering of the ice surface in Scharffenbergbotnen actually started.

5.2 Paleoclimate data (Paper IV)

Only few blue ice cores have been studied for paleoclimatic purposes (Table 1). We analysed a 101-m long continuous horizontal stable isotope record from the surface of the Scharffenbergbotnen BIA (SBB01H in Fig. 8) covering about a 500-year time period (Sinisalo and others, 2007). Before this work, the only horizontal stable isotope record from a BIA was extracted from Mt. Moulton (76° S, 135° W, 2800 m a.s.l, Fig. 1) covering about 140 000 years (Popp and others, 2004). However, that record does not include the Holocene since that part of the BIA was covered by snow when sampling was done. Although the surface ice may be hundreds of thousands of years old at some Antarctic BIAs the blue ice samples dealt with in this work represent mostly Holocene ice (10 500 BP to present) that was formed after the last transition between glacial and interglacial periods (Sinisalo and others, 2007).

The isotopic analysis of the SBB01H shows that BIAs can provide high resolution paleoclimate data that cannot be extracted from anywhere else (Fig. 9; Sinisalo and others, 2007). It should be noted, however, that the high resolution sample of the SBB01H was only 0.6 m long.

Table 1. Details of Antarctic blue ice cores. The drilling sites are indicated in Fig. 1 with the codes given in the first column under the name of the core.

Name	Location	Depth/ length (m)	Elev. (m a.s.l.)	Age (a BP)	Analyses	Reference
SY core (YM)	72°05'S 35°11'E	2150	101 (ver.)	55 000 – 61 000	Gas, chemistry, iso- topes	Moore and others, 2006
SBB01 (SBB)	74°35'S 11°03'W	1173	52 (ver.)	10 500 (+700, -300)	Isotopes	Sinisalo and others, 2007
SBB01H (SBB)	74°34'S 11°04'W	1187	100 (hor.)	4426 ±215*	Isotopes	M. Sigl and M. Schwikowski, Paul Scherrer Institut, personal communica- tion
Mt. Moulton (Mt.M)	76° S 135° W	2800	600 (hor.)	10 000 – 15 000	Gas, chemis- try, isotopes	Popp and others, 2004
MBI#1 (Mt.M)	76°04'S, 134°42'W	2820	~30 (ver.)	115 000 – 135 000	Gas, isotopes	Custer, 2006

*Age in the middle of the 100-m blue ice core. The age span of SBB01H is estimated to be about 500 years (Sinisalo and others, 2007).

In addition, we analysed the isotopic values from several other blue ice cores, and firn samples in Scharffenbergbotnen (Sinisalo and others, 2007). The differences in stable isotope values between blue ice and firn samples imply that the modern climate is about $1.0 \pm 0.3^\circ\text{C}$ warmer than the early Holocene optimum climate in Scharffenbergbotnen. Furthermore, the 10 500 year old SBB01 from the early Holocene (Fig. 8) originates from a warmer time period than SBB01H from mid Holocene. This work also emphasises that geophysical data must be combined with ice core analysis to get a reliable paleoclimate record.

5.3 Dating of surface blue ice (Paper III and IV)

We estimate the horizontal age gradient and the age of our blue ice samples in Scharffenbergbotnen BIA by adjusting a flowmodel (Grinsted and others, 2003) to match the radiocarbon ages (Van der Kemp and others, 2002; Van Roijen, 1996). The main limita-

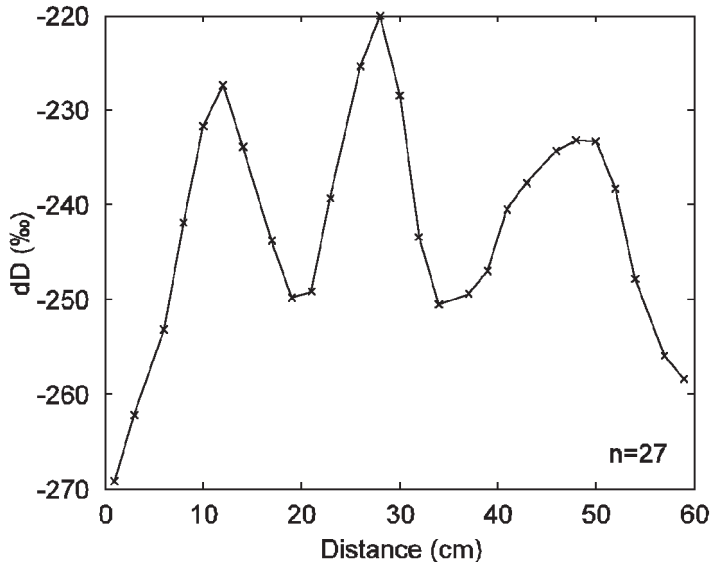


Fig. 9. Clear annual cycles in the high resolution δD analysis of the horizontal ice core SBB01H (Fig. 8). The annual layer thickness at mid-Holocene found at the surface of Scharffenbergbotnen BLA is about 20 cm of ice that corresponds to 160 mm w.e. (Sinisalo and others, 2007).

tion of the modelling was that temporal changes in geometry of the BIA could not be modelled. However, figure 10 shows that the modelling results are rather consistent with the age gradient estimated by following isochrones with GPR (Sinisalo and others, 2004), and high resolution isotopic analysis (Fig. 9; Sinisalo and others, 2007). The power spectrum of the high resolution isotopic analysis of SBB01H (Fig. 9) suggests a horizontal age gradient of about 5.4 a m^{-1} (Sinisalo and others, 2007), and the surface age gradient determined by dating of internal radar reflection horizons close to the current blue ice/snow transition zone along the flowline is about $3\text{-}6 \text{ a m}^{-1}$ (Sinisalo and others, 2004). Very recent ^{14}C dating of the SBB01H give an age of 4426 ± 215 years for the middle part of the horizontal ice core (Fig. 9; Michael Sigl, Margit Schwikowski, Paul Scherrer Institut, personal communication) that supports our dating based on the horizontal age gradient obtained from the high resolution isotopic analysis of SBB01H (Fig. 10), and indicates that the age gradient between SBB01 and SBB01H is fairly linear.

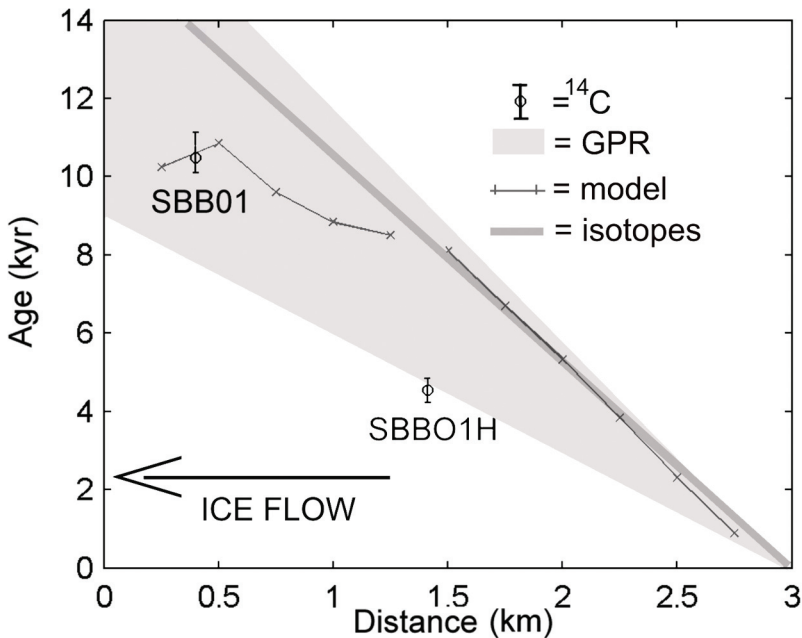


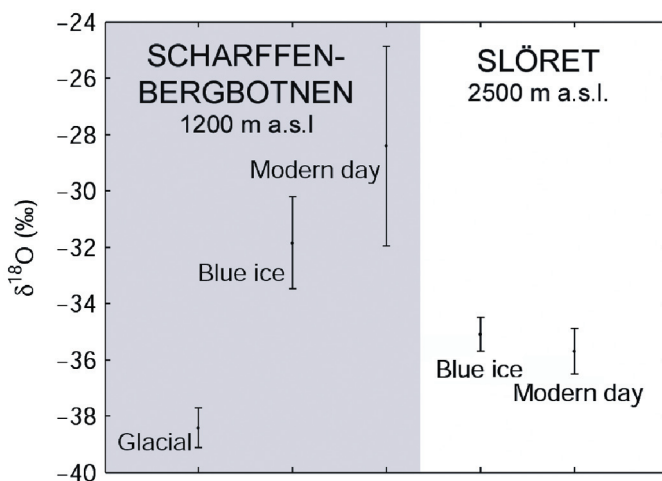
Fig. 10. Surface age relationship along the flowline of Scharffenbergbotnen (marked in Fig. 8). Horizontal age gradient suggested by the power spectrum of the high resolution isotopic analysis of SBB01H (Fig. 9; Sinisalo and others, 2007; gray line), and by dating of internal radar reflection horizons close to the current blue ice/snow transition zone along the flowline (Sinisalo and others, 2004; light gray). The model output with a linearly changing temporal and spatial surface velocity and accumulation rate reaching the present values in 11 000 years. The model was adjusted to match with the ^{14}C age of a vertical blue ice core (SBB01). The error bars for SBB01 are calculated using a radiocarbon calibration curve by Reimer and others (2004). The middle part of the SBB01H was very recently ^{14}C dated to 4426 ± 215 years BP (Michael Sigl, Margit Schwikowski, Paul Scherrer Institut, personal communication) The horizontal distance is measured starting from the bottom of the valley. The SBB01 (Table 1) is located at $x = 400$ m and the SBB01H at $x = 1400$ m. See Sinisalo and others (2004), and Sinisalo and others (2007) for more details.

5.4 On the age and stability of the BIAs (Paper IV)

We introduce a fast and easy way to make a first estimation of the age of a BIA. We only need a limited set of snow/firn and blue ice samples for isotopic analysis. Snow/firn samples from the accumulation area of a BIA represent the modern day isotopic values and isotopic values of the surface blue ice samples indicate whether the BIA originates from glacial or interglacial period. We know the isotopic variability of ice and snow in Holocene (e.g. Epica Community members, 2006), and can compare that with the measured difference between the samples. We have to take into account possible changes in the ice sheet thickness in the last glacial-interglacial cycle especially in the low elevation mountainous areas where the variations in the ice sheet thickness have been greatest (Pattyn and Declerq, 1998).

Based on the isotopic analysis, we found that the major part of the surface ice of two mountainous BIAs in Scharffenbergetotnen, and Slöret, Kirwanveggen mountain range (Fig. 8), are of Holocene origin (Fig. 11).

Fig. 11. The $\delta^{18}\text{O}$ values from the Scharffenbergetotnen valley (left) and Slöret (right). The modern day values are measured from snow/firn samples collected in the accumulation areas of the BIAs. The location of the blue ice sample from Slöret is marked in Fig. 8 (SL7). Glacial ice was only found in Scharffenbergetotnen showing clearly lower $\delta^{18}\text{O}$ values than the modern day samples (Sinisalo and others, 2007).



Our study supports the idea, that the changes in ice sheet thickness control the existence of the BIAs in the mountainous areas (Sinisalo and others, 2007) as also suggested by Bintanja (1999). The ice sheet elevation changes at the glacial termination are likely to have been most pronounced in the low elevation nunatak areas (Pattyn and Declair, 1998). The surface of the major part of the East Antarctic plateau ice sheet may have been about 100 m lower (Ritz and others, 2001; Pattyn, 1999; Jouzel and others, 1989), but in some places hundreds of meters higher in the last glacial than at present (Näslund and others, 2000; Hättestrand and Johansen, 2005). We found that the decrease of the surrounding ice sheet elevation after the LGM enabled Scharffenbergbotnen BIA to grow (Sinisalo and others, 2007). Most of the surface ice in the area is of Holocene origin although it is evident that there was a BIA in Scharffenbergbotnen at the last glacial maximum (LGM) in agreement with Hättestrand and Johansen (2005) but it was much smaller than today (Sinisalo and others, 2007).

Based on the $\delta^{18}\text{O}$ analysis, the high-elevation BIA in Slöret also originates in Holocene (Fig. 11). It is plausible to assume that a decrease of the ice sheet elevation after LGM is also responsible for the formation of the BIA in Slöret although the mechanism of its formation is different from Scharffenbergbotnen. Delisle and Sievers (1991) found in their radio-echo sounding study in Allan Hills that BIAs can form if ice thickness is reduced to about 350 m or less. Our GPR results show that the current thickness of the Slöret BIA varies between 100 and 350 m. The ice flow over the nunataks must have slowed down as the ice sheet elevation decreased after LGM allowing a BIA to form. Similar condition is likely to be required for all open-type of BIAs.

Bintanja (1999) suggested that many of the type I BIAs currently existing in Dronning Maud Land did not exist during at LGM. He found that the height of the outcropping mountain in comparison to the ice surface height seems to be a critical variable that has a large effect on the temporal variations in the extent of a type I BIA, as a thickening of the ice sheet leading to submergence of a nunatak will tend to make a type I BIA disappear. Our results show that also the type III BIAs can be sensitive to the changes in the ice sheet thickness. The area covered by blue ice and the number of individual BIAs vary mainly on an ice sheet thinning-thickening timescale. It is also likely that the BIAs accompanying the highest nunataks being the most stable ones (Bintanja, 1999).

Interestingly, radar internal reflection analysis in central East Antarctica in the foreground of the Transantarctic Mountains (Fig. 1) suggests that ablation may have been more prevalent during glacial periods than in present (Siegert and others, 2003). This indicates that in this part of East Antarctica more and larger BIAs had existed in the last glacial. This agrees with an overall Holocene increase in elevation of the East Antarctic ice sheet due to increased Holocene accumulation rates (Ritz and others, 2001), and highlights the differences between the ice sheet elevation history in the mountainous areas of Dronning Maud Land and in central East Antarctica and Transantarctic mountains.

5.5 Suggestions for future studies

In order to reach better accuracy for the surface age gradient over the whole BIA in Scharffenbergbotnen, more high resolution surface blue ice samples are needed for isotopic analysis. The length of the high resolution section from SBB01H is only 60-cm long (Fig. 9), and further analysis must be made to determine whether the surface age gradient remains constant over the whole BIA as suggested by the flow model (Grinsted and others, 2003; Sinisalo and others, 2007). A continuous 2.6 km long horizontal blue ice core was recovered for this purpose from Scharffenbergbotnen in austral summer 2006/07 but at this point we have no results

The isotopic dating method can be used to make an easy and quick estimate of the age of BIAs on glacial-interglacial timescales. For this method, only a few samples from the surface of the BIA and from the surrounding accumulation area are needed. This is a simple method to make the age estimate of a specific BIA.

The conditions at the glacier bed should be further studied in the BIAs in mountain ranges. It is still unclear whether the bed of such BIAs are frozen or not. The surface velocities are not necessarily directly related to creep flow alone. The mountain BIAs are situated in the area of the cold/warm transition at the bed as the ice sheet is cold based on the Antarctic plateau, while the ice is at the pressure melting point downstream of the mountains bordering the East Antarctic ice sheet (Huybrechts, 1992). This is essential for modeling the evolution of BIAs.

The dynamics of the Antarctic ice sheet can be studied using satellite image analysis of BIAs. Dated layers in deep ice cores may be geochemically correlated with tephra found in BIAs. Correlation of individual tephra layers, or sets of layers, in BIAs will also allow a better understanding of the geometry of the ice flow. The paleoclimate record obtained from surface blue ice samples can be extended over wide geographical areas, though at low resolution, by using satellite and aerial photographic images. This can be made by identifying and dating visible horizons on BIAs using the stratigraphic records from ice cores.

Although the overall changes in the BIA extent seem to be slow, the possible areal changes in individual BIAs, and in the total extent of Antarctic BIAs should be continued to be monitored by satellite image analysis.

BIAs located in different sectors close to Southern Ocean can also provide valuable information about the last glacial transition, as the Southern Ocean may trigger the transition into an interglacial mode of circulation (Knorr and Lohmann, 2003). Detailed paleoclimate data should be collected from the surface of the many BIAs that are much closer to the ocean than traditional deep coring sites.

6 REFERENCES

- Azuma, N., M. Nakawo, A. Higashi, and F. Nishio, 1985. Flow pattern near Massif A in the Yamato bare ice field estimated from the structures and the mechanical properties of a shallow ice core, *Mem. NIPR, Spec. Iss.* 39, 173-183.
- Bintanja, R., 2000. Surface heat budget of Antarctic snow and blue ice: interpretation of temporal and spatial variability. *J. Geoph. Res.*, vol. 105, no. D19, 24,387-24,407.
- Bintanja, R., 1999. On the glaciological, meteorological, and climatological significance of Antarctic blue ice areas. *Rew. Geophys.*, 37,3, p. 337-359. (1999RG900007).
- Bintanja, R., and C.H. Reijmer, 2001. Meteorological conditions over Antarctic blue-ice areas and their influence on the local surface mass balance. *J. Glaciol.*, 47 (156), 37-50.
- Bintanja, R., C.H. Reijmer, and S.J.M.H. Hulscher, 2001. Detailed observations of the rippled surface of Antarctic blue-ice areas. *J. Glaciol.*, Vol. 47, No. 158, 387-396.
- Bintanja, R., and M. R. van den Broeke, 1995a. The climate sensitivity of Antarctic blue ice areas, *Ann. Glaciol.*, 21, 157-191.
- Bintanja, R. and M. R. van den Broeke, 1995b. The surface energy balance of Antarctic snow and blue ice. *J. Appl. Meteor.*, 34, 902-926.
- Blunier, T., J. Chappellaz, J. Schwander, A. Dällenbach, B. Stauffer, T. F. Stocker, D. Raynaud, J. Jouzel, H. B. Clausen, C. U. Hammer, and S. J. Johnsen, 1998. Asynchrony of Antarctic and Greenland climate change during the last glacial period. *Nature*, 394(20), 739-743.
- Brown, I. C., and T. A. Scambos, 2004. Satellite monitoring of blue-ice extent near Byrd Glacier, Antarctica. *Ann. Glaciol.* 39, p. 223-230.
- Cassidy, W., R. Harvey, J. Schutt, G. Delisle, and K. Yanai, 1992. The meteorite collection sites of Antarctica. *Meteoritics* 27, 490-525.
- Cassidy, W. A., E. Olsen, and K. Yanai, 1977. Antarctica: A Deep-Freeze Storehouse for Meteorites. *Science* 198 (4318), 727. [DOI: 10.1126/science.198.4318.727]
- Corti, G., A. Zeoli, and M. Bonini, 2003. Ice-flow dynamics and meteorite collection in Antarctica. *Earth and Plan. Sci. Lett.* 215 (2003) 371-378.
- Crary, A. P. and C. R. Wilson, 1961. Formation of "Blue" Glacier Ice by Horizontal Compressive Forces. *J. Glaciol.*, Vol. 3, No. 30, 1045-1050.
- Custer, S. E., 2006. Eemian records of $\delta^{18}\text{O}_{\text{atm}}$ and CH_4 correlated to the Vostok EGT4 timescale from the Moulton Blue Ice Field, West Antarctica. *A senior thesis in Geosciences*, The Pennsylvania State University, USA. <http://www.geosc.psu.edu/undergrads/documents/documents/StantonCusterthesis.pdf>
- Delaygue, G., J. Jouzel, V. Masson, R.D. Koster, and E. Bard, 2000. Validity of the isotopic thermometer in central Antarctica: Limited impact of glacial precipitation seasonality and moisture origin. *Geophys. Res. Lett.*, 27, 2677-2680.
- Delisle, G. 1993. Global change, Antarctic meteorite traps and the East Antarctic ice sheet. *J. Glaciol.*, 39, 397-408.
- Delisle, G. and J. Sievers. 1991. Sub-ice topography and meteorite finds near the Allan Hills and the Near Western Icefield, Victoria Land, Antarctica. *J. Geophys. Res.*, E96, 15577-15587.
- EPICA Community Members, 2006. One-to-one hemispheric coupling of millennial polar climate variability during the last glacial. *Nature*, 444, 195-198.

- EPICA Community Members, 2004. Eight glacial cycles from an Antarctic ice core. *Nature* 429 (6992): 623-628. DOI:10.1038/nature02599.
- Faure G., and D. Buchanan, 1991. Ablation rates of the ice fields in the vicinity of the Allan Hills, Victoria Land, Antarctica. Contributions to Antarctic research II. *Antarctic Res. Ser.*, Vol 53, pp. 19-31.
- Fireman, E. L., 1986. Uranium-series dating of Allan Hills ice. *J. Geophys. Res.* 91, pp. D539–D544 (correction *J. Geophys. Res.* 91: 8393).
- Fireman E. L. and T. L. Norris, 1982. Ages and composition of gas trapped in Allan Hills and Byrd core ice. *Earth and Planetary Science Letters*, Volume 60, Issue 3, 339-350. doi:10.1016/0012-821X(82)90072-3
- Giaever, J., 1954 *The White Desert*. The Official Account of the Norwegian- British-Swedish Antarctic Expedition. Chatto & Windus, London 1954.
- Goldstein S. J., M. T. Murrell, K. Nishiizumi, and A. J. Nunn, 2004. Uranium-series chronology and cosmogenic ^{10}Be - ^{36}Cl record of Antarctic ice. *Chemical Geology*, 204, 125-143.
- Gonfiantini, R., 1984. Advisory group meeting on stable isotope reference samples for geochemical and hydrological investigations. Report to the Director General, International Atomic Energy Agency, Vienna.
- Grinsted, A., J. C. Moore, V. Spikes, and A. Sinisalo. 2003. Dating Antarctic Blue Ice Areas using a novel ice flow model. *Geoph. Res. Lett.* 30(19), 2005. (10.1029/2003GL017957).
- Grootes, P. M., 1990. ^{18}O results from blue-ice areas: “old” ice at the surface? In: Cassidy, W. and I. Whillams (Eds.), 1990. Workshop on Antarctic Meteorites, Stranding Surfaces, LPI tech. Rep. 90-03, Lunar Planet Inst., Houston, 67-69.
- Harvey, R.P., 2003. The origin and significance of Antarctic meteorites. *Chemie der Erde*, 63, 93-147. DOI: 10.1078/0009-2819-00031
- Hättestrand, C., and N. Johansen, 2005. Supraglacial moraines in Scharffenbergbotnen, Heimfrontfjella, Dronning Maud Land, Antarctica –significance for reconstructing former blue ice areas. *Antarctic Science* 17 (2), 225-236 (2005). DOI: 10.1017/S0954102005002634.
- Herron, M. M., and C. C. Langway, Jr. 1980. Firn densification: an empirical model. *J. Glaciol.*, 25(93), 373–385.
- Huss, G. R., 1990. Meteorite infall as a function of mass: Implications for the accumulation of meteorites on Antarctic ice. *Meteoritics* 25 (1990), 41-56.
- Huybrechts, P., 1992. The Antarctic ice sheet and environmental change: a three-dimensional modeling study. *Ber. Polarforsch.* 99, p. 1–241.
- Isaksson, E., and W. Karlén, 1994. High resolution climatic information from short firn cores, Western Dronning Maud Land, Antarctica. *Climatic Change*, 24, 421-434.
- Jonsson, S. 1992. Local climate and mass balance of a blue-ice area in western Dronning Maud Land, Antarctica. *Z. Gletscherkd. und Glazialgeol.*, 26 (1), [1990], 11-29.
- Jonsson, S. and P. Holmlund, 1990. Evaporation of snow and ice in Scharffenbergbotnen, Dronning Maud Land, Antarctica. *Ann. Glaciol.* 14: 342.
- Jouzel, J., G. Raisbeck, J.P. Benoist, F. Yiou, C. Lorius, D. Raynaud, J.R. Petit, N.I. Barkov, Y.S. Korotkevitch, and V.M. Kotlyakov, 1989. A comparison of deep Antarctic ice cores and their implications for climate between 65,000 and 15,000 years ago, *Quat. Res.*, 31, 135-150.

- Knorr, G. and G. Lohmann, 2003. Southern Ocean Origin for Resumption of Atlantic Thermohaline Circulation during Deglaciation. *Nature*, 424, 532-536
- Koeberl, C, 1990. Dust Bands in Blue Ice Fields in Antarctica and Their Relationship to Meteorites and Ice. Workshop on Antarctic Meteorite Stranding Surfaces. A Lunar and Planetary Institute Workshop held 13-15, 1988, at the University of Pittsburgh. Sponsored by Division of Polar Programs, National Science Foundation, and LPI. Edited by W. A. Cassidy and I. M. Whillans. *LPI Technical Report 90-03*, published by Lunar and Planetary Institute, 3303 NASA Road 1, Houston, TX 77058, 1990, p.70
- Lintinen, P. and J. Nenonen, 1997. Glacial history of the Vestfjella and Heimefrontfjella nunatak ranges in western Dronning Maud Land, Antarctica. In: Ricci, C.A. (ed.), *The Antarctic Region: Geological Evolution and Processes*. Siena: Universtà degli Studi di Siena, 845-852.
- Masson V., F. Vimeux, J. Jouzel, V.I. Morgan, M. Delmotte, P. Ciais, C.U. Hammer, S.J. Johnsen, V.Y. Lipenkov, E.M. Thompson, J-R. Petit, E.J. Steig, M. Stievenard, and R. Vaikmae, 2000. Holocene Climate Variability in Antarctica Based on 11 Ice-Core Isotopic Records. *Quat. Res.*, Vol. 54, 348 - 358.
- McIntosh, W. C., and N. W. Dunbar, 2004, High-precision $^{40}\text{Ar}/^{39}\text{Ar}$ dating of a 10 ka to 492 ka sequence of englacial tephra layers at Mt. Moulton, Antarctica: IAVCEI International Volcanological Congress.
- Mellor, M. and C. Swithinbank, 1989. Airfields on Antarctic glacier ice. *CRRELL Rep.* 89-21.
- Moore, J. C., F. Nishio, S. Fujita, H. Narita, E. Pasteur, A. Grinsted, A. Sinisalo, and N. Maeno, 2006. Interpreting ancient ice in a shallow ice core from the South Yamato (Antarctica) blue ice area using flow modeling and compositional matching to deep ice cores. *J. Geophys. Res.*, 111, D16302, doi:10.1029/2005JD006343.
- Nakawo, M, M. Nagoshi, and S. Mae, 1988. Stratigraphic record of an ice core from the Yamato meteorite ice field, Antarctica, *Ann. Glaciol.*, 10, 126-129.
- Naruse, R., and M. Hashimoto. 1982. Internal flow lines in the ice sheet upstream of the Yamato Mountains, East Antarctica, *Mem. NIPR spec. Iss.* 24, 201-203.
- Näslund, J.O., J. L. Fastook, and P. Holmlund, 2000. Numerical modeling of the ice sheet in western Dronning Maud Land, East Antarctica: impacts of present, past and future climates *J. Glaciol.* 46 (152), 54-66.
- Nishiizumi, K., D. Elmore, and P. W. Kubik, 1989. Update on terrestrial ages of Antarctic meteorites, *Earth Planet. Sci. Lett.*, 93, 299-313.
- Nishiizumi, K., L. R. Arnold, D. Elmore, R. D. Ferraro, H. E. Gove, R. C. Finkel, R. P. Beukens, K. H. Chang, and L. R. Kilius, 1979. Measurements of ^{36}Cl in Antarctic meteorites and Antarctic ice using a Van de Graaff accelerator. *Earth. Planet. Sci. Lett.*, 45, 285-292.
- Nishio, F., T. Katsushima, H. Ohmae, M. Ishikawa, and S. Takahashi, 1984. Dirt layers and atmospheric transportation of volcanic glass in the bare ice areas near the Yamato Mountains in Queen Maud Land and the Allan Hills in Victoria Land, Antarctica, *Mem. NIPR spec. Iss.* 34 , 160-173
- Nye, J. F. 1963. Correction factor for accumulation measured by the thickness of the annual layers in an ice sheet. *J. Glaciol.*, 4(36), 785-788.
- Orheim O., and B. Lucchitta, 1990. Investigating climate change by digital analysis of blue ice extent on satellite images of Antarctica. *Ann. Glac.* 14., p.211-215.

- Pattyn, F., 1999. The variability of Antarctic ice-sheet response to the climatic signal. *Ann. Glaciol.* 29, 273-278.
- Pattyn, F. and H. Declair, 1998. Ice dynamics near Antarctic marginal mountain ranges: implications for interpreting the glacial-geological evidence. *Ann. Glaciol.*, 27, 327-332.
- Perchiazzi, N., L. Folco, and M. Mellini, 1999. Volcanic ash bands in the Frontier Mountain and Lichen Hills blue-ice fields, northern Victoria Land. *Antarctic Science* 11 (3): 353-361.
- Petit, J.R., J. Jouzel, D. Raynaud, N.I. Barkov, J.-M. Barnola, I. Basile, M. Bender, J. Chappellaz, M. Davis, G. Delayque, M. Delmotte, V.M. Kotlyakov, M. Legrand, V.Y. Lipenkov, C. Lorius, L. Pépin, C. Ritz, E. Saltzman, and M. Stievenard, 1999. Climate and Atmospheric History of the past 420,000 years from the Vostok Ice Core, Antarctica. *Nature* 399: 429-436.
- Popp, T., T. Sowers, N. Dunbar, W. McIntosh, and J.W.C. White, 2004. Radioisotopically dated climate record spanning the last interglacial in ice from Mount Moulton, West Antarctica, *Poster Presented at the AGU Fall Meeting, December 2004. American Geophysical Union, San Francisco.*
- Reimer, P.J., M.G.L. Baillie, E. Bard, A. Bayliss, J.W. Beck, C.J.H. Bertrand, P.G. Blackwell, C.E. Buck, G.S. Burr, K.B. Cutler, P.E. Damon, R.L. Edwards, R.G. Fairbanks, M. Friedrich, T.P. Guilderson, A.G. Hogg, K.A. Hughen, B. Kromer, G. McCormac, S. Manning, C. Bronk Ramsey, R.W. Reimer, S. Remmele, J.R. Southon, M. Stuiver, S. Talamo, F.W. Taylor, J. van der Plicht, and C.E. Weyhenmeyer, 2004. INTCAL04 Terrestrial radiocarbon age calibration 0-26 cal kyr BP. *Radiocarbon* 46, 1029-1058.
- Ritz, C., V. Rommelaere, and C. Dumas, 2001. Modeling the evolution of Antarctic ice sheet over the last 420,000 years: Implications for altitude changes in the Vostok region. *J. Geophys. Res.*, 106(D23), 31,943–31,964.
- Robin, G. de Q. 1975. Velocity of radio waves in ice by means of a bore-hole interferometric technique. *J. Glaciol.*, 15(73), 151-159.
- Scherer, P.; Schultz, L.; Neupert, U.; Knauer, M.; Neumann, S.; Leya, I.; Michel, R.; Mokos, J.; Lipschutz, M. E.; Metzler, K.; Suter, M.; Kubik, P. W., 1997. Allan Hills 88019: an Antarctic H-chondrite with a very long terrestrial age. *Meteoritics & Planetary Science*, vol. 32, no. 6, pages 769-773
- Schultz, L., J. O. Annexstad, and G. Delisle, 1990. Ice movement and mass balance at the Allan Hills Icefield. *Antarctic J.*, US 25, pp. 94-95.
- Schytt, V., 1961. Glaciology II. E. Blue ice fields, moraine features and glacier fluctuations. *Norwegian-British-Swedish Antarctic Expedition, 1949-52, Scientific results*, vol. IV E., pp. 183-204.
- Siegert, M. J., R. C.A. Hindmarsh, and G. S. Hamilto, 2003. Evidence for a large surface ablation zone in central East Antarctica during the last Ice Age. *Quat. Res.* 59 (2003), 114–121. doi:10.1016/S0033-5894(02)00014-5
- Sinisalo, A, A. Grinsted and J. C. Moore, 2004. Dynamics of the Scharffenbergbotnen blue-ice area, Dronning Maud Land, Antarctica. *Ann. Glaciol.* 39, p. 417-423.
- Sinisalo, A., A. Grinsted, J. C. Moore, H. A. J. Meijer, T. Martma, and R. S. W. van de Wal, 2007. Inferences from stable water isotopes on the Holocene evolution of Scharffenbergbotnen blue ice area, East Antarctica. *J. Glaciol.* 53(182), p. 427-434.
- Sinisalo, A., J. Moore, R. van de Wal, R. Bintanja, and S. Jonsson, 2003a. A 14-year mass balance record of a blue ice area in Antarctica. *Ann. Glaciol.* 37, p. 213-218.

- Sinisalo, A., A. Grinsted, J. Moore, E. Kärkäs and R. Petterson, 2003b. Snow accumulation studies in Antarctica with ground penetrating radar using 50, 100 and 800 MHz antenna frequencies. *Ann. Glaciol.* 37. , p. 194-198.
- Spikes, V. B., 2000. Laser altimetry, mass balance, and meteorites: A two part study of ice streams and blue ice. *M. Sc. Thesis*, The Ohio State University.
- Takahashi, S., R. Naruse, N. Masayoshi, and S. Mae, 1988. A bare ice field in East Queen Maud Land, Antarctica, caused by horizontal divergence of snow. *Ann. Glaciol.*, 11, 156-160.
- Van den Broeke, M. R. and R. Bintanja, 1995. The interaction of katabatic wind and the formation of blue ice areas in East Antarctica, *J. Glaciol.*, 41, 395-407.
- Van der Kemp, W. J. M., C. Alderliesten, K. van der Borg, A. F. M. de Jong, R. A. N. Lamers, J. Oerlemans, M. Thomassen and R. S. W. van de Wal, 2002. In situ produced ^{14}C by cosmic ray muons in ablating Antarctic ice. *Tellus*, 54B, 186-192.
- Van Roijen, J. J., 1996. Determination of ages and specific mass balances from ^{14}C measurements on Antarctic surface ice. *Ph.D. thesis*, Faculty of Physics and Astronomy, Utrecht University.
- Van Roijen, J. J., R. Bintanja, K. van der Borg, M.R. van den Broeke, A.F.M. de Jong, and J. Oerlemans, 1994. Dry extraction of $^{14}\text{CO}_2$ and ^{14}CO from Antarctic ice. *Nuclear Instruments and Methods in Physics Research*, B 92: 331-334. doi:10.1016/0168-583X(94)96029-1.
- Van Roijen, J.J., K. van der Borg, A.F.M. de Jong, and J. Oerlemans, 1995. Ages, ablation and accumulation rates from ^{14}C measurements on Antarctic ice. *Ann. Glaciol.*, 2, 139-143.
- Watanabe, O., Jouzel, J., Johnsen, S., Parrenin, F., Shoji, H. and Yoshida, N. 2003. Homogeneous climate variability across East Antarctica over the past three glacial cycles. *Nature* 422: 509-512
- Weller, G. E., 1968. The heat budget and heat transfer processes in Antarctic plateau ice and sea ice. *ANARE Sci. Rep.*, Ser. A(4) Glaciology 102.
- Welten, K. C.; Lindner, L.; van der Borg, K.; Loeken, Th.; Schultz, L.; Romstedt, J.; Metzler, K., 1995. Antarctic Meteorites with Unusual Exposure and Terrestrial Histories. *Meteoritics*, vol. 30, no. 5, p. 598.
- Welten K. C., K Nishiizumi., and M. W. Caffee, 2000. Update on terrestrial ages of antarctic meteorites. *Lunar Planet. Sci.* XXXI, CD-ROM 2000.
- Whillans, I.M., and W.A. Cassidy, 1983. Catch a falling star; meteorites and old ice. *Science*, 222(4619), 55-57.
- Wilch, T.I., McIntosh, W.C., and Dunbar, N.W., 1999, Late quaternary volcanic activity in Marie Byrd Land: Potential $^{40}\text{Ar}/^{39}\text{Ar}$ dated time horizons in West Antarctic ice and marine cores. *Geological Society of America Bulletin*, v. 111, p. 1563-1580.
- Winther, J.-G., M. N. Jespersen, and G. E. Liston, 2001. Blue-ice areas in Antarctic derived from NOAA AVHRR satellite data. *J. Glaciol.* 47, 325-334.
- Winther, J.-G., 1994. Spectral bi-directional reflectance of snow and glacier ice measured in Dronning Maud Land, Antarctica. *Ann. Glaciol.*, 20, 1-5.
- Yoshida M., Ando H., Omoto K., Naruse R., Ageta Y., 1971. Discovery of meteorites near Yamato Mountains, East Antarctica. *Antartic Record* 39, 62-65.

PAPER I

A 14 YEAR MASS-BALANCE RECORD OF A BLUE-ICE AREA IN ANTARCTICA

Anna Sinisalo, John C. Moore, Roderik S.W. van de Wal,
Richard Bintanja, Stig Jonsson



Photo: FINNARP/Anna Sinisalo

A 14 year mass-balance record of a blue-ice area in Antarctica

Anna SINISALO,^{1,2} John C. MOORE,¹ Roderik S.W. VAN DE WAL,³
Richard BINTANJA,³ Stig JONSSON⁴

¹Arctic Centre, University of Lapland, Box 122, FIN-96101 Rovaniemi, Finland
E-mail: anna.sinisalo@uova.fi

²Department of Geophysics, Box 3000, University of Oulu, FIN-90014 Oulu, Finland

³Institute for Marine and Atmospheric Research, P.O. Box 80.005, Utrecht University,
Princetonplein 5, 3584 CC Utrecht, The Netherlands

⁴Department of Physical Geography, Stockholm University, S-106 91 Stockholm, Sweden

Abstract. Accumulation and ablation rates over an Antarctic blue-ice area spanning the 14 year period 1988–2002 are presented. Data were obtained by direct stake measurements. Large spatial and temporal variations in the net balance were observed without any clear trend over the entire period. There are marginally significant increases in snow accumulation, and in ablation in the blue-ice area farthest from the equilibrium zone (both at the 95% confidence level). The snow/blue-ice transition zone shows no change over the entire period of observation, and the blue-ice area near the zone shows no change in ablation rate over the 14 year period. The mass-balance gradient in Scharffenbergbotnen may have increased during the period 1988–2002. However, the changes are small, especially when compared with the changes observed elsewhere in Antarctica even relatively close to the blue-ice area. This may indicate that the blue-ice areas are relatively stable to changes in accumulation rate, and possibly temperature.

INTRODUCTION

There is a need to improve our knowledge of the flow dynamics and stability of Antarctic blue-ice areas in a changing climate (Bintanja, 1999). Blue-ice areas are known to have very old ice at the surface that can be a valuable resource for palaeoclimatic re-

search (e.g. Naruse and Hashimoto, 1982; Bintanja, 1999). However, to extract useful information from the ancient surface ice for palaeoclimate studies, or to study the stability of the Antarctic blue-ice areas as a part of largescale mass-balance research, detailed mass-balance and concurrent ice-flow measurements are needed. The state of balance of blue-ice areas over a period could also be estimated from these measurements.

The longest mass-balance record known to us from a blue-ice area is from Borgmassif in Dronning Maud Land where three stakes were measured over a 34 year interval (Brunk and Staiger, 1986). Ablation rates have been measured by direct stake measurements on several other Antarctic blue-ice areas, but most stake ablation records still only cover a relatively short period (e.g. Budd, 1967; Faure and Buchanan, 1991; Takahashi and others, 1994). The results are summarized by Bintanja (1999). We present accumulation and ablation rates for a blue-ice area spanning a period of 14 years. The results are compared with previous, only partially published, field measurements (Jonsson, 1992). We discuss the error sources in the data, and estimate the state of balance of the blue-ice area.

STUDY AREA

Scharffenbergbotnen is the best-studied blue-ice area in Antarctica, from a glaciological

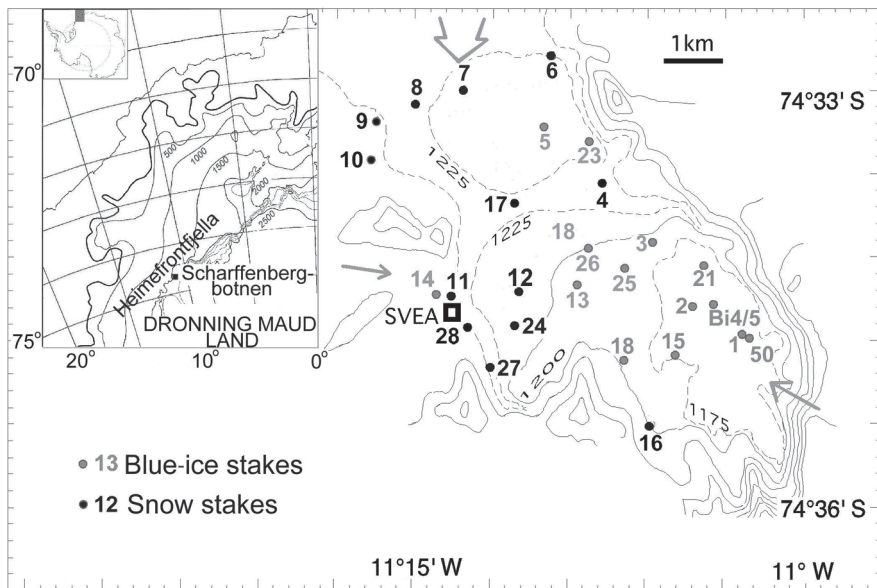


Fig. 1. The Scharffenbergbotnen study area close to the Swedish field station Svea (marked). The stakes located on snow are labelled in black, and the blue-ice stakes in grey.

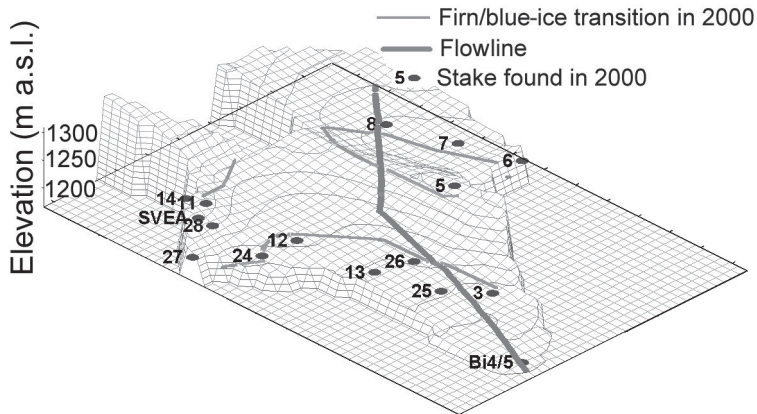


Fig. 2. Surface of Scharffenbergbotnen mapped in 2000. The stakes and the firn/blue-ice transition line that were measured in the same year are plotted. Other stakes shown in Figure 1 survived at least until 1994. The flowline section in Figure 4 is marked.

point of view. It is located in northwest Sivorgfjella, Heimefrontfjella, with an ice inflow from the surrounding inland ice sheet (Fig. 1). The main influx comes from the north-western entrance of the valley (shown by the large arrow in Fig. 1). There are minor inflows from the shallow, narrow southwestern portal and from ice entering the valley from a 400 m high icefall at the eastern end of Scharffenbergbotnen (shown by small arrows in Fig. 1). A visible boundary <1 km from the icefall, in the ice at the bottom of the valley, restricts the small icefall flow (Jonsson, 1992). This boundary also marks the end of a debris-covered area close to the mountains. Supraglacial till is found mainly at the eastern end of the valley and on the southern side where stakes 15, 16 and 18 were located. The mass-balance data from these stakes appear typical of blue ice.

The surface topography of the floor of the valley, mapped in 2000, is presented in Figure 2. The main blue-ice area is located in a depression at the southeastern end of the valley. There is a smaller blue-ice field, in a depression upstream of the main blue-ice area, on the northern side of the main entrance that is separated from the main blue-ice field by a snow ridge (stakes 4 and 17 in Fig. 1). Blue ice is also found above the Swedish research station Svea (stake 14 in Fig. 1). The ice transition between perpetual snow-covered areas and blue ice is a zone where snow patches are found on blue ice occasionally situated >100 m from the continuous snow-covered areas.

Figure 2 also shows the stakes that survived until 2000. Stake 28 was snow-covered between 2000 and 2002, but the rest of the stakes plotted in Figure 2 were also found in 2002. The study area is described in more detail by Jonsson (1992).

STAKE MEASUREMENTS

Originally a net of 34 stakes was established in the study area in 1988 (Jonsson,1992). The stakes were remeasured in 1990, 1992, 1993, 1994, 1998, 2000 and 2002. The mass-balance results are obtained from direct measurements on 12 stakes over the full 14 year period, and from 26 stakes over the 6 year period 1988–94. The positions of the 12 stakes and an additional 3 stakes installed in 1998 were measured with differential global positioning system (DGPS) in 2000 and 2002 (Javad Positioning System) to determine the ice-flow velocity. Two of the additional stakes (Bi4/5 in Fig. 1) were also used for mass-balance measurements for the period 1998–2002.

Table 1. Net balance ($mm\ m.e.\ a^{-1}$) for each stake in Scharffenbergbotnen valley for the observation period they survived. Error given is the standard deviation of the mean

Group 1: blue ice				Group 2: snow			
StakeNo.	Period			StakeNo.	Period		
	1988–94	1988–98	1988–2002		1988–94	1988–98	1988–2002
50	-82±45	–	–	4	75±60	–	–
1	-138±43	–	–	6†	-11±75	–	-2±75
2	-111±63	–	–	7	-15±40	-8±40	2±46
3*,†	-55±41	–	-30±41	8	-4±85	5±76	4±67
5*	-50±46	-56±46	-8±62	9	27±89	–	–
13*	-35±32	-38±29	-33±38	10	-6±76	8±76	–
14*	-42±56	-39±50	-21±54	11‡	-16 ±66	-9±60	-2±60
15	-100±56	–	–	12‡	-5±73	-2±73	4±73
18**	-65±62	–	–	16	-17±73	–	–
21*	-103±76	–	–	17	40±127	–	–
23	-108±18	-98±18	–	24	-26±72	-21±65	-11±60
25	-85±47	–	–	27	-1±97	6±87	14±87
26*	-37±34	–	-6±51	28	-36±161	45±161	–
All	-78±48	-58±36	-20±49	All	0±84	3±80	1±67

* Stakes on blue ice except in 1990 and 2002.

† Not measured in 1998.

‡ Stakes in some years on ice.

** Stake located on changing surface, mostly on firn ice.

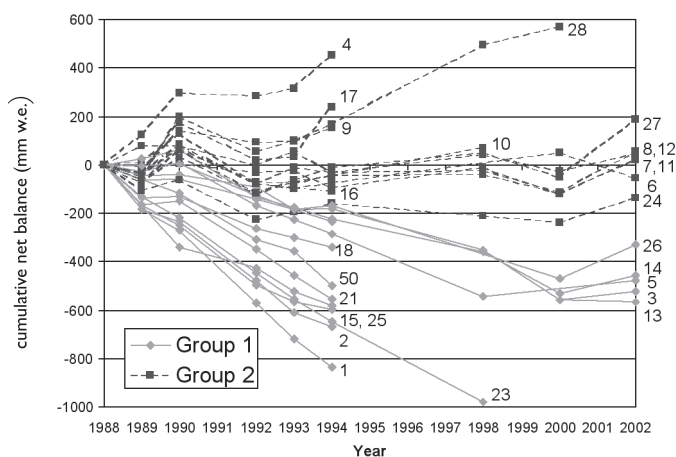


Fig. 3. Cumulative net balances for 26 stakes in Scharffenbergbotnen. Group 1 consists of the blue-ice stakes, and group 2 includes the snow stakes. Only the stakes at sites that are close to equilibrium have survived the full 14 years. The highest accumulation rate is found on the snow ridge between the two blue-ice areas (stakes 4 and 17).

RESULTS

We divided the stake data into two groups according to the surface conditions (Table 1). Group 1 consisted of stakes that were on blue ice for the whole period, and also stakes that had snow around them in 1990 and 2002 but were otherwise on blue ice. Group 2 included a few stakes that were occasionally on blue ice but usually on snow, along with stakes that were on snow for the whole period.

The cumulative net balance for each stake over the 14 year observation period is shown in Figure 3. Only 12 stakes survived the whole period, 5 of which were on blue ice. Most of the surviving stakes were located close to the equilibrium zone of the main blue-ice area in the Scharffenbergbotnen valley or the smaller blue-ice area upstream from the main blue-ice area (Fig. 1). Thus they were not buried by snow accumulation, or ablated from the blue ice. The measurements show high spatial and temporal mass-balance variability both within the two groups and, of course, between the blue-ice and snow groups. The measured net balance for each stake is presented in Table 1. The range of net balance values during the 14 year period along the main flowline is from $-186 \pm 36 \text{ mm w.e. a}^{-1}$ at stake 1 at the eastern end of the blue-ice area, to $208 \pm 132 \text{ mm w.e. a}^{-1}$ at stake 17 on the snow ridge.

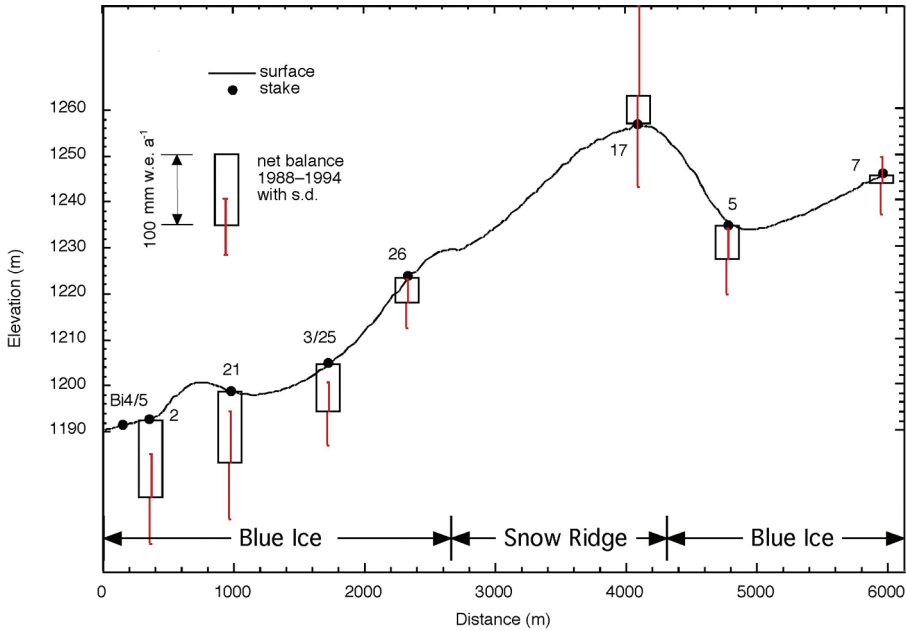


Fig. 4. A 6 km section of the surface profile of a flowline starting from the bottom of the southeastern depression of the main blue-ice field (see Fig. 2). A snow ridge separates the main blue-ice area from the smaller blue-ice field at the northwestern entrance to the valley. The stakes located close to the flowline are marked. The horizontal distance between the stakes marked and the centre line varies between 30 and 990 m, being 460 m on average. The average annual net balance at the stakes over the period 1988–94 are shown with standard deviation of the measurements.

The variation of the average annual net balance along a flowline ending near stakes 2 and Bi4/5, close to the bottom of the southeastern depression of the main blue-ice field (see Fig. 2), is presented in Figure 4. The figure shows that net balance along the line is positive only at the snow ridge separating the main blue-ice field from the smaller blue-ice depression. The year-to-year variation in net balance expressed by the ratio of the standard deviation to the mean is also largest at the snow ridge.

The areas of observed net accumulation over the 14 year period are also those where snowdrift is transported by the dominant easterly winds (Bintanja, 2000). The relative year-to-year variability in net balance is smaller on blue ice than on snow-covered areas (Table 1), perhaps because ephemeral snowdrift affects stake measurements on snow, but not on ice where snow accumulation is occasional. The highest annual variations in the net mass balance were observed on the western side of the valley, and on the snow ridge separating the main blue-ice field from the small blue-ice depression.

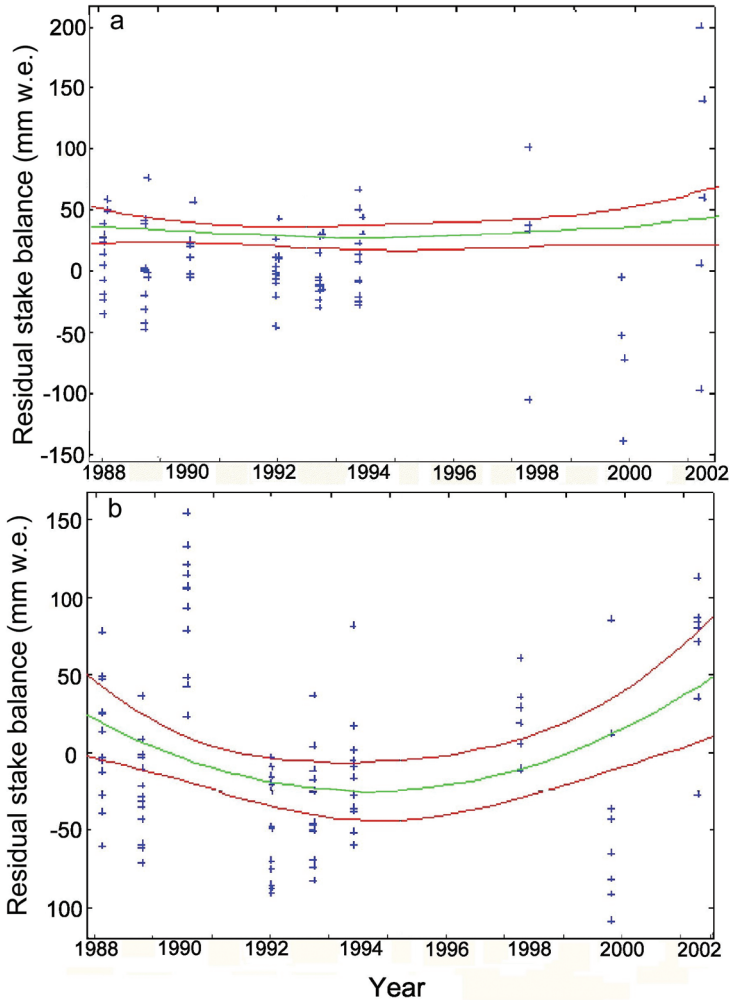


Fig. 5.

(a) Residual ablation for ice stakes (and those mostly on ice) with a robust quadratic fit and 95% confidence interval.

(b) Residual accumulation for snow stakes (actual accumulation minus linear trend at each stake) with a robust quadratic fit and 95% confidence interval.

TRENDS

We calculated the linear trend in balance for each stake over the entire period. For each stake we looked at the difference, at each measuring time, between the long-term linear trend and the actual value of the ablation or accumulation, i.e. the residual balance. The residuals in each group of stakes were fitted with the simplest non-linear function (a quadratic) with robust (or least-squares) estimation methods. Calculating 95% confidence limits to the quadratic curve allows any significant changes in balance trend over the whole period to be investigated. Figure 5 shows the results in water equivalent (w.e.) assuming a snow density of 400 kg m^{-3} . Each group is now discussed in turn.

Blue ice

The 1990 data were excluded from the analysis for stakes located on snow in that year, since the snow depth was not measured. Results of the residual analysis are shown in Figure 5a and suggest no change in ablation rate with time for the stakes on blue ice.

The mean ablation rate for the blue-ice stakes was -78 ± 48 mm w.e. a^{-1} (13 stakes) in 1988–94 and -20 ± 12 mm w.e. a^{-1} (5 stakes) in 1988–2002 (Table 1). The difference does not indicate a change in ablation rate but is actually determined by the location of the stakes that remained until 2002. None of the 12 stakes that survived the whole 14 year period on blue ice are located in the most severe ablation area, which is at the bottom of the depression at the southeastern end of the valley. Thus, the blue-ice ablation rate calculated for the whole period represents the ablation rate fairly close to the equilibrium zone (see Fig. 2).

In an attempt to extend the observation period for the southeastern end of the main blue-ice field, we also remeasured, in 2000 and 2002, a pair of stakes installed in 1998 in the vicinity of stake 2 (Bi4/5 in Figs 1 and 2). Bi4/5 was about 360 m from stake 2, 690 m from stake 1 and about 510 m from stake 21 (Fig. 1). The surface elevation of Bi4/5 was about the same as that of stakes 2 and 21 (± 5 m) and about 10 m higher than that of stake 1. Since the pair of stakes were located only 2 m apart and thus represent ablation almost at the same point, we use an average value for the ablation rate measured from them. The measured ablation rate for Bi4/5 for the period 1998–2002 was -146 ± 4 mm w.e. a^{-1} . The ablation rate at stakes 1, 2 and 21 for the period 1988–94 was -111 ± 28 mm w.e. a^{-1} . This result suggests that the ablation rate at the southeastern end, i.e. in the area with the highest ablation rate in the main blue-ice field, may have increased during the 14 year observation period, while close to the equilibrium zone it remained constant. However, the errors are large and the difference is just about at the 95% confidence level.

An inverse relation between the ablation rate and the ice surface elevation was found in Scharffenbergbotnen even though the variation in the blue-ice surface elevation is only 40 m (Fig. 6). The change in ablation rate was about 23 mm w.e. a^{-1} for a 10 m elevation change. Stake 50, located at the bottom of the depression, and stakes Bi4/5 were excluded from the calculation. Stake 50 stands at a site where surface melt-water gathers and refreezes, and Bi4/5 was measured over a different observational period.

Snow

The stakes on snow show a relative decrease in accumulation in the middle of the observing period, and a significant increase over the latter part of the period, particularly in the last 2 years (Fig. 5b).

Large temporal variations in net balance have been reported in the vicinity of the Scharffenbergbotnen valley (Holmlund and others, 1989; Jonsson, 1992; Isaks-

son and Karlén, 1994). The net accumulation within 20 km of Scharffenbergbotnen in 1988–89 was only one-third of the value in 1989–90 (Holmlund and others, 1989; Jonsson, 1992). The 1990 increase in accumulation is also observable in the data from the Scharffenbergbotnen valley, when some of the blue-ice group of stakes were even found on snow. A similar thing was observed in 2002.

Four of the snow stakes (stakes 6,11,16 and 24) show net ablation over their whole observation period. All these stakes are at the margins of blue ice. The average net mass balance for them is -6 ± 7 mm w.e. a^{-1} . The proximity of blue ice increases the sublimation rate on the snow, mainly because the surface temperatures are significantly higher on blue ice than on snow (Takahashi and others,1994; Bintanja and Van den Broeke,1995). Thus, the surface temperature is probably higher at the blue-ice/firn transition zone than on snow further away. The negative net balance on these snow stakes suggests that the area of the blue-ice field will tend to grow. However, short-term fluctuations in the extent of one particular blue-ice area are believed to be an indication of changes in surface wind speed (Bintanja,1999).

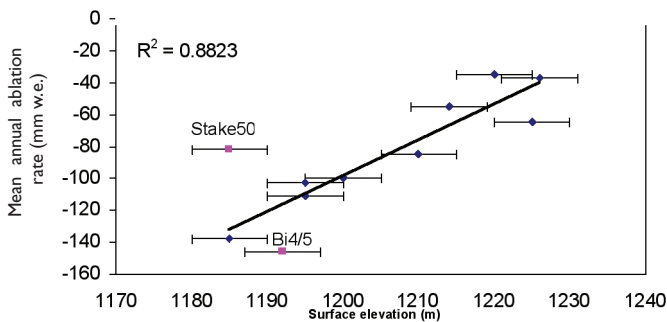


Fig. 6. The annual net balance for 11 stakes in the main blueice field in Scharffenbergbotnen vs the surface elevation in the period 1988–94. Stakes 50 and Bi4/5 were excluded from the trend-line calculation. Refreezing of the meltwater decreases the net ablation at stake 50. Bi4/5 was measured only in 1998–2002. The elevations for stakes that were not found and measured in 2000 are taken from Jonsson (1992).

VELOCITY

The maximum horizontal flow velocity in the main blue-ice field was $30 \pm 2 \text{ cm a}^{-1}$ at stake 3 close to the equilibrium line of the main blue-ice field. At the southeastern end of the blue-ice field the velocity is about half this value. The velocities indicate a mass influx from the east/northeast, right outside the northwestern entrance of the valley, where the horizontal velocity was about $117 \pm 2 \text{ cm a}^{-1}$ from the east/northeast at stake 6. The value is approximately twice as large as that reported earlier (Van Roijen, 1996; personal communication from P. Holmlund, 1992). The reason for this difference is unclear.

The vertical velocities were not measured over the blue-ice area since they are too small to be observed by the DGPS in such a short time period. Even if there was an increased net ablation over the blue-ice area, a reduced upward velocity could lead to the disappearance of the blue-ice area in the longer term through an increased transport of firn to the area. However, the time-scale for this kind of process is probably somewhat longer than for mass-balance effects on blue-ice areas.

ERROR ESTIMATION

The accuracy of each stake length measurement is $\pm 5 \text{ mm}$. Year-to-year variations can be partially caused by variations in the length of the measurement period, by temporary changes in the snow cover and by change in weather. The stakes could not be measured every year. When they were, logistical limitations sometimes prevented them from being measured at the end of the summer period or at exactly the same time of the year. For an individual year, this can lead to significant errors since the average summer ablation rates in blue ice are significantly higher than the average annual rates (Faure and Buchanan, 1991; Bintanja and others, 2001). The results obtained from bare blue ice may also include an additional error due to the rippled surface typical of blue-ice areas. The wave height of the ripples increases throughout the summer, as most ablation occurs in the wave troughs (Bintanja and others, 2001). The stakes were measured in relation to the level of the highest points of the surrounding ripples. This method has been found to underestimate the true ablation on bare blue ice by 6–15% (Bintanja and others, 2001). Large temporary changes in surface snow conditions in the blue-ice areas have also been reported during the summer seasons, and at the ice/snow margin the surface conditions may have changed from year to year. All these errors disappear, however, when many years of data are considered.

Originally the stake net was well distributed in order to observe the general features of the mass balance and the average net balance in the area. However, stakes installed in the accumulation area and the area of the highest ablation values are now lost,

so the average net balance value of the area now best represents the net balance in the areas close to the equilibrium line.

DISCUSSION

There is a relation between annual ablation rate and altitude for various blue-ice areas (Bintanja, 1999). Scharffenbergbotnen is a blue-ice area at 1200 m a.s.l., and the observed ablation rate is at the lower limit of expected values for its altitude. An inverse relation between the ablation rate and the ice-surface elevation that has also been reported from other blue-ice areas (Budd 1967; Faure and Buchanan, 1991) is observed in the main blue-ice field in Scharffenbergbotnen. We observe a gradient of about 25 cm w.e. per 100 m elevation change (Fig. 6) compared with only about 2.5 cm w.e. per 100 m observed by Faure and Buchanan (1991). The difference is probably due to the strong heating effect of the steep rock walls around Scharffenbergbotnen. We also observed that the distance to the rock correlates with the ablation rate for blue ice. In the Scharffenbergbotnen valley, the distance between most of the stakes and the rock increases with increasing elevation. Thus, it is difficult to estimate which part of the decrease in ablation rate is due to the increase in elevation and which part to the increase in distance to rock outcrops. It seems likely that rock heating dominates in comparison with other blue-ice areas.

Taken together, the results indicate that there has been little trend in net balance over the period studied. This, however, may be a logical consequence of the fact that survival of stakes near the equilibrium line biases the data towards that region. What is most interesting, however, in terms of blue-ice area sensitivity to climate change, is to study changes in the snow/blue-ice transition zone. There is some indication of a recent increase in accumulation in the snow-covered areas. Simultaneously, there appears to be an increase in ablation rates in the peak ablation area of the blue-ice area, while no change has occurred near the equilibrium zone. Increased ablation is expected in a warmer climate since the sublimation rate increases with increasing incoming longwave radiation (Bintanja and Van den Broeke, 1995). The increased snow precipitation onto the blue ice can decrease the sublimation rate only temporarily since any snow on blue ice tends to be blown away efficiently by gusty winds (Bintanja, 2001). This enables a negative surface mass balance to be maintained on blue ice by sublimation. Since there are so few measurements on blue ice and none in the area of highest ablation rates over the whole 14 year period, it is impossible to estimate whether the observed slight increase in the average net balance in snow in the Scharffenbergbotnen valley is balanced by the decreased values of net balance in bare blue ice.

Large spatial and temporal variations in net accumulation have been observed in Dronning Maud Land. Isaksson and Karlén (1994) discuss snow-accumulation variations in Dronning Maud Land between 1975 and 1988. The observation point closest

in that period to Scharffenbergbotnen was 27 km to the northwest of the valley, and showed a decreasing trend in the observation period. On the other hand, Isaksson and Karlén also found a 12% increase in accumulation from the period 1957–74 to 1975–88. Sommer and others (2000) found no trend in accumulation rates in Dronning Maud Land for the last few decades, but variability on decadal time-scales was about 20%. Large accumulation trends have been reported in several other places in Antarctica, and both trend and decadal-scale variation may be related to the Antarctic Oscillation (AAO) index (Thompson and Wallace, 2000). The large trend in the AAO over recent decades is presumably driven by the decrease in stratospheric ozone, intensifying the polar stratospheric vortex which leads to stronger westerly winds and to changing precipitation patterns in much of Antarctica. The rather striking changes due to AAO trends contrast markedly with the observations presented here, which seem to show only minor changes or none at all. Indeed the equilibrium zone appears to have undergone no change over the 14 year period of the observations, during which the AAO has been declining at about $3\% \text{ a}^{-1}$.

CONCLUDING REMARKS

The mass-balance results for the Scharffenbergbotnen blue-ice area can be summarized as follows:

- (1) Changes in accumulation and ablation rate have been slight. There is a marginally significant increase in snow accumulation over the latter part of the 14 year observation period (at the 95% confidence level).
- (2) There is a similarly marginally significant increase in ablation in the blue-ice area farthest from the equilibrium zone.
- (3) The snow/blue-ice transition zone shows no change over the whole period of observation, and the ablation rate shows no change over the 14 year period.

The results of direct stake measurements suggest that the mass-balance gradient in Scharffenbergbotnen may have become steeper during the period 1988–2002, but the equilibrium line has not changed. This may indicate that the blue-ice areas are relatively stable to change in accumulation rate, and possibly temperature. Since there are only a few detailed mass-balance studies on Antarctic blue-ice areas and since the time series are still relatively short, it is important to continue the direct net balance studies in order to obtain a longer time series to verify this presumption.

ACKNOWLEDGEMENTS

We would like to thank J. Vehviläinen for all his help in the field. We are also grateful to those who made the field measurements during the various Swedish Antarctic Research Programme (SWEDARP) expeditions to Antarctica in the period 1988–98, and to D. P. Zwartz for the field measurements in 2002. The 1999–2002 field logistics were provided by the Finnish Antarctic Research Programme (FINNARP) 1999–2002. The work is funded by the Finnish Academy. We also thank two anonymous reviewers for helpful comments.

REFERENCES

- Bintanja, R. 1999. On the glaciological, meteorological and climatological significance of Antarctic blue ice areas. *Rev. Geophys.*, 37(3), 337–359.
- Bintanja, R. 2000. The surface heat budget of Antarctic snow and blue ice: interpretation of temporal and spatial variability. *J. Geophys. Res.*, 105(D19), 24,387–24,407.
- Bintanja, R. 2001. Characteristics of snowdrift over a bare ice surface in Antarctica. *J. Geophys. Res.*, 106(D9), 9653–9659.
- Bintanja, R. and M. R. van den Broeke. 1995. The climate sensitivity of Antarctic blue-ice areas. *Ann. Glaciol.*, 21, 157–161.
- Bintanja, R., C.H. Reijmer and S. J.M.H. Hulscher. 2001. Detailed observations of the rippled surface of Antarctic blue-ice areas. *J. Glaciol.*, 47(158), 387–396.
- Brunk, K. and R. Staiger. 1986. Nachmessungen an Pegeln auf einem Blaueisfeld im Borgmassiv, Neuschwabenland, Antarktis. *Polarforschung*, 56(1–2), 23–32.
- BuðD, W. 1967. Ablation from an Antarctic ice surface. In Ōura, H., ed. *Physics of snow and ice. Vol. 1, Part 1*. Sapporo, Hokkaido University. Institute of Low Temperature Science, 431–446.
- Faure, G. and D. Buchanan. 1991. Ablation rates of the ice fields in the vicinity of the Allan Hills, Victoria Land, Antarctica. In Elliot, D.H., ed. *Contributions to Antarctic research II*. Washington, DC, American Geophysical Union, 19–31. (Antarctic Research Series 53.)
- Holmlund, P., E. Isaksson and W. Karlén. 1989. Massbalans, isro« relse och isdynamik. Preliminära resultat från fältsäsongen 1988/89 i Vestfjella och Heimefrontfjella. V. Dronning Maud Land, Antarktis. *Stockholms Univ. Naturgeogr. Inst. Forskningsrappr.* 73.
- Isaksson, E. and W. Karlén. 1994. Spatial and temporal patterns in snow accumulation, western Dronning Maud Land, Antarctica. *J. Glaciol.*, 40(135), 399–409.
- Jonsson, S. 1992. Local climate and mass balance of a blue-ice area in western Dronning Maud Land, Antarctica. *Z. Gletscherkd. Glazialgeol.*, 26(1), 1990, 11–29.
- Naruse, R. and M. Hashimoto. 1982. Internal flow lines in the ice sheet upstream of the Yamato Mountains, East Antarctica. *Natl. Inst. Polar Res. Mem., Special Issue* 24, 201–203.
- Sommer, S. and 9 others. 2000. Glacio-chemical study spanning the past 2 kyr on three ice cores

- from Dronning Maud Land, Antarctica.1. Annually resolved accumulation rates. *J. Geophys. Res.*, 105(D24), 29,411–29,421.
- Takahashi, S., Y. Ageta, Y. Fujii and O. Watanabe. 1994. Surface mass balance in east Dronning-Maud Land, Antarctica, observed by Japanese Antarctic Research Expeditions. *Ann. Glaciol.*, 20, 242–248.
- Thompson, D.W. J. and J.M. Wallace. 2000. Annular modes in the extratropical circulation. Part I: Month-to-month variability. *J. Climate*, 13(5), 1000–1016.
- VanRoijen, J. J. 1996. Determination of ages and specific mass balances from ^{14}C measurements on Antarctic surface ice. (Ph.D. thesis, Universiteit Utrecht, Faculteit Natuur- en Sterrenkunde, Utrecht.)

PAPER II

SNOW-ACCUMULATION STUDIES IN ANTARCTICA WITH GROUND PENETRATING RADAR USING 50, 100 AND 800 MHZ ANTENNA FREQUENCIES

Anna Sinisalo, Aslak Grinsted, John C. Moore,
Eija Kärkäs, Rickard Pettersson



Photo: FINNARP/John Moore

Snow-accumulation studies in Antarctica with ground penetrating radar using 50, 100 and 800 MHz antenna frequencies

Anna SINISALO,¹ Aslak GRINSTED,¹ John C. MOORE,¹
Eija KÄRKÄS,² Rickard PETTERSSON³

¹Arctic Centre, University of Lapland, Box 122, FIN-96101 Rovaniemi, Finland

E-mail: anna.sinisalo@urova.fi

²Division of Geophysics, Department of Physical Sciences, P.O. Box 64, University of Helsinki, FIN-00014 Helsinki, Finland

³Department of Physical Geography, Stockholm University, S-106 91 Stockholm, Sweden

Abstract. Snow radar profiles were measured in Dronning Maud Land, East Antarctica, in the vicinity of the Finnish research station Aboa during austral summer 1999/2000. The aim was to study the annual layering in the upper 50 m of the snowpack and to compare the results obtained by three radar antenna frequencies (50, 100 and 800 MHz). Intercomparison of the radar profiles measured by the three frequencies shows that some individual internal layers are visible with different antennas. Sparse accumulation-rate data from stake measurements and snow pits are compared with layer depths. The comparison reveals a great deal of scatter due to the large interannual variability in accumulation patterns. Using the radar layers as isochrones together with a model of depth–density–radarwave velocity allows the individual accumulation data to be integrated, and a better estimate of accumulation patterns is obtained. Using the radar layering seems to be a much better method of estimating accumulation rate in this region than using a short series of stake measurements, even in the absence of deep ice cores to directly date the radar layering.

INTRODUCTION

The mass balance of Antarctica is insufficiently well known. More data are desirable in the context of current and possible future changes in climate, and the concomitant response of the Antarctic ice sheet. Significant progress has been made using various

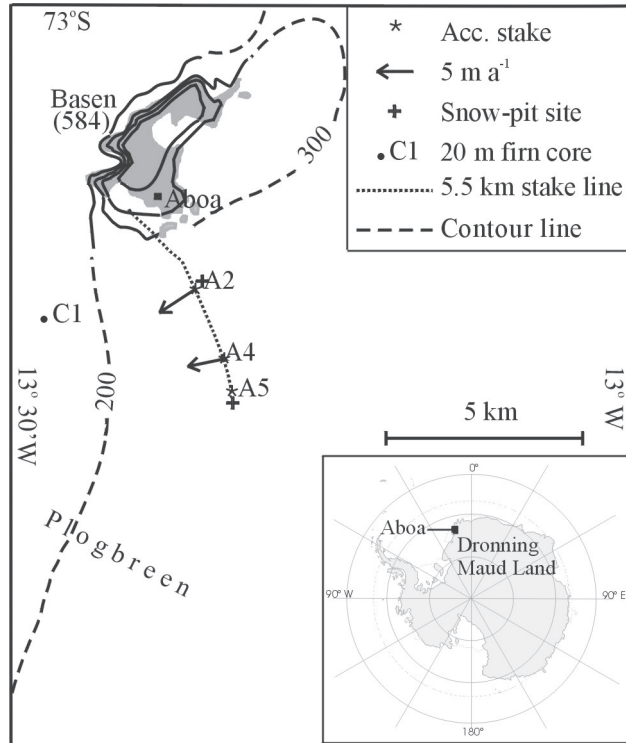
remote-sensing methods including groundbased and satellite radar sounding, but a major source of uncertainty is the probable large variability in accumulation and possibly snow properties both spatially and temporally, especially in regions close to the coast and in mountainous terrain. Accurate snow-accumulation data over these regions are required in order to obtain a reliable mass-balance estimate. Ground-penetrating radar (GPR) has been successfully used for snow-accumulation studies in Svalbard (Kohler and others, 1997; Pälli and others, 2002) and Antarctica (Richardson and others, 1997). The advantage of using GPR is that it is time-efficient; large areas can be covered quickly and the temporal and spatial variability in snow accumulation obtained. The disadvantage is that for the accumulation rates to be absolute rather than relative, the radar layers must be dated in at least one location (usually with an ice core). Once the depth–density profile is accounted for, and any layer thinning due to ice flow corrected for, the present and past accumulation rates can be found (e.g. Morse and others, 1998; Pälli and others, 2002). As we lack an ice core along our radar profile, we use the limited accumulation rate data from a few stakes and pits along the profile to estimate the age of radar layers.

Snow-accumulation studies usually employ high-frequency radars because of their high resolution (Richardson and others, 1997), but low-frequency radars (e.g. 50 MHz) can also be effective (Pälli and others, 2002). The lower frequencies are particularly useful for determining the accumulation rates further in the past or over longer time periods, as they have much greater penetration depths and tend to show only the strongest, most continuous reflectors. Few studies, however, have been based on the results obtained using different radar antenna frequencies. Fujita and others (1999) compare pulse radar frequencies of 60 and 179 MHz within the topmost 100–700 m of the surface of the East Antarctic ice sheet, and discuss the various scattering mechanisms. In this paper, we compare three different antenna frequencies for accumulation studies within the uppermost 50 m of the snowpack in Antarctica. We used a commercial Ramac GPR (Malå Geoscience).

FIELD DATA

A 5.5 km stake line (see Fig. 1) was measured with antenna frequencies of 50, 100 and 800 MHz in order to compare the reflection horizons and study the cause of the reflections. The line started on the glacier about 6 km from the Finnish research station Aboa. The first 5 km are on level terrain, while the last 500 m ascend the slope of the Basen nunatak to Aboa. The bedrock drops quickly away from Basen to give an ice thickness of 300–400 m along the profile (Ruotoistenmäki and Lehtimäki, 1997). Two snow pits and a 10 m core (A2) were drilled along this profile (Fig 1). Snow-accumulation-rate data for 2 years are available from several stakes along the line, and from several earlier

Fig. 1. Map of the Aboa area showing the radar transect and the location of the cores, snow pits, stakes and surface velocity vectors (arrows) for the A2 and A4 stakes.



sets of stake measurements along the profile, which has been on the area's main route southward for many years.

The radar technique involved driving the profile lines on a snowmobile carrying a differential global positioning system (GPS) (Javad Positioning System). The radar transmitter and receiver antennas for the 50 MHz measurements were mounted on a non-metallic sledge, which was pulled 7 m behind the snowmobile. The radar control unit and computer were mounted on the snowmobile together with the roving GPS receiver. The 800 and 100 MHz antennas were shielded units and could be pulled closer behind the snowmobile: the 100 MHz system was pulled about 5 m behind in its own sealed housing; the 800 MHz system was pulled about 2 m behind the snowmobile using rigid struts to keep it at a fixed distance. No trace stacking was done, and data were collected on a laptop computer. Table 1 shows the radar collection parameters. Post-processing of the radar data was done using the Haescan program (Roadscanners Oy). Amplitude zero-level correction was applied, background noise was removed and vertical high-pass and low-pass filtering in time domain was performed.

We compare our radar accumulation-rate data with those derived from snow-pit and core observations along the profile. The cores and the snowpits were sampled to delineate stratigraphy and density. Figure 2 shows the density profiles obtained from the A2 core and the 20 m C1 core obtained a few km to the west of the profile.

<i>Antenna frequency</i> MHz	<i>Number of samples</i>	<i>Time window</i> ms	<i>Trace interval</i> s	<i>Average trace interval</i> m
50	2048	4.762	0.5	1.7
100	2048	2.286	0.5	1.7
800	1024	1.968	0.25	0.8

Table 1. *Measurement parameters for each antenna in the GPR survey*

COMPARISON OF ANTENNA FREQUENCIES

Vertical resolution in firn of the 800, 100 and 50 MHz antennas estimated from their bandwidths is about 0.2, 1.4 and 2.5 m, respectively. Thus, the radar response measured with the lower frequencies does not originate from individual layers, but more likely it results from many reflectors as interference patterns (Moore, 1988; Kohler and others, 1997). For the two lower antenna frequencies, the data show no response from the upper 1–2 m due to the length of the transmitted pulse.

Figure 3 shows the radar stratigraphy for the three frequencies along the profile line. To compare the various reflections seen at the different frequencies, we picked the strongest, most continuous reflecting horizons that are visible in more than one profile with different antenna frequencies. The amplitude of the reflections varies from place to place, but we chose the layers that are generally visible throughout the profile. The large range in antenna properties means that only a few layers overlap, and we have picked out two layers that appear on more than one radar profile. We also marked layers 1 and 4, which are only visible in the 800 and 50 MHz data, respectively, to indicate the range of layering available with the different antennas. There are no single continuous reflecting horizons in the 800 MHz profile, but what appear more like reflection bands. The high resolution of the antenna and the relatively long horizontal trace interval (about 0.8 m) probably explains this. The high resolution allows scattering from very thin, discontinuous and weakly reflecting layers to be observed, confusing the general picture. Many strong, continuous layers are visible in the 100 and 50 MHz profiles (Fig. 3).

The subsurface undulation of the radar horizons is consistent in all the GPR profiles. It is widely accepted that the radar layers are isochrones (e.g. Richardson and others, 1997; Morse and others, 1998; Fujita and others, 1999) and that their depth is therefore related to accumulation rates and also to the ice flow. The surface ice-flow velocity is almost perpendicular to the profile (Fig. 1), but at 5 m a^{-1} , even ice that is 100 years old and 50 m deep will have originated only about 500 m away from the profile. The un-

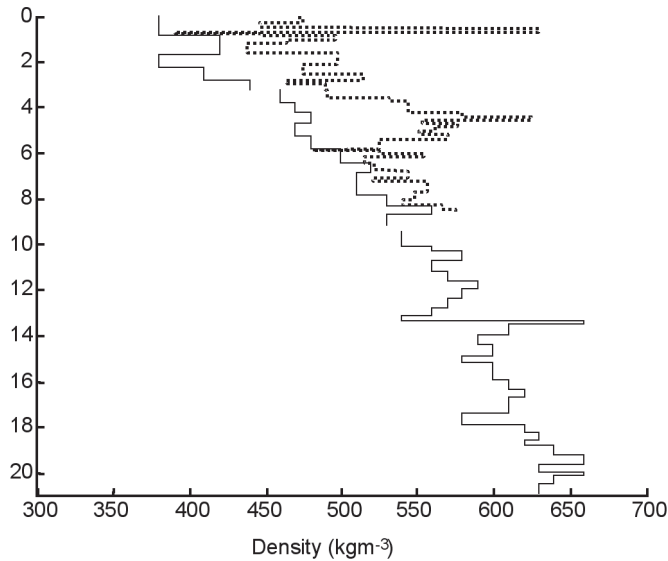


Fig. 2. Density profiles from the 20 m C1 (solid line) and 10 m A2 (dashed line) cores.

dulations of the radar horizons are clearly related to the surface topography along the profile (Fig. 4). There is a small surface hump at about 600–700 m along the profile. Figure 4 shows that the layers are shallowest near the top of this surface hump, though the exact horizontal position of this feature relative to the surface rise is to the north in the radar layers close to the surface and to the south in the deeper layers. The surface elevation is lowest in the beginning of the profile (southern end), and there is another surface trough at 1000 m (Fig. 4). The local layer depth maximum is 200–400 m north of the surface trough, and the depth maximum is further south in deeper layers. The horizontal displacement of the layer depth maximum shows more variation than the layer depth minimum at the surface hump. Ruotoistenmäki and Lehtimäki (1997) provide a map of bedrock topography along the profile, showing a local rise that is about 100 m higher than the bedrock elevation within 1 km on each side of it. This bedrock rise is in the vicinity of the observed surface hump, and must control the surface topography despite local accumulation-rate effects acting to smooth the topography.

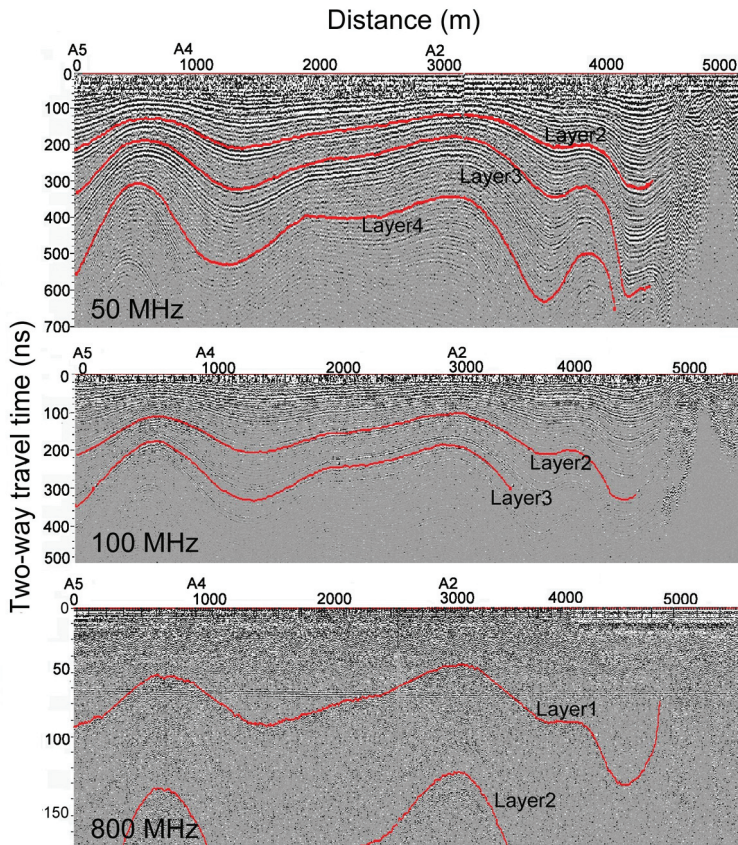


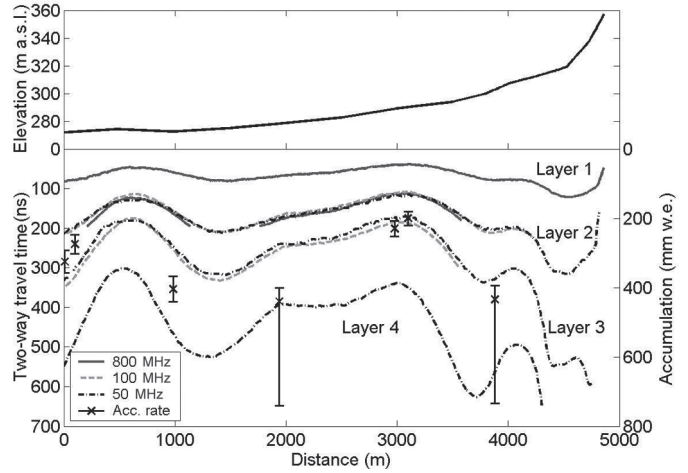
Fig. 3. The complete radar profiles at (top to bottom) 50, 100 and 800 MHz along the 5.5 km profile. Layers 1–4 are marked in the profiles, and ages are modelled at sites A5, A4 and A2 (Table 2).

ACCUMULATION RATES

Accumulation rates along the line are available from two sources. Detailed snow-pit stratigraphy gives accumulation rates at 0.1 and 3.1 km distance (Fig. 4), and from repeat measurements of stake exposure above the snow surface. We use density data from the two pits (at A5 and A2) to estimate water equivalent accumulation. Of five stakes originally placed along the 5 km section of line in January 1997 (personal communication from T. Ruotoistenmäki, 2000), two were not found (presumably they were buried, though they may have been blown away), so we have stake accumulation data spanning 2 years at three sites A5, A4 and A2 (at 0, 0.98 and 2.98 km distance). The buried stakes also give minimum accumulation rates; we assume that 20 cm of the stakes were above the snow surface but could not be seen (data at 1.94 and 3.88 km; Fig. 4).

It can be seen in Figure 4 that the accumulation rates follow the general pattern of highs and lows in the radar layering. However, a direct comparison requires conversion of the radar layering to a real snow depth and then to an age to verify that the layer is at a depth consistent with accumulation rates and density structure at the particular place along the profile. We can neglect the differential layer thinning due to ice flow, as we are

Fig. 4. Four layers seen in the radar profiles (Fig. 3): 800 MHz data shown as solid lines in dark grey, 100 MHz data as dashed lines in light grey, and 50 MHz data as dashdot lines in black. Layer 1 (top) is seen only in 800 MHz data; layer 2 in all data; layer 3 in 50 and 100 MHz data; and layer 4 only in 50 MHz data. The accumulation rates derived from the snow pits and stake measurements are shown as black squares with the error bars. Surface topography along the profile is shown at the top.



concentrating on the top 50 m of the 300–400 m thick ice sheet. To compare how well the accumulation rates measured from the stakes agree with the radar isochrones, we must model the densification rate and age–depth and radar–travel–time–depth relations at locations along the traverse. We do this using the densification model of Herron and Langway (1980) which requires knowledge of surface density, accumulation rate and 10m temperature. We have good data to do this at 0 km, where we have stake accumulation rates and densities from a snow pit, and at site A2 where we also have stake accumulation rates, the ice 10m temperature from the borehole (-17°C) and density. Site A4 (0.98 km) also has good accumulation-rate information, and we assume densities averaged between snow pits. With the Herron and Langway (1980) densification model, the radar two-way travel time t to any layer depth can then be calculated from the empirical equation (Robin, 1975)

$$t = \frac{1}{c} \left\{ \left[(1 + 0.85\rho) \sqrt{l_a^2 + 4D^2} \right] - l_a \right\}, \quad (1)$$

where c is the speed of light, ρ is the average snow density (relative to water) between the surface and a depth D , and l_a is the antenna separation (15 cm for the 800 MHz, 1 m for the 100 MHz and 2 m for the 50 MHz system). We neglect wave refraction within the snowpack since density changes have a negligible effect on wave path length with such small antenna separations.

Table 2 compares the model ages of the four prominent layers seen in Figures 3 and 4 by each antenna at three locations. There is clearly a lot of scatter in the ages derived for the layer. It may be that the radar layering is not an isochrone, possibly because

Table 2. *Model ages (years) of four layers at sites A2, A4 and A5.*

Location (distance in km in Fig. 3)	Layer 1	Layer 2	Layer 3	Layer 4
A5 (0)	15	42–43	69–73	120
A4 (0.98)	8	25–27	39–42	79
A2 (2.98)	9	29–31	47–50	97

Notes: Parameters used in the model: 10 m temperature = -17°C ; A5: $b = 0.325 \text{ m a}^{-1}$, $\rho_{\text{surface}} = 464 \text{ kg m}^{-3}$; A4: $b = 0.404 \text{ m a}^{-1}$, $\rho_{\text{surface}} = 435 \text{ kg m}^{-3}$; A2: $b = 0.23 \text{ m a}^{-1}$, $\rho_{\text{surface}} = 402 \text{ kg m}^{-3}$.

Layer 1: 800 MHz only; layer 2: all antennas except no 800 MHz data at A5; layer 3: 50 and 100 MHz antennas; layer 4: 50 MHz only.

of interference effects. However, the sensitivity to interference effects can be estimated by comparing the ages of layers with the different antennas, which is the range shown in each cell for layers 2 and 3 in Table 2 and is no more than a few years. The degree of scatter in the modeled ages is therefore largely due to the sensitivity of the model to the accumulation rate at each site, which is affected by the rather large interannual variability of precipitation and the snowdensity. Figure 2 shows that the density profiles of cores in the region can differ in the upper few metres, and the pit at A5 has a near-surface density of 464 kg m^{-3} compared with that at A2 of 402 kg m^{-3} . Isaksson and Karlén (1994) report the 1988 and 1989 accumulation rates along an earlier stake line on the same route with about a 50% lower accumulation in 1988 than in 1989. A firn core from about 30 km south of the profile spanning the years 1975–89 showed similar interannual variations and a net decrease from about 45 to 25 cm w.e. a^{-1} over the whole time period (Isaksson and Karlén, 1994). However, Sommer and others (2000) report that decadal variability of 20% in accumulation is typical of Dronning Maud Land, and Richardson and others (1997), on the basis of radar estimates of snow layering, conclude that the area exhibits generally static accumulation patterns with large year-to-year variations, probably due to variations in wind variability accentuated by the local nunataks. These results highlight the errors possible in estimating accumulation rates from very short series of measurements on stakes and on density data from a small number of snow pits.

We may assume that accumulation rates have not changed significantly over the past 100 years at any particular place along the radar profile, and therefore the best age estimate of the layers in Table 2 is the mean of the ages at each site. This procedure allows all the accumulation data to be utilized in a consistent way to derive a set of ages.

From the layer ages, the accumulation is then immediately available along the profile, using the densification model with Equation (1). Using this procedure, the long-term accumulation rate at A5 is rather more than that found from the pit and stake measurements from the last 2 years. If the surface snow density were closer to that at A2 (or indeed to the other pits and ice-core sites in the area, such as C1), then the modeled layer ages would be about 15% less, putting them very close to the A2 estimates.

It is clear that the accumulation-rate data given by each antenna are equally valid, so the difference between the antennas is about the trade-off between resolution and depth of penetration, as all seem adept at following layering that can give accumulation rates. Potentially the 800 MHz radar should reveal individual annual layers, but the variation in layer thickness along the profile in this mountainous region would require more closely spaced traces than are used here.

CONCLUSIONS

Comparison of radar profiles obtained at three different frequencies along a 5.5 km route highlights the complementary layering seen at each frequency. From the practical viewpoint of studying snow accumulation, the higher frequency (800 MHz) obviously gives the best resolution, especially in the upper few metres. However, the scattering of the radar energy from many individual points makes the snow layering harder to follow with the high-frequency antenna. Probably the performance would have been better with a shorter horizontal trace interval. The 50 and 100 MHz profiles give much clearer layering, as they tend to smooth local variations in the snowpack, at the expense of lower vertical resolution, and loss of signal in the upper metres. However, the layering at all frequencies is consistent in terms of its variability along the profile, and seems to be correlated with surface topography (reflecting bed topography) and with accumulation found from snow pits and stake measurements.

Using depth–density and depth–radar–travel-time relations, the age of radar layers can be estimated based on surface estimates of accumulation rate and temperature. We find that this gives ages with rather large scatter for continuous radar layers, which are known to be isochrones. However, the scatter is much more likely to be due to errors in the mass-balance data than to errors in radar interpretation caused by interference effects or lack of resolution. Once the age of a radar layer is determined, the accumulation rate follows from the depth–density–travel-time model used. The radar accumulation measurements have the advantage over traditional stake mass-balance measurements that they can be used to integrate the separate short time series from stake data into more reliable mass-balance measurements by utilizing the fact that the radar layers are isochrones.

ACKNOWLEDGEMENTS

We are grateful to J. Vehviläinen for his help in the field and for providing some of the density data. The 1999/2000 field logistics were provided by the Finnish Antarctic Research Programme (FINNARP) 2000. The work is funded by the Finnish Academy and the Thule Institute. Some GPS data were kindly supplied by E. Asenjo and I. Andersson of the Swedish Antarctic Research Programme (SWEDARP), and T. Ruotoistenmäki provided original stake data. We thank two anonymous reviewers for helpful comments.

REFERENCES

- Fujita, S. and 6 others. 1999. Nature of radio-echo layering in the Antarctic ice sheet detected by a two-frequency experiment. *J. Geophys. Res.*, 104(B6), 13,013–13,024.
- Herron, M.M. and C.C. Langway, Jr. 1980. Firn densification: an empirical model. *J. Glaciol.*, 25(93), 373–385.
- Isaksson, E. and W. Karlén. 1994. Spatial and temporal patterns in snow accumulation, western Dronning Maud Land, Antarctica. *J. Glaciol.*, 40(135), 399–409.
- Kohler, J., J. Moore, M. Kennett, R. Engeset and H. Elvehøy. 1997. Using ground-penetrating radar to image previous years' summer surfaces for mass-balance measurements. *Ann. Glaciol.*, 24, 355–360.
- Moore, J. C. 1988. Dielectric variability of a 130m Antarctic ice core: implications for radar sounding. *Ann. Glaciol.*, 11, 95–99.
- Morse, D.L., E.D. Waddington and E. J. Steig. 1998. Ice age storm trajectories inferred from radar stratigraphy at Taylor Dome, Antarctica. *Geophys. Res. Lett.*, 25(17), 3383–3386.
- Pälli, A. and 6 others. 2002. Spatial and temporal variability of snow accumulation using ground-penetrating radar and ice cores on a Svalbard glacier. *J. Glaciol.*, 48(162), 417–424.
- Richardson, C., E. Aarholt, S.-E. Hamran, P. Holmlund and E. Isaksson. 1997. Spatial distribution of snow in western Dronning Maud Land, East Antarctica, mapped by a ground-based snow radar. *J. Geophys. Res.*, 102(B9), 20,343–20,353.
- Robin, G. de Q. 1975. Velocity of radio waves in ice by means of a bore-hole interferometric technique. *J. Glaciol.*, 15(73), 151–159.
- Ruotoistenmäki, T. and J. Lehtimäki. 1997. Estimation of permafrost thickness using ground geophysical measurements, and its usage for defining vertical temperature variations in continental ice and underlying bedrock. *J. Glaciol.*, 43(144), 359–364.
- Sommer, S. and 9 others. 2000. Glacio-chemical study spanning the past 2 kyr on three ice cores from Dronning Maud Land, Antarctica. 1. Annually resolved accumulation rates. *J. Geophys. Res.*, 105(D24), 29,411–29,421.

PAPER III

DYNAMICS OF THE SCHARFFENBERGBOTNEN BLUE-ICE AREA, DRONNING MAUD LAND, ANTARCTICA

Anna Sinisalo, Aslak Grinsted, John Moore



Photo: FINNARP/Aslak Grinsted

Dynamics of the Scharffenbergbotnen blue-ice area, Dronning Maud Land, Antarctica

Anna SINISALO,^{1,2} Aslak GRINSTED,^{1,2} John MOORE¹

¹Arctic Centre, University of Lapland, P.O. Box 122, FIN-96101 Rovaniemi, Finland
E-mail: anna.sinisalo@ulapland.fi

²Department of Geophysics, University of Oulu, P.O. Box 3000, FIN-90014 Oulu, Finland

Abstract. Ground-penetrating radar (GPR) surveys in Scharffenbergbotnen valley, Dronning Maud Land, Antarctica, complement earlier, relatively sparse data on the ice-flow dynamics and mass-balance distribution of the area. The negative net surface mass balance in the valley appears to be balanced by the inflow. The flow regime in Scharffenbergbotnen defines four separate mass-balance areas, and about 60 times more ice enters the valley from the northwestern entrance than via the narrow western gate. We formalize and compare three methods of determining both the surface age gradient of the blue ice and the dip angles of isochrones in the firn/blue-ice transition zone: observed and dated radar internal reflections, a geometrical model of isochrones, and output from a flowline model. The geometrical analysis provides generally applicable relationships between ice surface velocity and surface age gradient or isochrone dip angle.

INTRODUCTION

Many Antarctic blue-ice areas (BIAs) are known to have very old ice at the surface (Whillans and Cassidy, 1983; Bintanja, 1999). However, the dating of the surface ice is still problematic. The easily recoverable ancient surface ice could be of great value for palaeoclimatic purposes if the dynamics and the internal structure of the BIAs were better known (Bintanja, 1999).

Scharffenbergbotnen is the best-studied Antarctic BIA from the glaciological point of view. However, the flow regime and the surface age distribution of the area are still partially unknown. Flow models and ¹⁴C analysis show that the age of most of the surface blue ice varies between 10 000 and 100 000 years (Van Roijen, 1996; Grinsted and others, 2003), but there are large differences in ages found by each method. No sig-

nificant changes in surface mass balance have been observed over a 14 year measuring period in Scharffenbergbotnen (Sinisalo and others, 2003a). The temporal mass-balance record from the area therefore suggests that the BIA is relatively stable. However, there are large spatial variations in accumulation rates in the valley.

Ground-penetrating radar (GPR) has been successfully used to study the spatial accumulation distribution elsewhere in Antarctica (e.g. Richardson and others, 1997; Sinisalo and others, 2003b). In this paper, we use GPR to study the spatial mass-balance distribution and the internal ice dynamics of Scharffenbergbotnen. We calculate the ages for continuous reflecting horizons taking them to be isochrones, which are then used to complement the accumulation data in the valley. There have been several attempts to model the ice flow in Antarctic BIAs (Naruse and Hashimoto, 1982; Whillans and Cassidy, 1983; Azuma and others, 1985). The ice flow has been modelled in Scharffenbergbotnen by Van Roijen (1996) and Grinsted and others (2003). The latter model is tested here by comparing the modelled isochrones with those observed by GPR near the equilibrium line between the firn and BIAs.

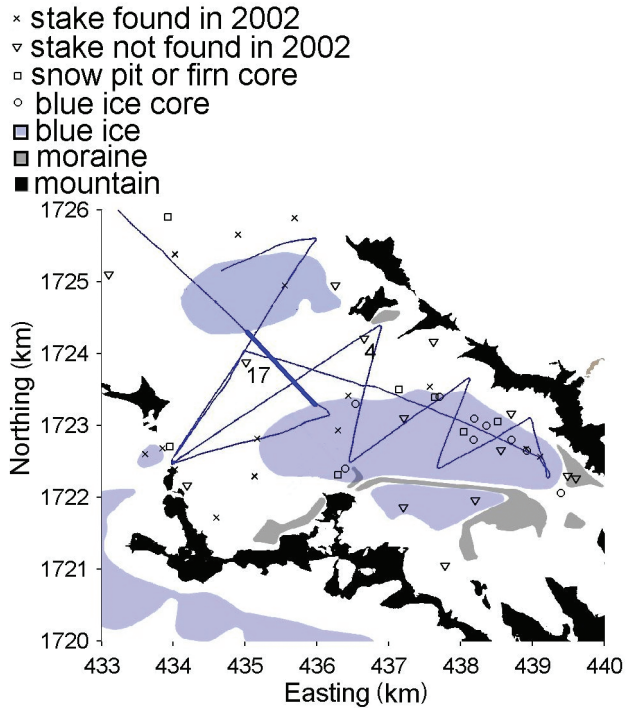
FIELD SITE

Scharffenbergbotnen, northwest Sivorgfjella, Heimefrontfjella, is a closed valley with an inflow from the surrounding ice sheet. There are two separate BIAs in the valley (Fig. 1). Although the BIAs are characterized by ablation, the surrounding glacier firn areas present positive accumulation, with equilibrium lines that approximately follow the perimeter of the BIAs. The large closed-type BIA dammed by the mountains covers the eastern part of the valley. A smaller, open-type BIA where the ice flow is not stopped by mountains forms a surface depression at the northwestern entrance. Ice apparently flows into the valley from the wide northwestern and the shallow, narrow western entrances, and from an icefall at the eastern end of the valley. The maximum ice thickness is about 1000 m (Herzfeld and Holmlund, 1990). The area is described in detail by Jonsson (1992) and Sinisalo and others (2003a). The age of the surface blue ice in Scharffenbergbotnen has been determined by ^{14}C analysis of shallow ice cores. From this analysis the surface ice appeared to be 1 ± 5 kyr old, though occasionally >24 kyr (Van Roijen, 1996). However, the oldest surface ice is >100 kyr old according to the latest flow model (Grinsted and others, 2003).

MEASUREMENTS AND METHODS

The GPR survey (Fig. 1) with precise global positioning system (GPS) was made using a 50 MHz Malå Geoscience pulse radar and the same settings as described in Sinisalo

Fig. 1. *Scharffenbergbotnen valley in western Dronning Maud Land, Antarctica. Map coordinates are Universal Transverse Mercator (UTM) zone 29C determined by precise differential GPS positions; the base map is based on Jacobs and Weber (1993) with map coordinates shifted by 75m eastward and 190m southward to match ground-control points. The GPR lines used to determine the mass-balance distribution in the valley are plotted; the data shown in Figures 3 and 5 are from the thicker-line section.*



and others (2003b). The objective of the survey was to track and date radar isochrones to map the mass balance in the valley, to determine the surface age gradient of the blue ice and to study the dip angles of the isochrones at the firn/blueice transition zone. It is essentially proven that the continuous reflecting horizons detected by GPR represent isochrones in the firn pack (Eisen and others, 2003a, b; Sinisalo and others, 2003b). The two-way travel times t_{tw} of the radar wavelet are converted to the real depths D by using Robin's (1975) expression

$$D = \frac{1}{2} \sqrt{(t_{tw}c - l_a \times 0.85\bar{\rho})(t_{tw}c + 2l_a + l_a \times 0.85\bar{\rho})} \times (1 + 0.85\bar{\rho})^{-1}, \quad (1)$$

where $c = 3 \times 10^8 \text{ ms}^{-1}$ is the speed of light in a vacuum, $\bar{\rho}$ is the mean density of the firn calculated from the surface to the depth D and $l_a = 2 \text{ m}$ is the antenna separation.

A correction for strain thinning of layers with depth must be made in order to calculate the age of the isochrones at each depth. In general, the layers followed are not very close to the bed, and a range of plausible layer-thinning models give very similar results. Hence, the layer thinning with depth is estimated using the simple model by Nye

(1963) which predicts the age T at a depth D_{we} (in water equivalent (w.e.)) via

$$T = -\frac{H}{a_c} \ln \left(1 - \frac{D_{we}}{H} \right), \quad (2)$$

where a_c is the mean accumulation rate in m w.e. a^{-1} , and H is the total ice thickness in m.w.e. The method used to calculate the age of a layer requires some knowledge of accumulation, which can be estimated from the relatively sparse and short-period stake measurements.

The mass-balance distribution was calculated from the stake measurements, firn-core, blue-ice-core and snow-pit studies and the GPR measurements made in the valley (Jonsson, 1992; Grinsted and others, 2003; Sinisalo and others, 2003a). The stakes were also used to measure the horizontal velocity field in the valley (Van Roijen, 1996; Grinsted and others, 2003; Sinisalo and others, 2003a). The locations of these are shown in Figure 1.

RESULTS

Radar isochrone dating

To estimate the surface age gradient in the vicinity of the BIAs from the GPR data the isochrones must be dated first. The density–depth profile was calculated from Herron and Langway (1980) assuming a constant average surface snow density of 400 kg m^{-3} , which appears to be independent of actual accumulation rates at many sites in Antarctica (Spencer and others, 2001). Ice-thickness data come from Herzfeld and Holmlund (1990). To test the dating method, the age of the same isochrone was calculated at its closest points to stakes 4 and 17 (Fig. 1) using the mean accumulation rates over a 6 year period measured from these two stakes (Sinisalo and others, 2003a). The stakes are located on firn, between the two BIAs (Fig. 1). The parameters used and the calculated depths and ages are shown in Table 1. The layer depths obtained correspond to a mean permittivity of 2.8–3.0 over the thickness of the firn pack above the layer. The error in the calculated age for the same layer at stakes 4 and 17 is about 6%. The result is satisfactory when taking into account errors in stake measurements (Sinisalo and others, 2003a).

Mass balance

It is essential to know the surface mass-balance gradient along the flowline in order to calculate the surface age gradient. The accumulation rates along the GPR profiles are calculated by tracking continuous layers. A 3 year mean of the accumulation measured by a Dutch automatic weather station (Fig. 1; Reijmer, 2001) was also used with the

Table 1. Age–depth calculation at the locations of stakes 4 and 17 and the Dutch automatic weather station (AWS) (see Fig. 1)

Stake	Accumulation rate m w.e.	Ice thickness m	Two-way travel time ns	Layer depth m w.e.	Calculated age years
4	0.075	240	527	37.1	542
17	0.040	800	286	19.2	486
AWS	0.284	1200	377	24.1	86

Note: The age and depth are calculated for the same layer at stakes 4 and 17 to test the dating method. The layer studied at the AWS is used to study the massbalance distribution outside of the valley and it is different from the one studied at the stakes.

GPR data to study the accumulation distribution outside of the valley, where no direct stake measurements are available.

Equations (1), (2) and the density–depth profiles are solved iteratively using the mean of the calculated ages for the layers at each GPR sounding along the GPR ground track. The ablation rates on the BIAs were found from stake measurements supplemented by rates from the ^{14}C analysis of ice cores (Van Roijen, 1996; Van der Kemp and others, 2002).

The surface mass-balance map based on the GPR, stake, snow-pit and ice-core measurements is presented in Figure 2a. This shows that the net surface mass balance in the valley is about $-215 \times 10^3 \text{m}^3 \text{a}^{-1}$ (Table 2).

The ice surface velocity is measured from stakes in the valley (Van Roijen, 1996; Sinisalo and others, 2003a) and then interpolated to cover the whole area. Figure 2b shows that the valley can actually be split into different massbalance zones based on the surface velocity data and on the moraine formations. The calculated inflow from the narrow western gate to area B is about $3.7 \times 10^3 \text{m}^3 \text{a}^{-1}$. Thus, the net surface mass balance, $-3.5 \times 10^3 \text{m}^3 \text{a}^{-1}$, of area B is almost exactly balanced by the inflow, and it can be said that area B is in steady state. The influx from the northwestern entrance is much more difficult to define due to sparsity of surface velocity data measured from the stakes. However, the influx through the entrance to area A as outlined in Figure 2b would have to be about $211 \times 10^3 \text{m}^3 \text{a}^{-1}$ to balance the net ablation in the valley. Area C is fed by local accumulation along the side-wall valley nunataks. The total ablation based on the stake measurements in area C is about $64 \times 10^3 \text{m}^3 \text{a}^{-1}$ and it must be balanced by the local accumulation if the area is in steady state. No stake-balance or veloc-

Table 2. *Mass-balance distribution in the valley*

	Net surface acc. 10^3m^3	Net surface abl. 10^3m^3	Total surface mass balance 10^3m^3	Estimated influx 10^3m^3
Area A	144.7	-355.9	-211.2	211
Area B	17.9	-21.4	-3.5	3.7
Total	162.6	-377.3	-214.7	215

Notes: The areas of the mass-balance calculation are outlined in Figure 2b. Influx A is calculated assuming a steady state, and influx B is calculated with a mean velocity of 0.1 m a^{-1} , mean depth of 80 m and width of 460 m.

ity data are available for area D at the eastern end of the valley. However, locations of the moraines and visible bands on aerial photographs (Jacobs and Weber, 1993) allow us to define the boundary between areas A and D. Calculating ablation rates for area D from stakes at the boundary between the areas gives a total ablation of $21 \times 10^3\text{m}^3 \text{ a}^{-1}$ which should be balanced by a flux from the accumulation area on the icefall itself and outside of the valley in steady state. If the area is in balance, a surface velocity of about 0.20 m a^{-1} is needed across the equilibrium line in area D, which is similar to the other measured velocities in the valley.

The visible features of the moraine formations in the valley seen in the aerial photographs provide evidence of flow behaviour in the past. The moraine ridge between areas A and C is well defined and thick. This moraine may indicate that the boundary between areas A and C has remained more or less stationary for a long time. In contrast, the boundary between areas A and B is less well defined and may remain fairly dynamic except for a short but thick moraine at the eastern end of the boundary. This is consistent with changing inflow through the narrow western gate as ice-sheet thickness changed over time. The icesheet elevation was about 20–40 m higher than at present in the vicinity of Scharffenbergbotnen about 6–12 kyr BP (Van Roijen, 1996; Näslund and others, 2000). This would increase flow by 50% through the gate assuming that the ice velocities were unchanged for the period. It would take about 10–20 kyr for this pulse of increased inflow to travel from the gate to the moraine between areas A and B.

The ice velocities and mass balance inside the Scharffenbergbotnen valley are much lower than those typical for the area (Richardson and others, 1997; Näslund and others, 2000; Fig. 2a) and therefore are not simply related to the climate conditions outside of the valley. The ice that enters the valley diverges as the flowline turns south, and slows considerably (Fig. 2b). The flow of ice into the valley is regulated by the extent of the divergence, which is heavily influenced by the ice-sheet mass balance. Much of the ice from the higher-elevation accumulation area does not flow into the valley, but passes across the northwestern valley entrance to the west. During periods of ice-sheet thick-

ening as modelled after the end of the glacial period (Van Roijen, 1996; Näslund and others, 2000), more ice flows into the valley, thereby raising the surface, and eventually inhibiting ice inflow. During periods of thinning, less ice flows into the valley until ablation of the BIA lowers the surface, thereby compensating for reduced influx.

Surface age distribution

The surface age distribution in the firn/blue-ice transition zone can be found in three ways: by the dated GPR isochrones, by considering the geometry of the isochrones and by a flowline model of Grinsted and others (2003).

Three dated GPR layers that were used to determine the surface age gradient are plotted in Figure 3. The ages for the layers were calculated from GPR data at the top of the snow ridge in the vicinity of stake 17 where the layers are flattest and the accumulation rate is higher than elsewhere on the snow area along the flowline. The isochrones were followed to the firn/blue-ice transition zone where they come up to the surface and allow us to determine the surface age gradient.

The along-flow surface age gradient (dT/dx) in the vicinity of the equilibrium line can also be found geometrically. In steady state

$$\frac{DT}{dt} = u \frac{\partial T}{\partial x} + w \frac{\partial T}{\partial z} = 1,$$

where t is time and the horizontal velocity u is constant. We assume that

$$w(x) = \begin{cases} b'x & x < 0 \\ a'x & x > 0 \end{cases}$$

where $w(x)$ is the vertical velocity gradient along the flowline, x is the distance of the outcropping layer from the equilibrium line, and b' and a' are the ablation and accumulation gradients along the flowline. Layer thinning can be ignored in the firn/blue-ice transition zone for the near-surface layers. In steady state it can be written

$$\frac{dT}{dx} = \frac{1}{u} \left(1 + \sqrt{\frac{b'}{a'}} \right). \quad (3)$$

If the ablation-rate and accumulation-rate gradients are similar, the righthand side of Equation (3) reduces to $\sim 2/u$. From Figure 2 it can be seen that a' is perhaps 1–2 times b' along the flowline, giving an age gradient from Equation (3) of 7–10 years m^{-1} using a mean surface velocity of 0.2 $m a^{-1}$ in the firn/blue-ice transition zone (Fig. 2b).

The flowline model (Grinsted and others, 2003) was used at very high resolution in the equilibrium zone and gave a surface age gradient of about 8 years m^{-1} , whereas the horizontal age gradient derived from the GPR data is about 3–6 years m^{-1} (Fig. 3). Thus, the flowline model and Equation (3) are very consistent, while the observed radar isochrones give a lower gradient. There are several possible reasons for the discrepancy.

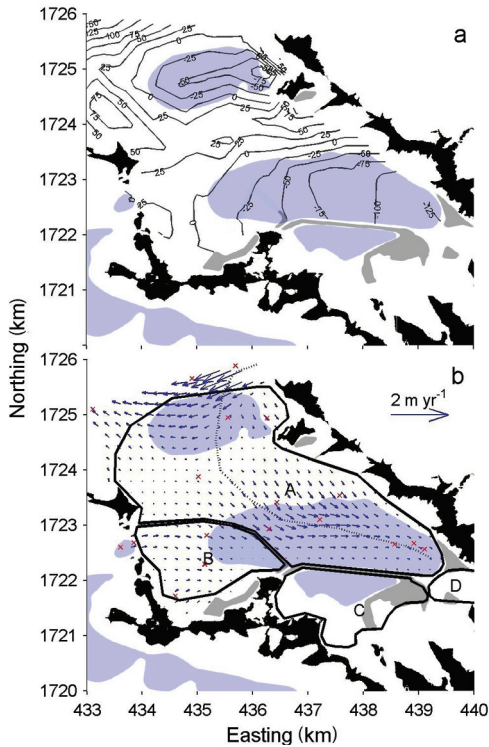


Fig. 2. Same as Figure 1, but showing (a) mass-balance distribution (mm m.e.) in the valley interpolated from stake, GPR, snow-pit and ice-core data; and (b) velocity distribution in the valley interpolated from stake data and areas of different ice origin. The modelled flowline (Grinsted and others, 2003) is shown as a dashed line in (b).

Model input data of accumulation rates are averaged over a larger area than is used in the age calculation for the GPR horizons near stake 17. The surface density doubles in the firn/blue-ice transition zone in a relatively short distance, so there is also a horizontal gradient for the permittivity. However, without any detailed measurements this has been ignored in the migration of the GPR isochrones. The equilibrium line may also have migrated over time, i.e. non-steadystate condition, though its impact is hard to estimate and appears contrary to recent observation (Sinisalo and others, 2003a).

Dip angles of isochrones

The dip angles of GPR layers can be compared with the dip angles from geometric arguments, and also with those from the flowline model isochrones (Grinsted and others, 2003). The GPR data were migrated to obtain true angles for the dipping horizons assuming a constant permittivity of 2.9, which is consistent with Table 1, and mean density of 800 kg m^{-3} for the firn pack above the layers. The angles are calculated from depths in m.w.e.

The processed GPR layers come up from the accumulation areas towards the BI-As at an angle of $1\text{--}7^\circ$ relative to the surface (Fig. 4). The measured angles are corrected by a factor of $1/\cos \theta$, where θ is the horizontal angle between the GPR ground track and the ice-flow vector, in order to obtain along-flow dip angles and to compare them

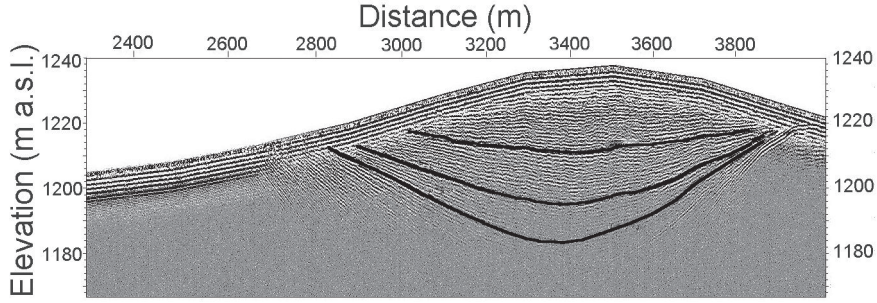


Fig. 3. A GPR section over the snow ridge between the BIAs in the valley (see Fig. 1). The main BIA is on the left side of the snow ridge, and the smaller BIA on the right side. Ice flows from right to left in the figure. Note that the data are not migrated, i.e. the dip angles of the layers appear steeper than they actually are. The ages of the marked layers are 504, 853 and 1122 years.

with the modelled isochrones.

Ideally, a single layer should be followed through each transition zone in the GPR data. However, this cannot be done due to the gaps in the data when they cross BIAs, so instead we consider layers from approximately the same depth. The angles in Figure 3 are calculated for two layers of 20 and 30 m maximum depth to give a range. For the layers at the northern entrance of the valley, the dip angles are low, as may be expected from the high velocity in the area. The 2° angle seen at the western edge of the main BIA is due to the very low ablation-rate gradient there rather than high velocities.

The dip angle of an isochrone can also be calculated if the horizontal velocity u and the ablation and accumulation gradients b' and a' are known. From the layer geometry, we obtain for the dip angle α

$$\begin{aligned} \tan \alpha &= \frac{\left(\frac{\partial T}{\partial x}\right)}{\left(\frac{\partial T}{\partial z}\right)} = -\frac{a'x\sqrt{\frac{b'}{a'}}}{u} \left(1 + \sqrt{\frac{b'}{a'}}\right) \\ &= -\frac{x}{u} \left(\sqrt{a'b'} + b'\right). \end{aligned} \quad (4)$$

Equation (4) shows the linear dependence of the dip angle on the horizontal distance x from the equilibrium line. This is consistent with the GPR data which show near-surface layers less steep than the deeper ones (Fig. 3). However, our goal here is to demonstrate the relative changes in the dip angles on different sides of the BIAs with different flow velocities and mass-balance gradients, and this we can do using layers from a small depth range.

The GPR layers and the flowline-model isochrones in the snow ridge between

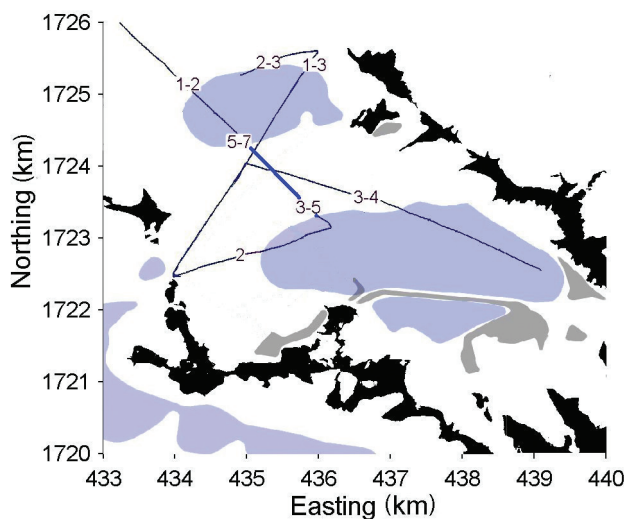


Fig. 4. Same as Figure 1, but showing the dip angles ($^{\circ}$) of isochrones relative to the surface from migrated GPR profiles across the equilibrium line to demonstrate the relative differences in them due to different horizontal velocities and mass-balance gradients. The angles are corrected for ice-flow direction to be true dip (see Fig. 2b).

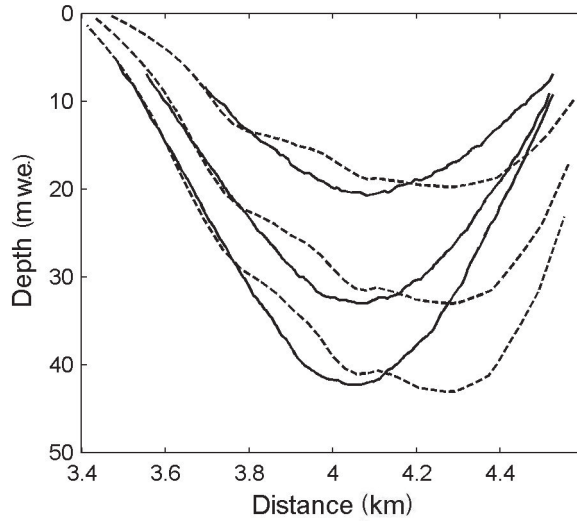
BIAs are plotted in Figure 5. The dip angles of both the observed and modelled isochrones are $3\text{--}5^{\circ}$ at the firn/blue-ice transition zone of the main BIA. There is a relative lack of agreement in the length of the isochrones, because the modelled flowline (Fig. 2b) and the GPR profile (Fig. 1) do not overlap all the way over the snow ridge. They separate at about 4 km in Figure 5 where the modelled flowline makes a curve whereas the GPR profile directly crosses it. As the ice flows from the small BIA to the firn area on the right side of the snow ridge in Figure 4, the layers dip more steeply, which is expected due to the lower surface velocity on that side of the ridge (Equation (4)) and is also predicted by the flowline model of Grinsted and others (2003).

CONCLUSIONS

The net surface mass balance in the Scharffenbergbotnen valley is about $-215 \times 10^3 \text{ m}^3 \text{ a}^{-1}$ which appears to be balanced by the inflow. The inflow through two gates and an icefall, together with accumulation along the valley sidewalls, leads to four separate mass-balance areas in the valley that are delineated by moraine formations. The limited evidence indicates that the area is close to balance, in which case about 60 times more ice enters the valley from the northwestern entrance than via the narrow western gate.

The blue-ice surface age distribution was obtained by three methods: by dated GPR isochrones, by considering the geometry of the isochrones and by a flowline model. They give values of $3\text{--}10 \text{ years m}^{-1}$ for the age gradient along a modelled flowline near the equilibrium line. The dated GPR isochrones give lower values ($3\text{--}6 \text{ years}$

Fig. 5. Modelled isochrones (dashed lines) and the measured GPR horizons from Figure 3 (solid lines) in the snow ridge between the BLAs. The GPR section shown here is marked with a thicker line in Figure 4.



m^{-1}) than are found from the calculations based on the geometry and the flowline model which are consistent with each other. The discrepancy may be caused by different accumulation rates used in the flowline model and in the age calculation for the GPR horizons. Some of the assumptions made in the GPR data processing may also be responsible, although the extent of their combined impact is difficult to estimate. The equilibrium line may have migrated over time, though its impact is also hard to estimate and appears contrary to recent observation (Sinisalo and others, 2003a).

The flowline model was originally designed for broaderscale dating of blue ice, but the comparison with observational data shows that it gives promising results even over small scales. Equation (3) can be used to make a first estimation of the surface age gradient of a BIA if the horizontal velocity and mass balance are known. Equations (3) and (4) can be used to estimate the ice velocity if GPR data over the outcropping isochrones are available and the mass-balance gradients are known.

ACKNOWLEDGEMENTS

We thank J. Vehviläinen for help in the field and for providing data, and R. Petterson for helping us to collect the old datasets. We also thank P. Jansson and an anonymous referee for useful comments. The Finnish Antarctic Research Programme (FINNARP) 1999–2001 provided field logistics. The work is funded by the Finnish Academy and the Thule Institute.

REFERENCES

- Azuma, N., M. Nakawo, A. Higashi, F. Nishio and S. Kawaguchi. 1985. Flow pattern near massif A in the Yamato bare ice field estimated from the structures and the mechanical properties of a shallow ice core. *Nat. Inst. Polar Res. Mem., Ser. Special Issue*, 39, 173–183. (Proceedings of the Seventh Symposium on Polar Meteorology and Glaciology, National Institute of Polar Research, Tokyo.)
- Bintanja, R. 1999. On the glaciological, meteorological and climatological significance of Antarctic blue ice areas. *Rev. Geophys.*, 37(3), 337–359.
- Eisen, O., F. Wilhelms, U. Nixdorf and H. Miller. 2003a. Identifying isochrones in GPR profiles from DEP-based forward modeling. *Ann. Glaciol.*, 37, 344–350.
- Eisen, O., F. Wilhelms, U. Nixdorf and H. Miller. 2003b. Revealing the nature of radar reflections in ice: DEP-based FDTD forward modeling. *Geophys. Res. Lett.*, 30(5), 1218–1221. (10.1029/2002GL016403.)
- Grinsted, A., J. C. Moore, V. Spikes and A. Sinisalo. 2003. Dating Antarctic blue ice areas using a novel ice flow model. *Geophys. Res. Lett.*, 30(19), 2005. (10.1029/2003GL017957.)
- Herron, M. M. and C. C. Langway, Jr. 1980. Firn densification: an empirical model. *J. Glaciol.*, 25(93), 373–385.
- Herzfeld, U. C. and P. Holmlund. 1990. Geostatistics in glaciology: implications of a study of Scharffenbergbotnen, Dronning Maud Land, East Antarctica. *Ann. Glaciol.*, 14, 107–110.
- Jacobs, J. and K. Weber. 1993. *Scharffenbergbotnen, 11° 118'W, 74° 137'S*. (Scale 1: 25 000.) Frankfurt am Main, Institut für Angewandte Geodäsie. (Geological Map.)
- Jonsson, S. 1992. Local climate and mass balance of a blue-ice area in western Dronning Maud Land, Antarctica. *Z. Gletscherkd. Glazialgeol.*, 26(1), [1990], 11–29.
- Näslund, J.-O., J. L. Fastook and P. Holmlund. 2000. Numerical modelling of the ice sheet in western Dronning Maud Land, East Antarctica: impacts of present, past and future climates. *J. Glaciol.*, 46(152), 54–66. (Erratum: 46(153), p. 353–354.)
- Naruse, R. and M. Hashimoto. 1982. Internal flow lines in the ice sheet upstream of the Yamato Mountains, East Antarctica. *Nat. Inst. Polar Res. Mem., Ser. Special Issue*, 24, 201–203. (Proceedings, 4th Symposium on Polar Meteorology and Glaciology, 1982.)
- Nye, J. F. 1963. Correction factor for accumulation measured by the thickness of the annual layers in an ice sheet. *J. Glaciol.*, 4(36), 785–788.
- Reijmer, C.H. 2001. Antarctic meteorology: a study with automatic weather stations. (Ph.D. thesis, University of Utrecht.)
- Richardson, C., E. Aarholt, S.-E. Hamran, P. Holmlund and E. Isaksson. 1997. Spatial distribution of snow in western Dronning Maud Land, East Antarctica, mapped by a ground-based snow radar. *J. Geophys. Res.*, 102(B9), 20,343–20,353.
- Robin, G. de Q. 1975. Velocity of radio waves in ice by means of a bore-hole interferometric technique. *J. Glaciol.*, 15(73), 151–159.
- Sinisalo, A., A. Grinsted, J. C. Moore, E. Kärkäs and R. Pettersson. 2003. Snow-accumulation studies in Antarctica with groundpenetrating radar using 50, 100 and 800 MHz antenna

- frequencies. *Ann. Glaciol.*, 37, 194–198.
- Sinisalo, A., J. C. Moore, R. S.W. van de Wal, R. Bintanja and S. Jonsson. 2003. A 14 year mass-balance record of a blue-ice area in Antarctica. *Ann. Glaciol.*, 37, 213–218.
- Spencer, M. K., R. B. Alley and T. T. Creyts. 2001. Preliminary firn densification model with 38-site dataset. *J. Glaciol.*, 47(159), 671–676.
- Van der Kemp, W. J. M. and 7 others. 2002. *In situ* produced ^{14}C by cosmic ray muons in ablating Antarctic ice. *Tellus*, 54B(2), 186–192.
- Van Roijen, J. J. 1996. Determination of ages and specific mass balances from ^{14}C measurements on Antarctic surface ice. (Ph.D. thesis, Universiteit Utrecht, Faculteit Natuur- en Sterrenkunde, Utrecht.)
- Whillans, I. M. and W. A. Cassidy. 1983. Catch a falling star: meteorites and old ice. *Science*, 222(4619), 55–57.

PAPER IV

INFERENCES FROM STABLE WATER ISOTOPES ON THE HOLOCENE EVOLUTION OF SCHARFFENBERGBOTNEN BLUE- ICE AREA, EAST ANTARCTICA

Anna Sinisalo, Aslak Grinsted, John C. Moore,
Harro A.J. Meijer, Tõnu Martma, Roderik S.W. van de Wal



Photo: FINNARP/ Aslak Grinsted

Inferences from stable water isotopes on the Holocene evolution of Scharffenbergbotnen blue-ice area, East Antarctica

Anna SINISALO,^{1,2} Aslak GRINSTED,^{1,2} John C. MOORE,¹
Harro A.J. MEIJER,³ Tõnu MARTMA,⁴ Roderik S.W.VAN DE WAL⁵

¹Arctic Centre, University of Lapland, PO Box 122, FIN-96101 Rovaniemi, Finland
E-mail: anna.sinisalo@ulapland.fi

²Department of Geophysics, Box 3000, University of Oulu, FIN-90014 Oulu, Finland

³Centre for Isotope Research (CIO), University of Groningen, Nijenborgh 4,
9747 AG Groningen, The Netherlands

⁴Institute of Geology, Tallinn University of Technology, 7 Estonia Avenue, EE-10143 Tallinn, Estonia

⁵Institute for Marine and Atmospheric Research Utrecht, Utrecht University,
3508 TA Utrecht, The Netherlands

Abstract. We show that it is possible to extract a high-resolution (annual) paleoclimate record from the surface of a blue-ice area (BIA). The variability of the surface stable-isotope values suggests that almost all the surface ice in Scharffenbergbotnen BIA, East Antarctica, is of Holocene age. The isotopic changes across the BIA show that the modern climate there is warmer than the climate in the early-Holocene optimum (11 kyr BP). A volume-conserving ice flow model for the BIA constrained by isotopic variability and layer thicknesses, and a series of ¹⁴C ages indicate both that the BIA has been smaller than now, and that the surface velocities were considerably smaller during the Last Glacial Maximum. Changes in ice-sheet thickness drive the BIA towards present-day conditions. The relatively young age of the majority of the BIA also explains the lack of meteorite finds in this area, and may be typical for many BIAs in low-elevation nunatak areas.

I. INTRODUCTION

Antarctic blue-ice areas (BIAs) are known to have old ice at the surface (e.g. Whillans and Cassidy, 1983; Nishiizumi and others, 1989; Bintanja, 1999). Ablation in Antarctic blue-ice areas above 1000m is overwhelmingly dominated by sublimation rather than

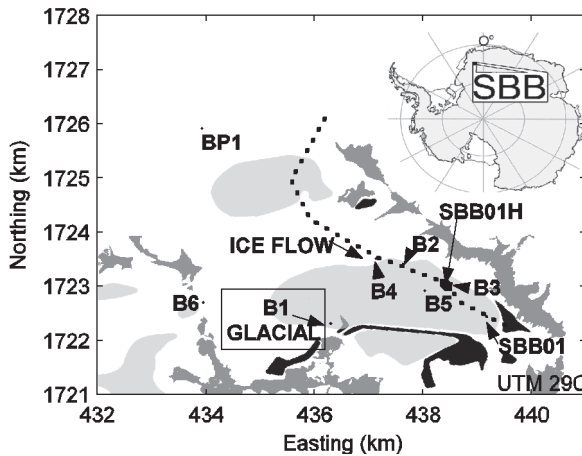


Fig. 1. Locations of the shallow blue-ice cores (B1–B5), firn core (B6), snow pit (BP1), the 100 m horizontal ice core (SBB01H) and the 52 m vertical core (SBB01) in Scharffenbergbotnen (SBB). Supraglacial moraines are marked in black, mountains in dark gray and blue ice in light gray. The ice flow is from northeast into the valley (dotted line). The ice passes through a small BIA and then terminates in the main BIA close to SBB01.

melting (Bintanja, 1999). Such ice is likely to contain a high-resolution paleoclimate record that is easier to access than traditional deep ice cores. The dating of surface blue ice is, however, demanding. Previously, blue-ice samples from various BIAs have been dated by terrestrial ages of meteorites found on their surface (e.g. Whillans and Cassidy, 1983; Nishiizumi and others, 1989), by ^{14}C dating of ice (Van Roijen and others, 1995; Van der Kemp and others, 2002), by radiometric dating of tephra layers found at the surface of BIAs (Wilch and others, 1999) and by stratigraphic comparison with ice cores (Moore and others, 2006).

Isotopic composition of polar snow and ice has been regarded as a valuable temperature proxy in East Antarctica for decades (e.g. Lorius and Merlivat, 1977). Here, we make use of the ratios of heavy to light atoms of both oxygen and hydrogen expressed as $\delta^{18}\text{O}$ and δD values, respectively. The deuterium-excess, d ($d = (\delta\text{D} - \delta)\delta^{18}\text{O}$), is assumed to depend mainly on the physical conditions in the source area for mid- and high-latitude precipitation. Changes in d are traditionally used as indicators of changes in the average temperature of oceanic moisture sources (Merlivat and Jouzel, 1979; Petit and others, 1991; Vimeux and others, 2001). However, Helsen and others (2006) showed that the vertical gradient in d excess over the moisture source area and the kinetic fractionation along the transport path have a prominent influence on the observed d values.

There are very few paleoclimate data records from Antarctic BIAs. The only continuous horizontal stableisotope record, i.e. a $\delta^{18}\text{O}$ record extracted from an ice sample cut from the surface of a BIA along the flowline, has been extracted from Mount Moulton (76°S , 135°W ; 2800 m a.s.l.) and covers 140 000 years (Popp and others,

2004). However, this record does not include the Holocene since that part of the BIA was covered by snow when sampling was done.

Here we focus on the surface blue ice in Scharffenbergbotnen BIA, Dronning Maud Land (DML), (74° S, 11° W; 1200 m a.s.l.), where there is some uncertainty in the dating. Some authors argue that glacial ice is present at the eastern end of the valley (Van Roijen, 1996; Grinsted and others, 2003), but others have suggested, in general terms, that BIAs in DML may have been an accumulation area during the glacial period (Bintanja, 1999). In this paper, we show that almost all the surface ice in the area is Holocene, based on the variability of the stable-isotope values. We study the spatial and temporal isotopic changes in the BIA in terms of climate variability, and compare results with other East Antarctic sites. Finally, we show results of a simple model on how the dynamics of the BIA may have evolved since the Last Glacial Maximum (LGM).

2. BACKGROUND

2.1. Study area

Scharffenbergbotnen (Fig. 1) is the best-studied Antarctic BIA. It is a valley located in the Heimefrontfjella mountain range at the edge of the Antarctic plateau about 350 km from the coast. Several studies have been made of its mass balance (Jonsson and Holmlund, 1990; Jonsson, 1992; Sinisalo and others, 2003), ice flow and surface age distribution (Van Roijen, 1996; Grinsted and others, 2003; Sinisalo and others, 2004), on the blue-ice surface properties (Bintanja and others, 2001) and on the moraines in the area (Lintinen and Nenonen, 1997; Hättestrand and Johansen, 2005).

The meteorological conditions in the valley and surrounding area are described in detail by, for example, Bintanja and Van den Broeke (1995a, b), Bintanja (2000a, b), Bintanja and Reijmer (2001) and Reijmer (2001). The annual average temperature is about -20°C and wind speed is $\sim 7\text{ m s}^{-1}$ (Reijmer, 2001). Scharffenbergbotnen is located in the lee side of the nunataks, and geostrophically and katabatically forced winds blow from easterly directions (Bintanja, 2000b). The precipitation is characterized by a highly intermittent accumulation record (Reijmer and Van den Broeke, 2003) with large spatial variations in the valley (Sinisalo and others, 2003). The present-day moisture source area is in the southern Atlantic Ocean (Reijmer, 2001; Helsen and others, 2006).

The meteorological conditions over the BIA differ from those over the snow-covered surroundings as the air over the BIA is warmer and the relative humidity is lower than over a snow site (Bintanja and Reijmer, 2001). These conditions contribute to the observed high sublimation rates of blue ice. Surface sublimation over the BIA is significantly higher than over snow (Bintanja and Reijmer, 2001), being $>0.1\text{ m w.e. a}^{-1}$ at the southeastern end of the valley (e.g. Sinisalo and others, 2003). Slight surface melting occurs during a few high-insolation days in the BIA. The surface water film, however, is

subsequently refrozen and removed by sublimation.

The main BIA in Scharffenbergbotnen is of the closed type, i.e. the ice has no outflow from the valley (Grinsted and others, 2003), and therefore it must have old ice at the surface if it is in steady state. According to geomorphological studies of Hättestrand and Johansen (2005), the difference between the surface elevation in Scharffenbergbotnen and outside the valley is greater today than when the ice sheet was thickest, which probably occurred during the LGM. The debris cover of the supraglacial moraines on the surrounding slopes in and outside Scharffenbergbotnen suggests that the ice surface in the valley was 200–250 m higher, and the elevation of the surrounding ice sheet only 50–150 m higher, at the LGM than today (Hättestrand and Johansen, 2005). The elevation decrease in the valley probably occurred gradually after the surrounding ice-sheet elevation had decreased after the LGM and ice overflow of the nunataks at the eastern end of the valley became insignificant. A decrease in surface elevation relative to the surrounding nunataks results in stronger katabatic flow, which has a positive feedback to the extent of a BIA (Van den Broeke and Bintanja, 1995). The moraine structures strongly suggest that the inner part of Scharffenbergbotnen must have been a local ablation area during the LGM; i.e. a BIA has long existed in the valley (Hättestrand and Johansen, 2005).

2.2. Sample locations

A 52 m long vertical ice core (SBB01 in Fig. 1) was drilled in the innermost part of the valley close to the end of the current flowline during the austral summer of 1997/98 (R. Bintanja and others, unpublished information). A 100 m horizontal ice core (SB-B01H in Fig. 1) was collected, using electric chainsaws, from the surface of the BIA 1 km upstream from SBB01 in 2003/04. Approximately the top 20 cm was cut off from the samples in order to remove a possible refrozen meltwater layer in the high-insolation period, and to avoid any other disturbances from surface processes that may have influenced the ice composition.

In addition, a 10 m firn core (B6) and five 3m shallow cores (B1–B5) were drilled in the austral summer 1999/2000 (Fig. 1). In the same field season, a 2m snow pit (BP1) was also sampled at the northwestern entrance to the valley (Fig. 1). The details of the subsampling of the blue-ice cores and snow and firn samples are collated in Table 1.

2.3. Previous dating of Scharffenbergbotnen blue ice

Several blue-ice samples were dated using the ^{14}C method described by Van Roijen and others (1994) and Van der Kemp and others (2002) and converted to calendar ages using the radiocarbon calibration curve of Reimer and others (2004). The surface ages at the main BIA varied between 4000 and 14 000 years along the flowline (Fig. 1). These ages, however, have large uncertainties of up to several thousands of years. The ^{14}C age

for the uppermost 45 m section of the SBB01 is 9300 ± 400 years (Van der Kemp and others, 2002) which corresponds to a calibrated calendar age of 10 500 (+700, -300) years. Unfortunately, a vertical age span cannot be determined for the ice core from the ^{14}C data.

Van Roijen (1996) used a numerical model of the ice flow in the valley based on the shallow-ice approximation and compared its results to the ^{14}C dating of the ice samples. He obtained surface ages of up to 60 000 years at the end of the flowline at the eastern end of the valley using three different surface velocity and mass-balance scenarios. Grinsted and others (2003) modelled the ice flow in the valley with a volume-conserving model which assumes constant ice-sheet geometry over time, i.e. steady-state flow. The flowline (Fig. 1) was chosen based on the measured velocity data (Van Roijen, 1996; Sinisalo and others, 2003) and is more realistic than the flowline that Van Roijen (1996) used, although the differences are not crucial. Grinsted and others (2003) used the measured accumulation and surface velocities (Van Roijen, 1996; Sinisalo and others, 2003) as input parameters, and obtained very old ages ($\sim 100\,000$ years) for the ice at the end of the flowline. The difference between the modelled ages is most likely due primarily to different grid resolutions at the end of the flowline where the ages are highest.

3. METHODS

3.1. Isotopic analysis

The $\delta^{18}\text{O}$ and δD analyses of the SBB01H and SBB01 cores were made at the Centre for Isotope Research, University of Groningen, The Netherlands. The $\delta^{18}\text{O}$ measurements were performed with a Sira-10 isotope-ratio mass spectrometer with an adjacent $\text{CO}_2\text{-H}_2\text{O}$ isotopic equilibrium system. The δD measurements were performed using a continuousflow system, consisting of a Eurovector chromium reduction oven coupled to a GVI Isoprime. The accuracy (combined uncertainty) of $\delta^{18}\text{O}$ analysis was $\pm 0.06\text{‰}$ and of δD $\pm 0.7\text{‰}$. The $\delta^{18}\text{O}$ analysis of the 3m blue-ice cores, and the 10 m firn core and 2 m snow pit was performed at the University of Technology, Tallinn, Estonia, using a Finnigan- MAT Delta-E mass spectrometer. Combined uncertainty of the analyses was better than $\pm 0.1\text{‰}$. The $\delta^{18}\text{O}$ and δD are both presented with respect to the international consensus Vienna Standard Mean Ocean Water – Standard Light Antarctic Precipitation (V-SMOW–SLAP) scale (R. Gonfiantini, unpublished information). The accuracy of d excess is $\pm 1.3\text{‰}$.

3.2. Isotopic paleothermometer

We use the isotope record as an indicator of local temperature change in Scharffen-

bergbotnen and compare it with other sites from East Antarctica. Although the time-spans of the individual isotope samples from the blue-ice cores are not known, based on present-day accumulation rates (Sinisalo and others, 2003), it is plausible to assume that most of our samples span time periods of several years to centuries. Hence, the influence of seasonal extreme isotopic and temperature values that could invalidate the classical temperature interpretation of isotopic variability is minimized (Helsen and others, 2005). However, it is necessary to make corrections both for elevation changes in Scharffenbergbotnen during the Holocene and for different ocean surface isotopic composition in the early Holocene. Thus, we calculate a change in $\delta^{18}\text{O}$ values due to temperature change, $\Delta\delta^{18}\text{O}_{\text{temp}}$, as

$$\Delta\delta^{18}\text{O}_{\text{temp}} = \delta^{18}\text{O}_m - (\Delta\delta^{18}\text{O}_{\text{EC}} + \gamma_m\Delta\delta^{18}\text{O}_{\text{SW}}), \quad (1)$$

where $\delta^{18}\text{O}_m$ is the difference between the average $\delta^{18}\text{O}$ values measured at two sites of different age (Fig. 1), $\Delta\delta^{18}\text{O}_{\text{EC}}$ is the change associated with elevation change in time, $\Delta\delta^{18}\text{O}_{\text{SW}}$ is the change in isotopic composition of ocean surface waters in time due to deglaciation and $m (= 0.6)$ is the temporal sensitivity of $\delta^{18}\text{O}$ to the changes in marine isotopic composition (Vimeux and others, 2002; Kavanaugh and Cuffey, 2003).

In addition, there are other factors, such as changes in the water-vapor source area (Kavanaugh and Cuffey, 2003), changes in precipitation seasonality (Werner and others, 2001) and changes in the strength of the temperature inversion (Van Lipzig and others, 2002), which may have influenced isotopic changes in the Holocene. We assume here that these factors are secondary and can be discarded. We justify this assumption for some cases in section 4.2.

The decrease in surface elevation of 200–250 m in Scharffenbergbotnen during the Holocene (Hä ttestrand and Johansen, 2005) corresponds to a change of 9.3–12‰ in δD (1.2–1.5‰ in $\delta^{18}\text{O}$) using the present-day altitudinal lapse rate for $\delta^{18}\text{O}$ values of 5.8‰ km^{-1} (Isaksson and Karlén, 1994). This lapse rate is calculated for $\delta^{18}\text{O}$ values measured from 10m firn cores covering 15–30 years of accumulation along a traverse that crossed the Scharffenbergbotnen area. We calculate a standard error, EC, for $\Delta\delta^{18}\text{O}_{\text{EC}}$ of $\pm 0.1\text{‰}$. The $\Delta\delta^{18}\text{O}_{\text{SW}}$ was about +1.1‰ at the LGM compared with the present value (Labeyrie and others, 1987), and it was still +0.2‰ at 10 000 years BP (Waelbroeck and others, 2002).

The temperature change corresponding to a known $\Delta\delta^{18}\text{O}_{\text{temp}}$ can be calculated using the present-day spatial isotopic temperature gradient in Antarctica as a surrogate for the temporal isotopic temperature gradient (Delaygue and others, 2000; Masson and others, 2000; Jouzel and others, 2003). In this study, we use an isotopic temperature gradient of 1.16‰ K^{-1} from Isaksson and Karlén (1994). The gradient is greater than found elsewhere in Antarctica but it is calculated for samples drilled very close to our study area. We estimate that the error, $\sigma_{\text{temp}} = \pm 0.28\text{‰ K}^{-1}$.

Core	Depth/length m	Number of samples	Sample length cm
SBB01	25.9–31.1	25	1
		23	3
		10	18–26
SBB01H	100.4	87	45–140 (average 112)
		27	2
B1–B5	2.7–3.0	4	2
B6	10.0	28	2–24
BP1	2.1	17	2–3

Table 1. Sampling depth/length, number of subsamples (n) and length of each subsample for the vertical blue-ice core B1–B5 and SBB01, for the firn core B6, the snow pit BP1 and the horizontal blue-ice core, SBB01H

4. RESULTS AND DISCUSSION

The mean values of the stable-isotope ratios, $\delta^{18}\text{O}$, and the population standard deviations (in‰) for each core or pit are presented in Figure 2. The confidence interval (at 95‰ level) was less than $\pm 0.7\%$ for all the $\delta^{18}\text{O}$ mean values. Table 2 shows measured $\delta^{18}\text{O}$ and δD values and the population standard deviations (in ‰) for SBB01 and SBB01H.

4.1. Age estimation of blue ice

Different climatic periods have different signatures in stable isotopes (e.g. Petit and others, 1999). We determine whether the samples at a given site were deposited during a glacial or an interglacial period simply from the isotopic composition.

A rapid change of $\sim 40\%$ in δD (5‰ in $\delta^{18}\text{O}$) in Antarctic ice is an indicator of a change between interglacial and glacial climates (e.g. EPICA Community Members, 2006). Climate variability within the Holocene as measured along the EDML core (75° S, 0° E; 2900 m a.s.l.), the closest deep core to the study site in East Antarctica, causes changes of $< 2\%$ in $\delta^{18}\text{O}$ in the centennial-scale variability, and the maximum difference in decadal means of $\delta^{18}\text{O}$ is $\sim 5\%$ for Holocene ice (H. Oerter, <http://doi.pangaea.de/10.1594/PANGAEA.264634>). The standard deviation of the $\delta^{18}\text{O}$ values measured from B2–B5 in Figure 1 is $< 1.8\%$, and the difference between $\delta^{18}\text{O}$ values measured from B2–B5 and the present-day value of -28.5% , taken as an average from

Core	Number of samples	Mean $\delta^{18}\text{O}$ %	Std dev. $\delta^{18}\text{O}$ %	Mean δD %	Std dev. δD %	Mean d %	Std dev. d %
SBB01H all	69 ^a , 87 ^b	-31.9	0.9	-251.6	7.3	3.7	0.9
SBB01 all	58	-30.9	0.4	-238.5	3.0	8.6	1.1

^aNumber of $\delta^{18}\text{O}$ samples.

^bNumber of δD samples.

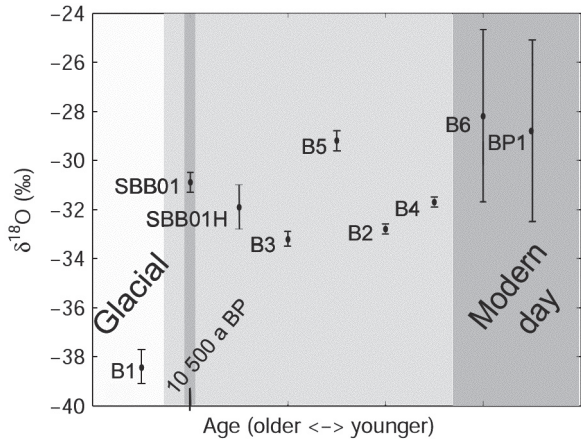
Table 2. *The mean values of the stable-isotope ratios $\delta^{18}\text{O}$ and δD and the population standard deviations (in %) for the vertical blue-ice core SBB01 and the horizontal blue-ice core SBB01H, the number of the samples and calculated deuterium excess, d*

B6 and BP1, is $<4\%$. In addition, geomorphological evidence suggests the blue-ice samples B2–B5 originate from a higher elevation (Hä ttestrand and Johansen, 2005). The correction of the elevation change would make the difference in $\delta^{18}\text{O}$ values between the blue-ice samples and present-day samples even smaller. Thus, we simply conclude that most of the main BIA in Scharffenbergbotnen is of Holocene origin.

SBB01, dated at 10 500 years, is located close to the bottom of the valley where the oldest surface ice along the current flowline occurs (Fig. 1). The most negative $\delta^{18}\text{O}$ value measured in the valley is, however, from B1. It is 9.9‰ lower than the present $\delta^{18}\text{O}$ value, which indicates that the ice in that particular sample, drilled from the southern margin of the main BIA (Fig. 1), originates from the glacial period. The oldest ^{14}C -dated sample was found in the same part of the BIA (Van Roijen, 1996), with a calibrated calendar age of more than 28 000 years BP.

In the high-resolution $\delta^{18}\text{O}$ data of a 60 cm long section from SBB01H we clearly see three annual cycles (Fig. 3). We determine, from the power spectrum of Figure 3, that the horizontal age gradient at that location is ~ 5.4 years m^{-1} . The result agrees with the surface age gradient of 3–6 years m^{-1} determined by dating of internal radar reflection horizons close to the current blue-ice/snow transition zone along the flowline (Sinisalo and others, 2004). This was the only high-resolution section of the SBB01H. The flow model of Grinsted and others (2003) gives an almost constant surface age gradient over the BIA. It is therefore reasonable to extrapolate this age gradient over the 100 m horizontal ice core, SBB01H. Thus we find that the horizontal ice core covers about 540 years. Similarly extrapolating over the 1 km distance between SBB01 and SBB01H gives an age of about 5000 years for SBB01H, as the SBB01 core is dated at 10 500 years BP. This age is, of course, a rough approximation and we shall return to it later in relation to the flow model.

Fig. 2. Measured $\delta^{18}\text{O}$ values for the shallow blue-ice cores (B1–B5), firn core (B6), snow pit (BP1), the 100 m horizontal ice core (SBB01H) and the 52 m vertical core (SBB01) marked in Figure 1 with their population standard deviations. The samples are ordered by their relative age along the x axis from the sample with the oldest ^{14}C age (B1) to the firn and snow samples (B6 and BP1) representing the present-day values in the valley.



No significant periodicities were found in the high-resolution isotopic data from a 1m section of the vertical core SBB01. We assume that the age–depth relationship is linear for the vertical ice core since the core penetrates only a small fraction of the total ice thickness (Herzfeld and Holmlund, 1990). The isochrones in the BIA, according to flow models, are strongly inclined at the SBB01 drilling site, which is close to the bottom of the valley where vertical flow dominates (Van Roijen, 1996; Grinsted and others, 2003). This means that the vertical core is not perpendicular to the isochrones and the annual layers seem much thicker since the core cuts them obliquely. As the ice is relatively old, we can expect it to have experienced more strain thinning of annual layers. We can also expect that diffusion will act to smooth high-frequency variability in the core, relative to the signals in SBB01H. Therefore it is not surprising that there are no high-frequency cycles present in the SBB01 core, and that the 5 m section of ice used to extract the mean isotopic values (Table 2) samples a large number of years.

4.2. Low-frequency changes

Several isotopic records from East Antarctica exhibit a clear early-Holocene optimum immediately following the end of the last ice age from 11 500 to 9000 years BP (Masson and others, 2000). Thus, it is plausible to assume that 10 500 year old SBB01 represents the early-Holocene optimum that is generally defined as the warmest climatic period during the Holocene. In Scharffenbergbotnen, however, our results show that the present-day climate is warmer than in the early-Holocene optimum. We use a value of -28.5‰ (average from B6 and BP1; Fig. 2) for present-day $\delta^{18}\text{O}$ in the valley. The change in $\delta^{18}\text{O}$ between SBB01 (Table 2) and the modern level is 932.4‰ (19‰ in δD). Equation (1) gives a $\Delta\delta^{18}\text{O}_{\text{temp}}$ value of $1.2\pm 0.2\text{‰}$ for $\Delta\delta^{18}\text{O}_{\text{SW}} = 0.2\pm 0.1\text{‰}$

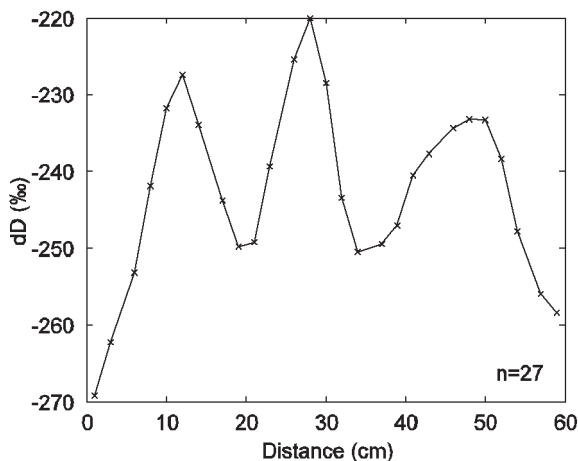


Fig. 3. Results of the high-resolution δD analysis measured from a 60 cm section of the horizontal core SBB01H.

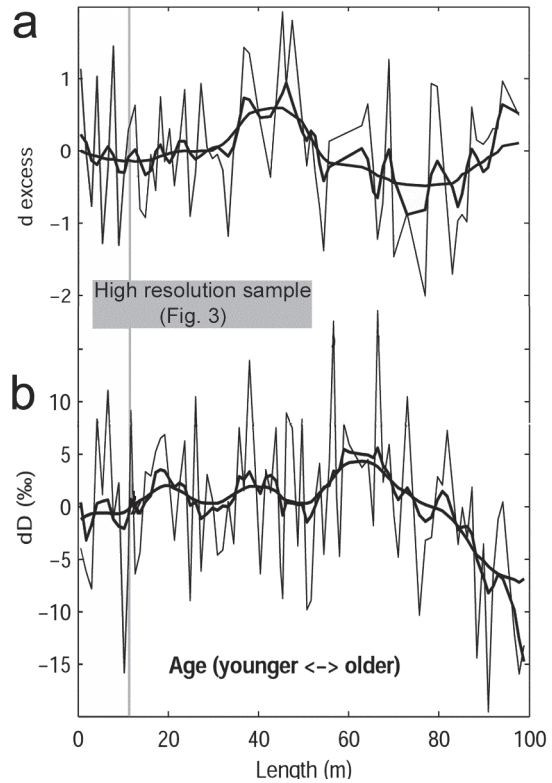
and an elevation change of 225 m. According to the isotopic temperature gradient (Isaksson and Karlén, 1994), this corresponds to a warming of $\sim 1.0 \pm 0.3^\circ\text{C}$ since the early Holocene optimum.

In contrast to the measurements in Scharffenbergbotnen, Masson and others (2000) found an opposite change in several isotopic records in East Antarctica between the early-Holocene optimum and modern levels. The decreasing trends found elsewhere in East Antarctica are probably the result of an overall Holocene increase in elevation of the East Antarctic ice sheet (Masson and others, 2000), due to increased Holocene accumulation rates (Ritz and others, 2001).

The SBB01 core has a 1‰ higher mean value in $\delta^{18}\text{O}$ (and $\sim 13\text{‰}$ higher δD) than the horizontal core SBB01H (Table 2). The $\delta^{18}\text{O}$ values of SBB01H are also lower than the present-day value of -28.5‰ by $\sim 3.4\text{‰}$ (27‰ lower for δD). We know that there was an elevation decrease of 200–250 m in Scharffenbergbotnen between the LGM and the present day (Hättestrand and Johansen, 2005), and that the elevation must have changed gradually. Thus, we use $\Delta\delta^{18}\text{O}_{\text{EC}} = 0.6\text{‰}$ and $\Delta\delta^{18}\text{O}_{\text{SW}} = 0$ for mid-Holocene and present-day values. From Equation (1) we find $\Delta\delta^{18}\text{O}_{\text{temp}} \approx -1.60.1\text{‰}$ between SBB01 and SBB01H, and $\Delta\delta^{18}\text{O}_{\text{temp}} \approx 2.80.2\text{‰}$ between SBB01H and the present-day samples. These changes correspond to a cooling of $\sim 1.4 \pm 0.4^\circ\text{C}$ and warming of $\sim 2.4 \pm 2.0^\circ\text{C}$, respectively.

There is a decrease of 11‰ in δD (1.4‰ in $\delta^{18}\text{O}$) in the last 40 m section at the downstream end of the SBB01H isotope profile (Fig. 4b). Oerter and others (2004) found that changes in precipitation seasonality in DML can cause trends in the $\delta^{18}\text{O}$ profile of $\sim 2\text{‰}$ within a 200 year period. That and influences of many source-region climate changes, however, are unlikely for the first half of the trend (60–80 m in Fig. 4)

Fig. 4. The variability of d excess (a) and δD values (b) of the horizontal SBB01H core: the d excess and δD records (gray), longterm trend as the first reconstructed component of the singular spectrum analysis (SSA) (e.g. Ghil and others, 2002) using an embedding dimension of 10 (thick black line), and the partial reconstruction as the sum of the first and second component of the SSA (thick gray line). SBB01H is 100m long and oriented along the flowline (Fig. 1). The youngest ice is found at $x = 0$. Older ice, ~ 540 years, is found downstream at $x = 100$ m.



as they are expected to cause anticorrelated changes in d excess with δD (Kavanaugh and Cuffey, 2003; Oerter and others, 2004). Thus, using Equation (1) we calculate that the change of -4.6‰ in δD between 60 and 80 m (Fig. 4) corresponds to a temperature change of $\sim 0.5 \pm 0.2^\circ\text{C}$ using the temperature–isotope relationship of Isaksson and Karlén (1994).

4.3. Changes in blue-ice dynamics since LGM

In this paper, we have shown that the BIA has not been in steady state throughout the Holocene. However, according to the moraine studies (Hättestrand and Johansen, 2005), the inner part of Scharffenbergbotnen was a local ablation area at the LGM because otherwise the supraglacial debris would have been transported from the valley.

The generally young age of the surface ice is the result of the past mass-balance and flow regime. We can explore some possible scenarios with a volume-conserving flow model that does accommodate temporally variable surface velocity, ice thickness and mass balance along the flowline with parameterized variation of ice rheology with

depth to produce particle trajectories and isochrones (Grinsted and others, 2003). There is no unique solution for how the BIA has changed over the last glacial cycle as there are only very few constraints on the surface age. We study three simple cases that produce surface ice ages comparable to those calculated from ^{14}C ages (Van Roijen, 1996; Van der Kemp and others, 2002). As the most accurate ^{14}C age was measured for SBB01, we define it to be the most important age to match. The cases are:

- i. different surface velocity in the past;
- ii. different accumulation rate in the past;
- iii. a combination of cases i and ii.

In the following we discuss each case in turn.

i. Different horizontal ice velocity

There must have been less inflow through the northwestern gate to the valley (Fig. 1) at the LGM than today because the surface elevation difference between the valley and its surroundings was smaller. Additionally, there must have been inflow from other directions as the ice flowed over the mountains, at least at the eastern end of the valley (Hättestrand and Johansen, 2005), though there must have been a net inward flow to preserve the BIA. Thus, the surface velocities must have been lower at the LGM than today.

It is not possible, however, to produce Holocene ages for SBB01 with the flow model using smaller surface velocities for the BIA in the past. On the contrary, the surface velocity would have to have been many times higher over the whole Holocene than the current measured velocity profile if it alone was responsible for the measured Holocene age. It is clear that different surface velocity alone cannot explain the young surface ice in the BIA.

The distance between SBB01 and the current equilibrium-line altitude, determined from the accumulation and ground-penetrating radar data, is ~ 2600 m (Sinisalo and others, 2004). Based on the geometry, the mean surface velocity needed for an age of 10 500 years BP for the SBB01 site is 0.5 m a^{-1} , if the surface velocities had been constant through time and the size of the BIA had not changed. This is 70% larger than the maximum velocity (0.3 m a^{-1}) that is measured in the valley (Sinisalo and others, 2003), and contradicts the evidence for lower surface velocities in the past. With a current average surface velocity of 0.14 m a^{-1} in the valley (Sinisalo and others, 2003), the 10 500 year old ice in SBB01 would have originated only 1500 m upstream. This is inside the present-day ablation area, so we conclude that the equilibrium line has probably moved over time and that the BIA was smaller in the past.

ii. Different accumulation rate

Many studies suggest increased accumulation in Antarctica during the Holocene in comparison with the LGM (e.g. Udisti and others, 2004). The results from the EDML core for the past 7000 years, however, show decreasing accumulation during the past 4000 years (Oerter and others, 2004). It is only possible to produce an age of 10 500 years for SBB01 with the flow model by increasing the accumulation rate earlier in the Holocene from the present observations. We get the best fit to the calibrated ^{14}C ages by adding a linear accumulation rate gradient of $2.2 \times 10^{-5} \text{ m a}^{-2}$ to the current measured accumulation rates at all positions along the flowline, so that the accumulation rates reach the present values in 11 000 years (Sinisalo and others, 2003). The model output gives a nearly linear surface age gradient over the whole BIA of about 4 years m^{-1} , which suggests SBB01H is ~ 6600 years old. The horizontal age gradient of 5.4 years m^{-1} estimated from the SBB01H high-resolution data (Fig. 3) is in reasonable agreement with the 4 years m^{-1} considering that only three cycles were measured isotopically, and natural accumulation variability over 3 years may typically be 30% (e.g. Isaksson and others, 1996; Sinisalo and others, 2003).

iii. Different ice flow regime in the valley

To model the scenario of both lower velocity and higher accumulation rate as suggested by the results of cases i and ii, we choose to linearly change the temporal and spatial surface velocity and accumulation rate for the flow model. We assume that the whole valley was an accumulation area in the glacial period (prior to 11 000 years BP) with an accumulation rate of $0.13 \text{ m w.e. everywhere}$ along the flowline, and a starting velocity of zero. We let the surface velocity and the accumulation rate change linearly over time so they reach the present values at 0 years BP. This leads to an ablation area, i.e. a BIA, with surface ages matching the ^{14}C ages, even if the whole valley begins as an accumulation area and there is no inflow through the northwestern gate (Fig. 5). Of course, this scenario is not modelled realistically as the flow model is purely prescriptive, but it is included here to suggest the possibility of negligible ablation area in the last glacial period.

The best-fit model to the ^{14}C ages gives a surface age gradient of $\sim 2.8 \text{ years m}^{-1}$ between SBB01 and SBB01H. This suggests that SBB01H is about 8000 years old (Fig. 5). In general, the modelled surface age gradients agree with the earlier studies of dated GPR reflection horizons that gave values of $3\text{--}6 \text{ years m}^{-1}$ at the firn/blue-ice transition zone (Sinisalo and others, 2004).

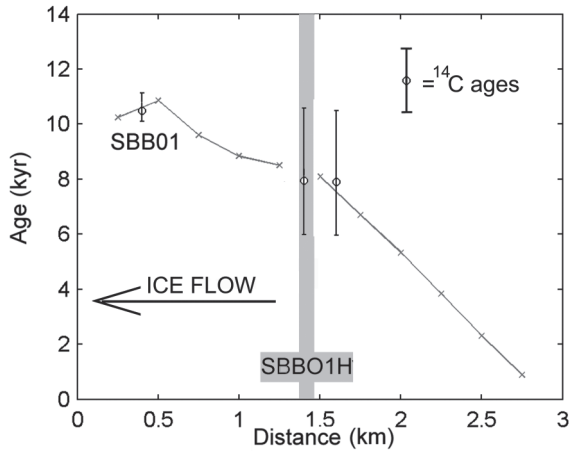


Fig. 5. The calibrated ^{14}C ages (Van Roijen, 1996; Van der Kemp and others, 2002) along the flowline (Fig. 1) and model output with a linearly changing temporal and spatial surface velocity and accumulation rate reaching the present-day values in 11 000 years. The starting accumulation rate was 0.13 m w.e. everywhere along the flowline and the surface velocity was zero. The error bars for SBB01 are calculated using a radiocarbon calibration curve of Reimer and others (2004). Only those of the other blue-ice cores (Van Roijen, 1996) that were located within 50 m of the flowline were plotted. There is thus an error associated with projecting the measurements onto the flowline. The relationship between error and distance was estimated by fitting a straight line to the relative difference between two ^{14}C measurements against their distance. The horizontal distance is measured starting from the bottom of the valley. SBB01 is located at $x = 400$ m and SBB01H at $x = 1400$ m.

5. CONCLUSIONS

In this study we show that most of the main BIA in Scharffenbergbotnen is Holocene ice, based on the $\delta^{18}\text{O}$ values in blue ice and snow. The $\delta^{18}\text{O}$ values in SBB01 support the previous ^{14}C dating of SBB01 and rule out the possibility that the ice close to the bottom of the valley originates from the East Antarctic plateau or from a glacial period.

The oldest surface ice in the valley was found close to the moraines on the southern side of the main BIA in Scharffenbergbotnen where the $\delta^{18}\text{O}$ value was most negative (sample B1 in Fig. 1). The calibrated calendar age (Reimer and others, 2004) at that part gave an age >28 000 years BP (cf. Van Roijen, 1995: ^{14}C age >24 000 years BP).

The oldest ice may have remained at the southern margin 'isolated' from the main flow. However, there is no indication of where this ice originates. We showed that it is possible to extract a high-resolution paleoclimate record from the BIA even with an annual resolution. However, we need a longer horizontal isotopic profile from the BIA in order to study how the surface age gradient varies and to determine the age of SBB01H reliably.

The differences in stable-isotope values between blue-ice and firn samples imply that the modern climate is about $1.0 \pm 0.3^\circ\text{C}$ warmer than the climate in the early-Holocene optimum in Scharffenbergbotnen. Further, the 10 500 year old SBB01 originates from a warmer period than the mid-Holocene SBB01H.

According to our simple flow modelling it is possible that the whole of Scharffenbergbotnen was an accumulation area at the LGM. However, previous studies of supraglacial moraines and ^{14}C dating, together with $\delta^{18}\text{O}$ values at the southern margin of the main BIA, indicate that the BIA existed during the LGM. Therefore we suggest that the BIA was smaller than it currently is, and that the surface velocities were considerably smaller at the LGM. The young age of the major part of the BIA also explains the lack of meteorite finds in this area, and may be typical for many BIAs in low-elevation nunatak areas, where the ice-sheet elevation changes at the glacial termination are likely to have been most pronounced (Pattyn and Declerq, 1998). It is clear that the evolution of the BIA requires a full diagnostic flow model, and we are presently setting up a finite-element scheme solving the full polythermal Stokes equations (Le Meur and others, 2004).

ACKNOWLEDGEMENTS

We are grateful to K. Virkkunen and J. Vehviläinen for help with fieldwork and for preparing samples for analysis. We also thank the Dutch field team drilling SBB01, and the Finnish Forestry Research Institute Rovaniemi. We thank F. Vimeux and an anonymous reviewer for critical comments that improved the manuscript substantially, and D. Peel for his efforts as the Scientific Editor. The Finnish Antarctic Research Program (FIN-NARP 1999–2001 and 2003–04) provided field logistics. Financial support was also obtained from the Netherlands Organization for Scientific Research (NWO) by a grant of the Netherlands Antarctic Programme. The work was primarily funded by the Academy of Finland and the Thule Institute. Part of this work was also funded by the Arctic graduate school ARKTIS and by grants from the Faculty of Natural Sciences, Oulu University, and the University Pharmacy Foundation (Oulu).

REFERENCES

- Bintanja, R. 1999. On the glaciological, meteorological and climatological significance of Antarctic blue ice areas. *Rev. Geophys.*, 37(3), 337–359.
- Bintanja, R. 2000a. Mesoscale meteorological conditions in Dronning Maud Land, Antarctica, during summer: a qualitative analysis of forcing mechanisms. *J. Appl. Meteorol.*, 39(12), 2348–2370.
- Bintanja, R. 2000b. The surface heat budget of Antarctic snow and blue ice: interpretation of temporal and spatial variability. *J. Geophys. Res.*, 105(D19), 24,387–24,407.
- Bintanja, R. and C.H. Reijmer. 2001. Meteorological conditions over Antarctic blue-ice areas and their influence on the local surface mass balance. *J. Glaciol.*, 47(156), 37–50.
- Bintanja, R. and M.R. van den Broeke. 1995a. The climate sensitivity of Antarctic blue-ice areas. *Ann. Glaciol.*, 21, 157–161.
- Bintanja, R. and M.R. van den Broeke. 1995b. The surface energy balance of Antarctic snow and blue ice. *J. Appl. Meteorol.*, 34(4), 902–926.
- Bintanja, R., C.H. Reijmer and S.J.M.H. Hulscher. 2001. Detailed observations of the rippled surface of Antarctic blue-ice areas. *J. Glaciol.*, 47(158), 387–396.
- Delaygue, G., J. Jouzel, V. Masson, R.D. Koster and E. Bard. 2000. Validity of the isotopic thermometer in central Antarctica: limited impact of glacial precipitation seasonality and moisture origin. *Geophys. Res. Lett.*, 27(17), 2677–2680.
- EPICA Community Members. 2006. One-to-one coupling of glacial climate variability in Greenland and Antarctica. *Nature*, 444(7116), 195–198.
- Ghil, M. And 10 others. 2002. Advanced spectral methods for climatic time series. *Rev. Geophys.*, 40(1), 1003. (10.1029/2000RG000092.)
- Grinsted, A., J.C. Moore, V. Spikes and A. Sinisalo. 2003. Dating Antarctic blue ice areas using a novel ice flow model. *Geophys. Res. Lett.*, 30(19), 2005. (10.1029/2003GL017957.)
- Hättestrand, C. and N. Johansen. 2005. Supraglacial moraines in Scharffenbergbotnen, Heimfrontfjella, Dronning Maud Land, Antarctica: significance for reconstructing former blue ice areas. *Antarct. Sci.*, 17(2), 225–236.
- Helsen, M.M., R.S.W. van de Wal, M.R. van den Broeke, D. van As, H.A.J. Meijer and C.H. Reijmer. 2005. Oxygen isotope variability in snow from western Dronning Maud Land, Antarctica and its relation to temperature. *Tellus*, 57B(5), 423–435.
- Helsen, M.M. and 6 others. 2006. Modelling the isotopic composition of Antarctic snow using backward trajectories: simulation of snow pit records. *J. Geophys. Res.*, 111(D15), D15109. (10.1029/2005JD006524.)
- Herzfeld, U.C. and P. Holmlund. 1990. Geostatistics in glaciology: implications of a study of Scharffenbergbotnen, Dronning Maud Land, East Antarctica. *Ann. Glaciol.*, 14, 107–110.
- Isaksson, E. and W. Karlén. 1994. High resolution climatic information from short firn cores, western Dronning Maud Land, Antarctica. *Climatic Change*, 26(4), 421–434.
- Isaksson, E., W. Karlén, N. Gundestrup, P. Mayewski, S. Whitlow and M. Twickler. 1996. A century of accumulation and temperature changes in Dronning Maud Land, Antarctica. *J. Geophys. Res.*, 101(D3), 7085–7094.

- Jonsson, S. 1992. Local climate and mass balance of a blue ice area in western Dronning Maud Land, Antarctica. *Z. Gletscherd. Glazialgeol.*, 26(1), 11–29.
- Jonsson, S. and P. Holmlund. 1990. Evaporation of snow and ice in Scharffenbergbotnen, Dronning Maud Land, Antarctica. *Ann. Glaciol.*, 14, 342–343.
- Jouzel, J. and 6 others. 2003. Magnitude of isotope/temperature scaling for interpretation of central Antarctic ice cores. *J. Geophys. Res.*, 108(D12), 4361–4370.
- Kavanaugh, J.L. and K.M. Cuffey. 2003. Space and time variation of $\delta^{18}\text{O}$ and δD in Antarctic precipitation revisited. *Global Biogeochem. Cycles*, 17(1), 1017. (10.1029/2002GB001910.)
- Labeyrie, L.D., J.C. Duplessy and P.L. Blanc. 1987. Variations in mode of formation and temperature of oceanic deep waters over the past 125,000 years. *Nature*, 327(6122), 477–482.
- Le Meur, E., O. Gagliardini, T. Zwinger and J. Ruokolainen. 2004. Glacier flow modelling: a comparison of the Shallow Ice Approximation and the full-Stokes equation. *C. R. Phys.*, 5(7), 709–722.
- Lintinen, P. and J. Nenonen. 1997. Glacial history of the Vestfjella and Heimefrontfjella nunatak ranges in western Dronning Maud Land, Antarctica. In Ricci, C.A., ed. *The Antarctic region: geological evolution and processes*. Siena, Università degli Studi di Siena, 845–852.
- Lorius, C. and L. Merlivat. 1977. Distribution of mean surface stable isotope values in East Antarctica: observed changes with depth in the coastal area. *LAHS Publ.* 118 (Symposium at Grenoble 1975 – *Isotopes and Impurities in Snow and Ice*), 127–137.
- Masson, V. and 13 others. 2000. Holocene climate variability in Antarctica based on 11 ice-core isotopic records. *Quat. Res.*, 54(3), 348–358.
- Merlivat, L. and J. Jouzel. 1979. Global climatic interpretation of the deuterium–oxygen 18 relationship for precipitation. *J. Geophys. Res.*, 84(C8), 5029–5033.
- Moore, J.C. and 7 others. 2006. Interpreting ancient ice in a shallow ice core from the South Yamato (Antarctica) blue ice area using flow modeling and compositional matching to deep ice cores. *J. Geophys. Res.*, 111(D16), D16302. (10.1029/2005JD006343.)
- Nishiizumi, K., D. Elmore and P.W. Kubik. 1989. Update on terrestrial ages of Antarctic meteorites. *Earth Planet. Sci. Lett.*, 93(3–4), 299–313.
- Oerter, H., W. Graf, H. Meyer and F. Wilhelms. 2004. The EPICA ice core from Dronning Maud Land: first results from stableisotope measurements. *Ann. Glaciol.*, 39, 307–312.
- Pattyn, F. and H. Declerq. 1998. Ice dynamics near Antarctic marginal mountain ranges: implications for interpreting the glacial-geological evidence. *Ann. Glaciol.*, 27, 327–332.
- Petit, J.R., J.W.C. White, N.W. Young, J. Jouzel and Y. Korotkevich. 1991. Deuterium excess in recent Antarctic snow. *J. Geophys. Res.*, 96(D3), 5113–5122.
- Petit, J.R. and 18 others. 1999. Climate and atmospheric history of the past 420,000 years from the Vostok ice core, Antarctica. *Nature*, 399(6735), 429–436.
- Popp, T., T. Sowers, N. Dunbar, W. McIntosh and J.W.C. White. 2004. Radioisotopically dated climate record spanning the last interglacial in ice from Mount Moulton, West Antarctica.
- Reijmer, C.H. 2001. Antarctic meteorology: a study with automatic weather stations. (PhD thesis, University of Utrecht.)
- Reijmer, C.H. and M.R. van den Broeke. 2003. Temporal and spatial variability of the surface mass balance in Dronning Maud Land, Antarctica, as derived from automatic weather

- stations. *J. Glaciol.*, 49(167), 512–520.
- Reimer, P.J. and 27 others. 2004. IntCal04 terrestrial radiocarbon age calibration, 0–26 cal kyr BP. *Radiocarbon*, 46, 1029–1058.
- Ritz, C., V. Rommelaere and C. Dumas. 2001. Modeling the evolution of Antarctic ice sheet over the last 420,000 years: implications for altitude changes in the Vostok region. *J. Geophys. Res.*, 106(D23), 31,943–31,964.
- Sinisalo, A., J.C. Moore, R.S.W. van de Wal, R. Bintanja and S. Jonsson. 2003. A 14 year mass-balance record of a blue-ice area in Antarctica. *Ann. Glaciol.*, 37, 213–218.
- Sinisalo, A., A. Grinsted and J. Moore. 2004. Dynamics of the Scharffenbergbotnen blue-ice area, Dronning Maud Land, Antarctica. *Ann. Glaciol.*, 39, 417–422.
- Udisti, R. and 8 others. 2004. Stratigraphic correlation between the EPICA-Dome C and Vostok ice cores showing the relative variations of snow accumulations over the past 45 kyr. *J. Geophys. Res.*, 109(D8), D08101. (10.1029/2003JD004180.)
- Van den Broeke, M.R. and R. Bintanja. 1995. The interaction of katabatic winds and the formation of blue-ice areas in East Antarctica. *J. Glaciol.*, 41(138), 395–407.
- Van der Kemp, W.J.M. and 7 others. 2002. In situ produced ^{14}C by cosmic ray muons in ablating Antarctic ice. *Tellus*, 54B(2), 186–192.
- Van Lipzig, N.P.M., E. van Meijgaard and J. Oerlemans. 2002. The effect of temporal variations in the surface mass balance and temperature-inversion strength on the interpretation of ice-core signals. *J. Glaciol.*, 48(163), 611–621.
- Van Roijen, J.J. 1996. Determination of ages and specific mass balances from ^{14}C measurements on Antarctic surface ice. (PhD thesis, Utrecht University)
- Van Roijen, J.J., R. Bintanja, K. Van der Borg, M.R. van den Broeke, A.F.M. De Jong and J. Oerlemans. 1994. Dry extraction of $^{14}\text{CO}_2$ and ^{14}CO from Antarctic ice. *Nucl. Instrum. Meth. Phys. Res. B*, 92(1–4), 331–334.
- Van Roijen, J.J., K. Van der Borg, A.F.M. De Jong and J. Oerlemans. 1995. Ages, ablation and accumulation rates from ^{14}C measurements on Antarctic ice. *Ann. Glaciol.*, 21, 139–143.
- Vimeux, F., V. Masson, G. Delaygue, J. Jouzel, J.R. Petit and M. Stievenard. 2001. A 420 000 year deuterium excess record from East Antarctica: information on past changes in the origin of precipitation at Vostok. *J. Geophys. Res.*, 106(D23), 31,863–31,873.
- Vimeux, F., K.M. Cuffey and J. Jouzel. 2002. New insights into Southern Hemisphere temperature changes from Vostok ice cores using deuterium excess correction. *Earth Planet. Sci. Lett.*, 203(4), 829–843.
- Waelbroeck, C. and 7 others. 2002. Sea-level and deep water temperature changes derived from benthic foraminifera isotopic records. *Quat. Sci. Rev.*, 21(1–3), 295–305.
- Werner, M., M. Heimann and G. Hoffmann. 2001. Isotopic composition and origin of polar precipitation in present and glacial climate systems. *Tellus*, 53B(1), 53–71.
- Whillans, I.M. and W.A. Cassidy. 1983. Catch a falling star: meteorites and old ice. *Science*, 222(4619), 55–57.
- Wilch, T.I., W.C. McIntosh and N.W. Dunbar. 1999. Late Quaternary volcanic activity in Marie Byrd Land: potential $^{40}\text{Ar}/^{39}\text{Ar}$ dated time horizons in West Antarctic ice and marine cores. *Geol. Soc. Am. Bull.*, 111(10), 1563–1580.